Exploring the roles of sediment production by Photozoan and Heterozoan biotas on the evolution of carbonate system geometries through forward modelling

Examples from Mallorca and Menorca

Timothy Oluwatobi TELLA

Kumulative Dissertation

zur Erlangung des akademischen Grades
"doctor rerum naturalium"
(Dr. rer. nat.)
in der Wissenschaftsdisziplin

Sedimentologie

**eingereicht an der
Mathematisch-Naturwissenschaftlichen Fakultät
Institut für Geowissenschaften
der Universität Potsdam**

Ort und Tag der Disputation: 09.02.2023, Potsdam.

Table of Contents

List of Figures

List of Tables

Abstract

The role of biogenic carbonate producers in the evolution of the geometries of carbonate systems has been the subject of numerous research projects. Attempts to classify modern and ancient carbonate systems by their biotic components have led to the discrimination of biogenic carbonate producers broadly into Photozoans, which are characterised by an affinity for warm tropical waters and high dependence on light penetration, and Heterozoans which are generally associated with both cool water environments and nutrient-rich settings with little to no light penetration. These broad categories of carbonate sediment producers have also been recognised to dominate in specific carbonate systems. Photozoans are commonly dominant in flat-topped platforms with steep margins, while Heterozoans generally dominate carbonate ramps. However, comparatively little is known on how these two main groups of carbonate producers interact in the same system and impact depositional geometries responding to changes in environmental conditions such as sea level fluctuation, antecedent slope, sediment transport processes, etc. This thesis presents numerical models to investigate the evolution of Miocene carbonate systems in the Mediterranean from two shallow marine domains: 1) a Miocene flat-topped platform dominated by Photozoans, with a significant component of Hetrozoans in the slope and 2) a Heterozoan distally steepened ramp, with seagrass-influenced (Photozoan) inner ramp. The overarching aim of the three articles comprising this cumulative thesis is to provide a numerical study of the role of Photozoans and Heterozoans in the evolution of carbonate system geometries and how these biotas respond to changes in environmental conditions. This aim was achieved using stratigraphic forward modelling, which provides an approach to quantitatively integrate multi-scale datasets to reconstruct sedimentary processes and products during the evolution of a sedimentary system.

In a Photozoan-dominated carbonate system, such as the Miocene Llucmajor platform in Western Mediterranean, stratigraphic forward modelling dovetailed with a robust set of sensitivity tests reveal how the geometry of the carbonate system is determined by the complex interaction of Heterozoan and Photozoan biotas in response to variable conditions of sea level fluctuation, substrate configuration, sediment transport processes and the dominance of Photozoan over Heterozoan production. This study provides an enhanced understanding of the different carbonate systems that are possible under different ecological and hydrodynamic conditions. The research also gives insight into the roles of different biotic associations in the evolution of carbonate geometries through time and space. The results further show that the main driver of platform progradation in a Llucmajor-type system is the lowstand production of Heterozoan sediments, which form the necessary substratum for Photozoan production.

In Heterozoan systems, sediment production is mainly characterised by high transport deposits, that are prone to redistribution by waves and gravity, thereby precluding the development of steep margins. However, in the Menorca ramp, the occurrence of sediment trapping by seagrass led to the evolution of distal slope steepening. We investigated, through numerical modelling, how such a seagrass-influenced ramp responds to the frequency and amplitude of sea level changes, variable carbonate production between the euphotic and oligophotic zone, and changes in the configuration of the paleoslope. The study reinforces some previous hypotheses and presents alternative scenarios to the established concepts of high-transport ramp evolution. The results of sensitivity experiments show that steep slopes are favoured in ramps that develop in high-frequency sea level fluctuation with amplitudes

between 20 m and 40 m. We also show that ramp profiles are significantly impacted by the paleoslope inclination, such that an optimal antecedent slope of about 0.15 degrees is required for the Menorca distally steepened ramp to develop.

The third part presents an experimental case to argue for the existence of a Photozoan sediment threshold required for the development of steep margins in carbonate platforms. This was carried out by developing sensitivity tests on the forward models of the flat-topped (Llucmajor) platform and the distally steepened (Menorca) platform. The results show that models with Photozoan sediment proportion below a threshold of about 40% are incapable of forming steep slopes. The study also demonstrates that though it is possible to develop steep margins by seagrass sediment trapping, such slopes can only be stabilized by the appropriate sediment fabric and/or microbial binding. In the Photozoan-dominated system, the magnitude of slope steepness depends on the proportion of Photozoan sediments in the system. Therefore, this study presents a novel tool for characterizing carbonate systems based on their biogenic components.

Zusammenfassung

Die Rolle von biogenen Karbonatproduzenten bei der Ausbildung der Geometrien von Karbonatablagerungen war bereits Gegenstand mehrerer Forschungsarbeiten. Bisherige Versuche, moderne und alte Karbonatsysteme anhand ihrer biotischen Komponenten zu klassifizieren, führten dazu, dass biogene Karbonatproduzenten generell unterschieden werden in Photozoen, welche sich durch eine starke Neigung zu warmen, tropischen Gewässern und eine hohe Abhängigkeit von der Lichtdurchflutung auszeichnen, und in Heterozoen, die im Allgemeinen mit kühlen Wasserumgebungen mit wenig bis gar keiner Lichtdurchflutung assoziiert werden. Dabei wurde auch festgestellt, dass diese beiden Haupttypen von Karbonatproduzenten in bestimmten Karbonatsystemen dominierend sind. Photozoen sind in der Regel auf Karbonatplattformen mit flachem Oberbereich und steilen Rändern vorherrschend, während Heterozoen generell in Karbonatrampen dominieren. Allerdings herrscht immer noch große Unkenntnis darüber, wie diese Karbonatsysteme und ihre Geometrien auf Veränderungen der Umweltbedingungen, wie z. B. Schwankungen des Meeresspiegels, vorherige Geometrien der Karbonatablagerungen, Prozesse des Sedimenttransports, usw., reagieren. In dieser Dissertation werden numerische Modelle vorgestellt, mit Hilfe derer die Entwicklung miozäner Karbonatsysteme im Mittelmeerraum anhand des Beispiels zweier Flachwasserbereiche untersucht werden: 1) eine miozäne Plattform mit flachem Oberbereich, die von Photozoen dominiert wird, und 2) eine von Seegras beeinflusste und distal steil abfallende Rampe die von Heterozoen dominiert wird. Das übergeordnete Ziel der drei wissenschaftlichen Publikationen, aus denen diese kumulative Dissertation aufgebaut ist, beinhaltet die numerische Analyse der Rolle von Photozoen und Heterozoen bei der Entwicklung der Geometrien von Karbonatsystem, und die anschließende Auswertung, wie diese Biotope auf Veränderungen der Umweltbedingungen reagieren. Dies wurde mit Hilfe der stratigraphischen Vorwärtsmodellierung realisiert, welche einen methodologischen Ansatz zur quantitativen Integration von Datensätzen unterschiedlichster Größenordnungen bietet, um sedimentäre Prozesse und deren Produkte im Laufe der Entwicklung eines Sedimentsystems zu rekonstruieren.

In einem von Photozoen dominierten Karbonatsystem, wie das der miozänen Llucmajor-Plattform im westlichen Mittelmeerraum, zeigt die stratigraphische Vorwärtsmodellierung in Übereinstimmung mit belastbaren Daten, die aus einer umfangreichen Reihe von Sensitivitätstests gewonnen wurden, wie die Geometrie des untersuchten Karbonatsystems durch die komplexe Interaktion von photozoischen und heterozoischen Biotopen als Reaktion auf variable Umgebungsbedingungen wie Meeresspiegelschwankungen, Struktur des Substrates, Prozesse der Sedimentation und die Dominanz von Photozoen gegenüber Heterozoen bestimmt wird. Diese Analyse führt zu einem erweiterten Verständnis über den Aufbau und die Entwicklung der verschiedenen Arten von Karbonatsystemen, die unter den jeweiligen ökologischen und hydrodynamischen Umgebungsbedingungen potenziell möglich sind. Zusätzlich bieten die in dieser Dissertation vorgestellten Forschungsergebnisse neue Einblicke über die Rolle der verschiedenen biologischen Vergesellschaftungen bei der zeitlichen und räumlichen Entwicklung der Geometrie eines karbonatischen Flachwasserablagerungsraums. Außerdem konnte bewiesen werden, dass der Hauptfaktor, der für die Progradation einer Plattform des Llucmajortypus verantwortlich ist, die Karbonatproduktion durch Heterozoen während der ´lowstand´- Phase ist, wodurch sich das Substrat bildet, welches für die Karbonatproduktion durch Photozoen notwendig ist.

In heterozoischen Systemen ist die Sedimentproduktion vor allem durch Prozesse mit hoher Transportdynamik gekennzeichnet, und unterliegt einer Sedimentumverteilung, die durch Wellenbewegungen und gravitative Prozesse ausgelöst wird, wodurch das Ausbilden steiler Plattformränder verhindert wird. In der Karbonatrampe von Menorca jedoch führte das Vorkommen von Sedimentablagerungen, die durch Seegras stabilisiert wurden, zur Versteilerung des distalen Bereichs der Karbonatrampe. Mit Hilfe numerischer Modelle wurde untersucht, wie eine solche von Seegras beeinflusste Rampe auf die Frequenz und Amplitude von Meeresspiegelschwankungen, auf die unterschiedlich ausgeprägte Karbonatproduktion innerhalb der euphotischen und der oligophotischen Zone, sowie auf Veränderungen in der Struktur der vorherigen Geometrie der Rampe, reagiert. Das Ergebnis dieser Analyse untermauert einige der früheren Hypothesen, bietet aber auch alternative Szenarien zu den bereits etablierten Konzepten der Entstehung und Entwicklung von Karbonatrampen, welche durch eine hohe Transportdynamik gekennzeichnet sind. Die Ergebnisse der „Sensitivitätsanalysen" zeigen, dass sich in einer Karbonatrampe bevorzugt steilere distalere Bereiche ausbilden, wenn die Entwicklung der Rampe durch hochfrequente Meeresspiegelschwankungen mit einer Amplitude zwischen 20 m bis 40 m geprägt wurde. Es konnte außerdem gezeigt werden, dass das Profil einer Rampe stark von der ursprünglichen Hangneigung beeinflusst wird, und ein optimaler Neigungswinkel des vorherigen Hanges von ungefähr 0.15 Grad benötigt wird, damit eine Rampe, wie die des Menorcatypus die im distalen Bereich steiler wird, sich ausbilden kann.

Im dritten Teil der Dissertation wird ein experimentelles Fallbeispiel vorgestellt, welches Hinweise auf das Vorhandensein eines spezifischen Schwellenwerts innerhalb der photozoischen Karbonatproduktion liefert, der essenziell für die Entwicklung von steilen Plattformrändern ist. Zu diesem Zweck wurden Sensibilitätstests für die Vorwärtsmodelle der Plattform mit flacher Topografie des oberen Bereiches (Llucmajor) und der im distalen Bereich steiler werdenden Plattform (Menorca) durchgeführt. Die Ergebnisse zeigen, dass Modelle, die einen Anteil an von Photozoen produzierten Sedimenten aufweisen, der unter einem Schwellenwert von etwa 40 % liegt, nicht in der Lage sind, steile Plattformränder auszubilden. Diese Analyse beweist auch, dass es grundsätzlich möglich ist, steile Plattformränder durch die Stabilisierung durch Seegras, welches Sediment einfängt und aufnimmt, aufzubauen. Voraussetzung dafür ist allerdings das Vorhandensein einer geeigneten internen Sedimenttextur und/oder der Verfestigung der Sedimente durch mikrobielle Aktivität. In Systemen, die durch Photozoen dominiert werden, hängt die Größe des Hangneigungswinkel stark vom Anteil des innerhalb des Systems photozoisch produzierten Sediments ab. In dieser Arbeit wird deshalb eine neue Herangehensweise zur Charakterisierung von Karbonatsystemen eingeführt, die auf deren Inhalt an biogenen Komponenten beruht.

Acknowledgements

Chapter 1
INTRODUCTION

The evolution of carbonate systems in geologic record: The present is a keyhole to the past

Observations and studies of modern shallow marine carbonate systems have shown that carbonate systems in the geologic record are significant paleoclimatic, paleoecological and paleogeographic archives from which meaningful geological reconstructions can be made (Milliman et al., 1974; Cabioch et al., 1999; Cornacchia et al., 2021). Modern carbonate systems also permit the possibility of drawing parallels with ancient carbonates as the former provides direct measurement of ecological and bio-physico-geochemical parameters in modern environments (Hallock, 1988; James, 1997; Mutti and Hallock, 2003a). Understanding the conditions under which ancient carbonate systems developed is therefore significantly dependent on improved knowledge of modern carbonates. However, inferring depositional processes of carbonate systems that developed over long geologic time from short-lived modern analogues could preclude the conclusive interpretation of the geometric evolution of carbonate systems in the geologic record. For example, the geometries of several carbonate systems have been misinterpreted due to the incompleteness of outcrop data and limitations arising from the scale of observation (Burchette and Wright, 1992). These interpretation limitations are however managed through the many classification schemes of carbonate systems, which can aid interpolation of the carbonate geometries beyond available data by observing the descriptive criteria for the classification scheme. One such classification scheme uses the dominant biotic association present in a carbonate system to classify it as either Heterozoan or Photozoan (James, 1997). Using such a classification requires understanding the response of biogenic carbonate producers, especially as such biotas reflect responses to ecological stresses in their geometries (Pomar, 2001b, 2001a; Schlager, 2005). Again, such investigations rely on modern analogues which may not be completely representative of ancient systems which have experienced several biotic evolution and extinctions (Edinger and Risk, 1995; Pomar and Hallock, 2008). The implication of the incompleteness of inferences of ancient carbonates from modern systems implies that caution should be taken to abate the uniformitarian bias. To avoid this bias, the study

of carbonate systems needs to be carried out by comparing carbonates within the same geological time interval such as the Miocene.

Carbonate geometries and biogenic carbonate production

Carbonate geometries in geologic records have been classified to vary between homoclinal ramps and flat-topped steep-margin platforms (Read, 1985; Pomar, 2001b; Bosence, 2005). Ramps typically are characterised by gentle dips from proximal to distal, without significant slope breaks (Ahr, 1973; Burchette and Wright, 1992), while flat-topped platforms are recognised by their well-defined slope breaks and steep margins (Tucker et al., 1990; Pomar, 2001b). Between these end members are geometric profiles that include distally steepened ramps, ramps with shoal water complexes, isolated platforms, drowned platforms, and several forms of rimmed carbonate shelves (Read, 1985).

The geometry of shallow water carbonate systems is connected to factors such as tectonic setting, eustatic oscillation, oceanographic factors, and climate (Wilson, 1975; Bosence, 2005). However, a major control on carbonate geometry is the type of biogenic carbonate sediment producers (Schlager, 2003; Reijmer, 2021). Biogenic carbonate associations have been classified essentially by climate zonation and marine temperature into different fields. These include: Chlorozoan, Chloralgal or Foramol (Lees, 1975); Chlorozoan, Chloralgal, Rhodalgal, Bryoalgal or Molechfor (Carannante et al., 1988). In addition to temperature zonations, light-dependence and their trophic requirements allow the distinction into Photozoan or Heterozoan (James, 1997). This distinction can be further subclassified into euphotic, oligophotic, mesophotic and aphotic contributors (Pomar, 2001b). Mutti and Hallock (2003) have shown how carbonate systems change along two different axes, temperature zonation (tropical, warm-temperate, cold-temperate or polar) and concentrations of trophic resources. In fact, in an otherwise warm water environment, the presence of cold and nutrient-ladened water (e.g., upwelling) in shallow marine carbonate environments, can result in Heterozoan biota. For our research purposes, we adopt primarily the classification of James, 1997) and Pomar (2001b).

Photozoan biotas, which are defined as an assemblage comprising light-dependent biotas such as green algae and zooxanthellate corals (because of the light-dependence of these symbionts), tend to form flat-topped platforms with steep flanks

and are associated with high-transport carbonate systems (Pomar, 2001b; Williams et al., 2011). Heterozoans on the other hand require little to no light, and include organisms such as coralline algae, bryozoans, foraminifera, molluscs and ahermatypic corals. Carbonate systems dominated by Heterozoans are usually ramps (Pomar and Kendall, 2008a; Williams et al., 2011). However, the connection between carbonate-producing biotas and carbonate system geometries is not yet fully understood, as different types of carbonate-producing biotas can coexist in the same system.

Motivation and Aims of the project

The motivation of this thesis is to provide a numerical-modelling-based contribution to the discussion on the relationship between biogenic carbonate production and the geometry of carbonate platforms, especially how the dominance of Photozoan versus Heterozoan carbonate production and their interplay results in specific geometries. Although many studies have advanced our understanding of carbonate production in relation to different carbonate systems (e.g., Carannante et al., 1988; James, 1997; Schlager, 2000, 2003; Pomar, 2001b, 2001a; Reijmer, 2021), the interaction between the two main types of carbonate producers in impacting the evolution of carbonate geometries is relatively poorly explored. This thesis attempts to address through stratigraphic forward modelling the following questions:

- Is the relationship between dominant biogenic carbonate production and carbonate system geometries predictive? If yes, can this relationship be predicted by investigating carbonate system evolution through process-based numerical modelling?

- How do Photozoan and Heterozoan biotas within the same system respond to changes in environmental conditions, and how does this impact the geometries?

- Do carbonate system geometries truly shift from ramp geometries to flat-topped platforms (FTPs) because of the ecological responses of carbonate factories to changing environmental conditions? Or are these geometric turnovers mainly a result of a change in carbonate production efficiency in which ramps are simply a transitional phase that will eventually evolve into FTP if sufficient time and improved production efficiency are allowed?

To answer these questions, the following research hypotheses were tested through stratigraphic forward modelling:

I.   Carbonate geometries are dependent on the dominant carbonate factory, i.e., Photozoan factories will result in flat-topped platforms, while Heterozoan factories will result in ramps.

II. The responses of Heterozoan and Photozoan biotas to changing environmental and ecological conditions are different and are reflected in the geometry of carbonate systems.

III. If a transition from ramps to flat-topped platform geometries is possible, a threshold of Photozoan sedimentation is required for an FTP to evolve from a ramp.

Stratigraphic forward modelling in carbonate research

Stratigraphic forward modelling (SFM) is a process-based numerical modelling established on the principle that sedimentary architecture is the response of sedimentary systems to the complex interaction between accommodation changes, sediment supply and sediment dispersion in a basin. Applied to carbonate systems, SFM relates the processes of carbonate sediment production, accommodation variation through tectonics and eustasy, and sediment transport by waves and gravity through a generalised diffusion formula that relates sediment flux Q_s with a topographic slope S by a diffusion coefficient K as given by the equation:

$$Q_s = KS \tag{1}$$

The technique has been used successfully in several studies to investigate the process of carbonate systems development (e.g., Bice, 1988; Bosence et al., 1994; Aurell et al., 1998; Williams et al., 2011; Sultana et al., 2021) thereby improving our understanding of the controls on the observed facies and architectural heterogeneity of carbonate systems. Various models with strong carbonate simulation capabilities through multidisciplinary integration of oceanographic, sedimentological, biological, physical and chemical principles. These include SEDPAK (Strobel et al., 1989), CARBONATE (Bosence and Waltham, 1990), DIONISOS (Granjeon and Joseph, 1999), REPRO (Hüssner et al., 2001), and several others. We use the DIONISOS model in this thesis for its flexibility of sediment diffusion of multiple grain sizes at diverse depositional environments.

We applied stratigraphic forward models to two Miocene carbonate platforms (Mallorca and Menorca) in the Mediterranean to test concepts of ramp and flat-topped platform development, and to quantify the impact of Photozoan and Heterozoan carbonate production on the geometries of carbonate systems. This location offers a unique opportunity to study a carbonate ramp and a flat-topped platform with biotas of the same age interval. This study was done by developing models referenced to the lower Tortonian distally steepened ramp in Menorca and the upper Tortonian – lower Messinian reef complex in Mallorca. Multiple sensitivity experiments were then carried out to investigate how parameters such as carbonate production modes, bathymetric configuration, sea level fluctuation and sediment transport control the evolution of carbonate systems.

Geologic setting of the Mediterranean (Menorca, Mallorca)

The reference carbonate systems of the models in the thesis are the upper Miocene Menorca ramp and the Llucmajor platform of Mallorca. They are situated in the Balearic Islands of the western Mediterranean (Figure 1.1).
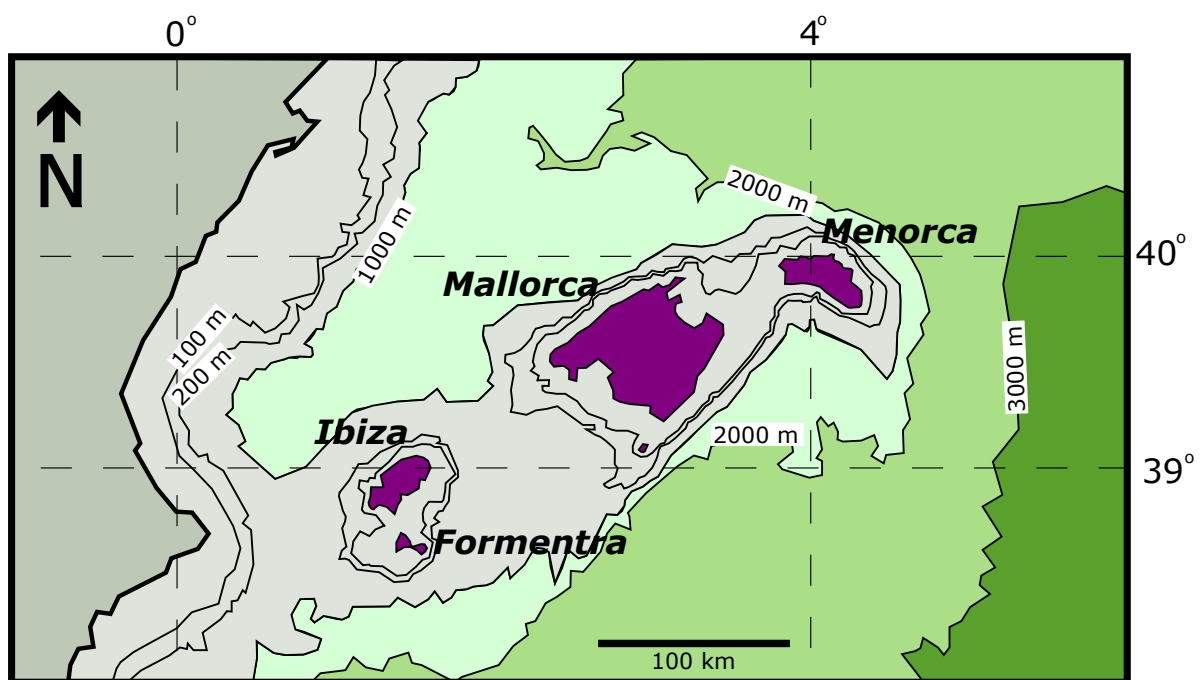
Figure 1.1: Map of the Balearic Islands in the Western Mediterranean contours show topographic variation (Modified from Pomar, 2004).

Both the Menorca and Mallorca carbonate systems represent an important unit of the Miocene sediments of the western Mediterranean as they significantly preserve

records of palaeoceanographic and paleoclimatic changes during the interval (Esteban, 1979; Pomar et al., 2002; Mateu-Vicens et al., 2008).

Series	Stages	Planktonic Forams Biochronozones	Stratigraphic Units	
			Mallorca	Menorca
Holocene				
Pleistocene		N23	Palma Silts & eolianites	eolianites
		N22		
Pliocene		N21		
	3.5 My	N20	San Jordi Calcarenites	
		N19	Son Mir Calcisiltites	
	5.2	N18	Santayi Lm / Bonanova Marls **?** Gypsum & Grey Marls	
Upper Miocene	Messinian 6.3	N17	Reef Complex Unit	Reefal Unit
	Tortonian	N16	Heterostegina Calcisiltites Unit	Lower Bar Unit

Figure 1.2: stratigraphic units of Mallorca and Menorca and their relationship with the Reef Complex Unit (Llucmajor platform) and the Lower Bar Unit (Menorca ramp) (Modified from Pomar, 2004)

The Miocene sediments of the western Mediterranean in relation to the carbonate systems of Menorca and Mallorca is given in Figure 1.2. These rocks represent post-tectonic sedimentary units overlying folded and thrust Mesozoic to Mid-Miocene rocks.

Thesis Organisation

The questions and hypotheses outlined herein were addressed in results that have been grouped in three journal articles which make up chapters 2, 3 and 4 of this doctoral thesis. These chapters have either been published, accepted or in preparation for submission. A summary of the chapters of this thesis is presented as follows:

Chapter 2 presents a quantitative investigation of the roles of changing biogenic carbonate production on the evolution of carbonate platforms, with the Llucmajor

platform in Mallorca as a case study. We presented a multi-class approach to carbonate sediment simulation, which offers flexibility for investigating the responses of individual biotic classes to changing environmental conditions. The results affirm earlier concepts of Photozoan versus Heterozoan effect in determining the geometry of carbonate systems. We also showed in this chapter that Heterozoans are an important component of highly prograding reef complexes. This chapter was published in 2022 in Petroleum Geoscience (DOI: 10.1144/petgeo2021-053) and the authors are Tella, Winterleitner and Mutti.

Chapter 3 presents a forward model referenced to the upper Miocene distally steepened Menorca ramp and shows how Photozoans and Heterozoans interact with hydrodynamics and basinal changes to control the profile of carbonate ramps. The results show the influence of sea level change parameter, paleoslope, variation in the dominance of Photozoan versus Heterozoan carbonate production on carbonate ramp evolution. This chapter has been published in Sedimentary Geology (DOI: 10.1016/j.sedgeo.2022.106267) and the authors are Tella, Winterleitner, Morsilli and Mutti.

Chapter 4 argues for the existence of a minimum Photozoan sediment threshold required for the development of steep margins in carbonate systems. This was achieved by subjecting the flat-topped Llucmajor (Mallorca) model and the distally steepened Menorca ramp model to sensitivity experiments. By investigating at what point steep margins begin to develop through the gradual increase of the proportion of Photozoan sediments, our models strongly suggest that a minimum of 43.4% Photozoan proportion is required in a carbonate system for steep margins to form. We also showed that carbonate systems can be better classified by including the proportion of Photozoan sediments in the system in the existing classification schemes. This chapter is ready for submission to Basin Research.

Chapter 5 is a synthesis of the results of the three previous chapters discussing the main results of the thesis.

Chapter 2
INVESTIGATING THE ROLE OF DIFFERENTIAL BIOTIC PRODUCTION ON CARBONATE GEOMETRIES THROUGH STRATIGRAPHIC FORWARD MODELLING AND SENSITIVITY ANALYSIS: THE LLUCMAJOR EXAMPLE

ABSTRACT

The geometry of carbonate platforms reflects the interaction of several factors. However, the impact of carbonate-producing organisms has been poorly investigated so far. This study applies stratigraphic forward modelling (SFM) and sensitivity analysis to examine, referenced to the Miocene Llucmajor platform, the effect on platform geometry of changes of the dominant biotic production in the oligophotic and euphotic zones. Our results show that the complex interplay of carbonate production rates, bathymetry and accommodation variation controls the platform geometry. The main driver of progradation is the oligophotic production of rhodalgal sediments during the lowstands. This study demonstrates that platform geometry and internal architecture vary significantly according to the interaction of the predominant carbonate-producing biotas. The input parameters for this study are based on well-understood Miocene carbonate biotas with characteristic euphotic, oligophotic and photo-independent carbonate production in which it is crucial that each carbonate-producing class is modelled explicitly within the simulation run and not averaged with a single carbonate production-depth profile. This is important in subsurface exploration studies based on stratigraphic forward models where the overall platform geometry may be approximated through calibration runs and constrained by seismic surveys and wellbores. However, the internal architecture is likely to be over-simplified, without an in-depth understanding of the target carbonate system and transfer to forward modelling parameters.

Keywords: Carbonate systems, stratigraphic forward modelling, Miocene, platform geometries, biota, euphotic, oligophotic, corals, rhodalgal, sensitivity analysis.

INTRODUCTION

The evolution of carbonate systems has traditionally been linked to relative sea level and regional tectonics as the first-order controls over geometries and facies associations (Kendall and Schlager, 1981; Handford and Loucks, 1993), in concert with climate and ocean circulation, which affect temperature, nutrients and ocean chemistry and the type of carbonate producing organisms through time (Milliman et al., 1974; Stanley and Hardie, 1998; Mutti, 2019). Many studies have focused on how these boundary conditions impact carbonate-producing organisms (e.g., Chave, 1967; Lees and Buller, 1972; Carannante et al., 1988; Nelson, 1988; James, 1997; Mutti and Hallock, 2003) and how these translate into geometrical and facies properties of carbonate systems and carbonate factories (Schlager, 1992, 2005; James, 1997). Geometries of carbonate systems, ranging from reef-rimmed to homoclinal ramps and a range of forms in between (Ahr, 1973; Ginsburg and James, 1974; Read, 1985; Handford and Loucks, 1993; Williams et al., 2011), can be linked to dominant biota at any given time during the evolution of the platform (e.g., James and Bone, 1991; James, 1997; Pomar et al., 2012a). Based on ecological and depositional requirements, carbonate sediment-producing biotas have been grouped into various categories (Purdy, 1963; Lees and Buller, 1972; Lees, 1975; Carannante et al., 1988; James, 1997; Pomar, 2001b, 2001a; Halfar et al., 2004; Schlager, 2005; Wilson and Vecsei, 2005; Roberts and Bally, 2012; Michel et al., 2018; Brandano et al., 2019). Due to the ability of many euphotic carbonate-producing biota, such as hermatypic corals, to withstand wave action, they are able to construct rimmed platforms, while the creation of low-angle ramps by many known oligophotic biotas is a consequence of their susceptibility to dispersion by currents (Pomar, 2001b; Williams et al., 2011). Several authors have described the transition from ramp to rimmed platforms and vice versa (e.g., Biddle et al., 1992; Pomar, 2001a; Schlager, 2005; Benisek et al., 2009; Tomás et al., 2010) and highlighted that changes in accommodation space availability is the driving force to initiate this ramp to rimmed-reef transition but also recognize that a shift in platform geometry might be linked to the temporal evolution of the dominant carbonate factory (Pomar, 2001a; Pomar and Hallock, 2007; Janson et al., 2010; Pomar et al., 2012a). This case study highlights how architectural changes occur in synchrony with a shift of the predominant carbonate factory at a given time and can

be related to changes of the environmental conditions causing a shift from oligophotic production to euphotic sediment production or vice versa.

Pomar and Haq (2016) showcased how the interaction of different factors specific to carbonate system results in a variety of platforms by contrasting sequence stratigraphic responses in clastic and carbonate environments. Different biota and their respective carbonate factories have the capacity to control platform geometry and facies dynamics through ecological constraints on platform growth rate (James and Bone, 1991; Burchette and Wright, 1992; Williams et al., 2011). Furthermore, the complex interplay between coexisting and competing carbonate biota in a given system has a first-order control on sediment rigidity (e.g., framework builders vs. sediment grains), grain size and shape of produced sediments and their spatial and temporal arrangements (Pomar, 2001a; Williams et al., 2011). The analysis of these processes and their role in shaping carbonate geometries is difficult to assess in a quantitative way due to sparse data sets from field observations. Recent advances in stratigraphic forward modelling (SFM) of carbonate systems (Granjeon and Joseph, 1999; Warrlich et al., 2002; Burgess et al., 2006, 2013; Williams et al., 2011; Hawie et al., 2015; Kolodka et al., 2016; Salles et al., 2018a; Zhang et al., 2019; Li et al., 2020; Pall et al., 2020) offer a powerful tool for quantitative analysis of carbonate systems development through time and space and for testing the impact of different controls over platform evolution. Extensive research using SFM has been undertaken in recent years (Burgess et al., 2006; Williams et al., 2011; Nader et al., 2018; Salles et al., 2018b; Al-Salmi et al., 2019; Hawie et al., 2019; Sultana et al., 2021), yet there has not been a significant focus on numerical modelling investigating the role of carbonate producing biota on platform geometry.

The aim of this study is to quantitatively analyse the effect of the temporal and spatial change of the dominant carbonate producing organisms and their differential rates of production on the resultant platform geometry, and to investigate how different carbonate factories interact to generate depositional geometries by employing stratigraphic forward modelling. We focussed our modelling on (1) investigating the sensitivity of platform geometries to biotic sediment production, (2) understanding how euphotic versus oligophotic carbonate production drive changes in platform geometry, and (3) how changes in initial bathymetry (at the onset of platform development) influence platform geometry, especially the extent of platform progradation.

We chose the Miocene Llucmajor carbonate system of Mallorca (Spain, Western Mediterranean) as a reference for this study, as the setting has been the focus of numerous and fundamental studies addressing the controls over stratigraphic and facies architecture and its evolution (Esteban, 1979; Pomar, 1993; Pomar and Ward, 1994, 1995; Pomar et al., 1996, 2012b; Pomar and Hallock, 2007; Sàbat et al., 2011a). The platform is a reef-rimmed carbonate system built by reef-building euphotic corals and green algae in the shallow water and upper slope domain, and oligophotic rhodalgal communities in the deeper slope (Carannante et al., 1988; Pomar et al., 2012a), both interacting as sea level fluctuates to create the platform progradational and aggradational sequences. The superbly exposed and extensively studied carbonate sequences allow for direct validation and calibration of the modelling results. Two numerical models of the platform architecture and its facies distribution of the platform have hitherto been created (Bosence et al., 1994; Hüssner et al., 2001). The model of Bosence et al. (1994) provides a numerical representation of the platform architecture, and consequently a stratigraphy-based interpretation of the episodic development of the facies as sea level fluctuates. Hüssner et al. (2001) used superimposed multiple synthetic sea level curves to simulate the platform development and internal geometry with a focus on achieving a close match with the outcrop data. However, both models did not address the impact of different carbonate biota on the evolution of the platform. The here presented study focuses on the role and impact of biotic carbonate production by creating a stratigraphic forward model constrained by published outcrop data (Pomar, 1991, 1993, 2020; Pomar and Ward, 1995; Pomar et al., 1996; Pomar and Haq, 2016) with a series of sensitivity analyses. The latter was used to investigate the possible platform responses that would result under varied conditions of carbonate production and accommodation. We herein present modelling-based evidence for the impact of differential carbonate production rates (with a focus on euphotic corals versus oligophotic rhodalgal sediment production) on platform geometries and how these interact spatially and temporally with changing accommodation space to define carbonate platform architecture.

THE MALLORCA CASE STUDY

Pomar et al. (1983) first described the upper Tortonian to lower Messinian Llucmajor reef complex in Mallorca (Figure 2.1a) as a reef-rimmed carbonate complex predominantly constructed by biogenic carbonate production (Pomar, 1991) and

strongly influenced by frame-building corals (Pomar et al., 1996). It overlies the lower Tortonian Heterostegina unit, which also outcrops in Menorca as a rhodalgal ramp known as the lower bar unit (Pomar et al., 1996; Morsilli and Pomar, 2012). This reef complex has been the subject of many studies, which were focused on its sedimentological and structural evolution and its sequence stratigraphic architecture (Esteban, 1979; Pomar, 1991, 1993; Qing Sun and Esteban, 1994; Pomar and Ward, 1995; Pomar et al., 1996, 2012a, 2017; Asprion et al., 2009; Sàbat et al., 2011b; Morsilli and Pomar, 2012; Pomar and Haq, 2016).
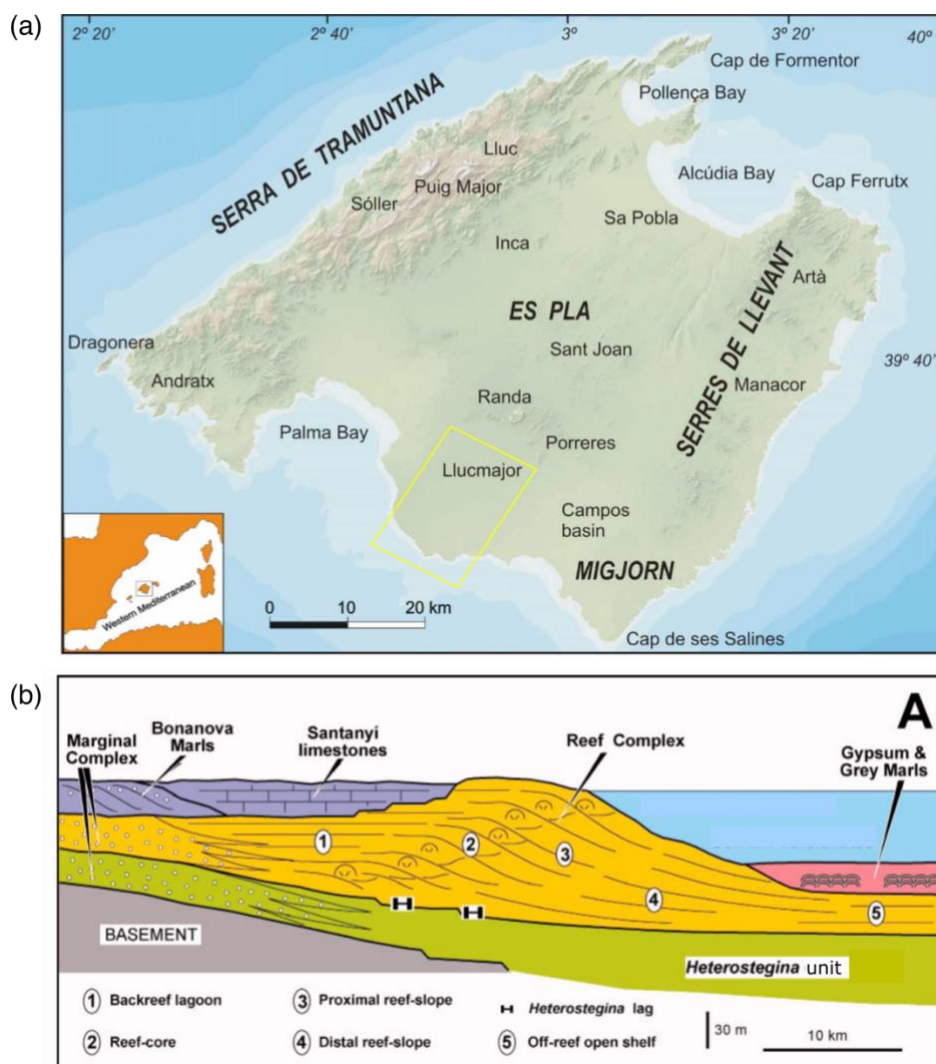
Figure 2.1: (a) Map of the Mallorca Island. The inset shows the island in relation to the other Balearic Islands of the Western Mediterranean. The yellow box is the model area of interest (modified from Ginés et al., 2012). (b) A cross-section illustrating the Upper Miocene, Pliocene and Pleistocene stratigraphic units of Mallorca Island, which is used as a reference for this model. Numbered units represent the depositional facies of the reef complex. Units 3 and 4 make up the forereef slope (modified from Pomar et al., 1996).

Pomar (1991) described in detail the facies architecture of the Llucmajor platform from proximal to distal setting (Figure 2.1b) as consisting of four main depositional facies; backreef lagoon, reef core, proximal and distal reef slopes which make up a forereef slope, and off-reef open shelf, arranged in basic building blocks referred to as sigmoids. A "sigmoid" is a sigmoid-shaped depositional unit comprising horizontal lagoonal beds transiting basinward into reef core facies, which in turn passes into a clinoformal reef-slope and a horizontal open-shelf bed (Pomar and Ward, 1994). The lateral and vertical superposition of sigmoids have been described as resulting from the highest frequency eustatic rise or highstand succeeded by a fall that produces an erosional truncation of the previously deposited units. These sea level variations that created the sigmoids correspond to the 7th order sea level variations of Haq et al. (1988) and 6th order sea level variations of Abreu and Haddad (1998). Thus, a sigmoid with most or all of it preserved from erosion will show the transitional co-occurrence of the four main depositional facies (Figure 2.2) of the reef complex (Pomar, 1991).The shallow water depositional facies, backreef lagoon and reef core facies, are mainly constituted of corals, red algae, mollusks, foraminifera, rhodoliths, bryozoans, etc. The deeper facies represented by the forereef slope and open shelf, are constituted of red algal biostromes, rhodoliths, mixed with reworked Halimeda and coral fragments, mollusks, planktonic foraminifera, deep water oyster (Pomar et al., 1996). Thus, the Llucmajor reef complex comprises euphotic, oligophotic and photo-independent biotic carbonate producers and production processes which interplay to generate its stratigraphic architecture (Figure 2.2).

An important characteristic of the reef complex is the euphotic coral morphological zonation of the reef-core depositional facies. The shallow-marine reef-building community of the reef-core comprises three depth-dependent, vertically-zoned coral forms with characteristic colonial morphologies (Pomar, 1991), all generating rigid frameworks (Pomar and Kendall, 2008a). A lower (relatively deeper water) zone of dish corals which commonly overlies the reef-slope, approximately 10 m thick, indicates the transition from the reef core facies to the slope facies, with a basal segment rich in Halimeda (Pomar et al., 1996). The corals in this zone are characteristically wavy plates that are up to 30 cm in diameter. Overlying the dish coral zone is the branching coral zone of intermediate water depths, with an irregular preservation and thickness varying from 2 to 7 m (Pomar, 1991). The shallowest zone

comprises the massive corals characterised by a high resilience to wave energy and highly photo-dependent.
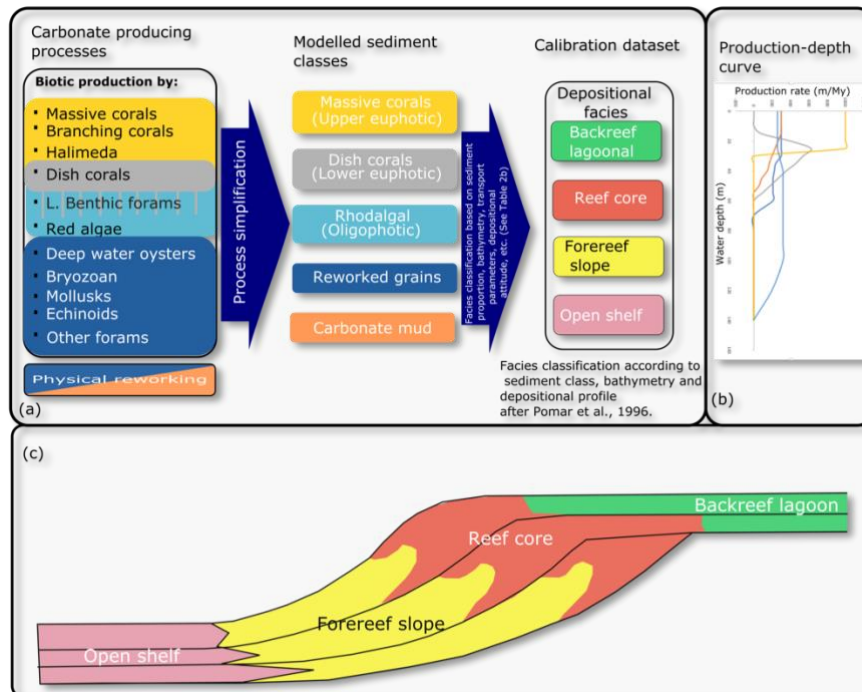
Figure 2.2: Overview of carbonate sediment production processes and their use in stratigraphic forward modelling: (a) a selection of processes involved in carbonate production and how they translate into modelled sediment classes and their relationship with the facies model; (b) the production–depth profile of the modelled sediment classes; and (c) cross-sectional sketch of ideal sigmoids showing the distribution of depositional facies (modified from Pomar, 2001a).

In the oligophotic setting where rhodalgal biotas thrive, sediments are produced as a base over which the corals grow intermittently trailing sea level oscillations (Pomar et al., 2012a). The rhodalgal biota, though also influenced by light penetration, are more productive during sea level lowstands when radiant energy has a higher competence to reach the basin floor (Pomar, 1993; Pomar et al., 2012a).

DATABASE AND METHODS

The data used for this study include published facies descriptions and geometries from outcrop sections and 70 water wells which penetrated the facies of the Llucmajor platform (Pomar and Ward, 1995). Studies on the growth and accumulation rates of Miocene carbonate platforms were also utilised for our constraining of the carbonate

production rates (Adey and Vassar, 1975; Bosscher and Schlager, 1993; Bosence et al., 1994; Montaggioni, 2005; Schlager, 2005; Pomar et al., 2012a). The model was developed using DIONISOS (a diffusion-oriented simulator) and a global sensitivity analysis was carried out using CougarFlow (Granjeon and Joseph, 1999; Gervais et al., 2016, 2018). The model parameterisation is summarised in Tables 2.1 and 2.2. The input parameters were constrained within documented ranges through experimental runs to obtain a best fit set of input parameters that produced a model consistent with observed outcrop and published data (Figure 2.3).
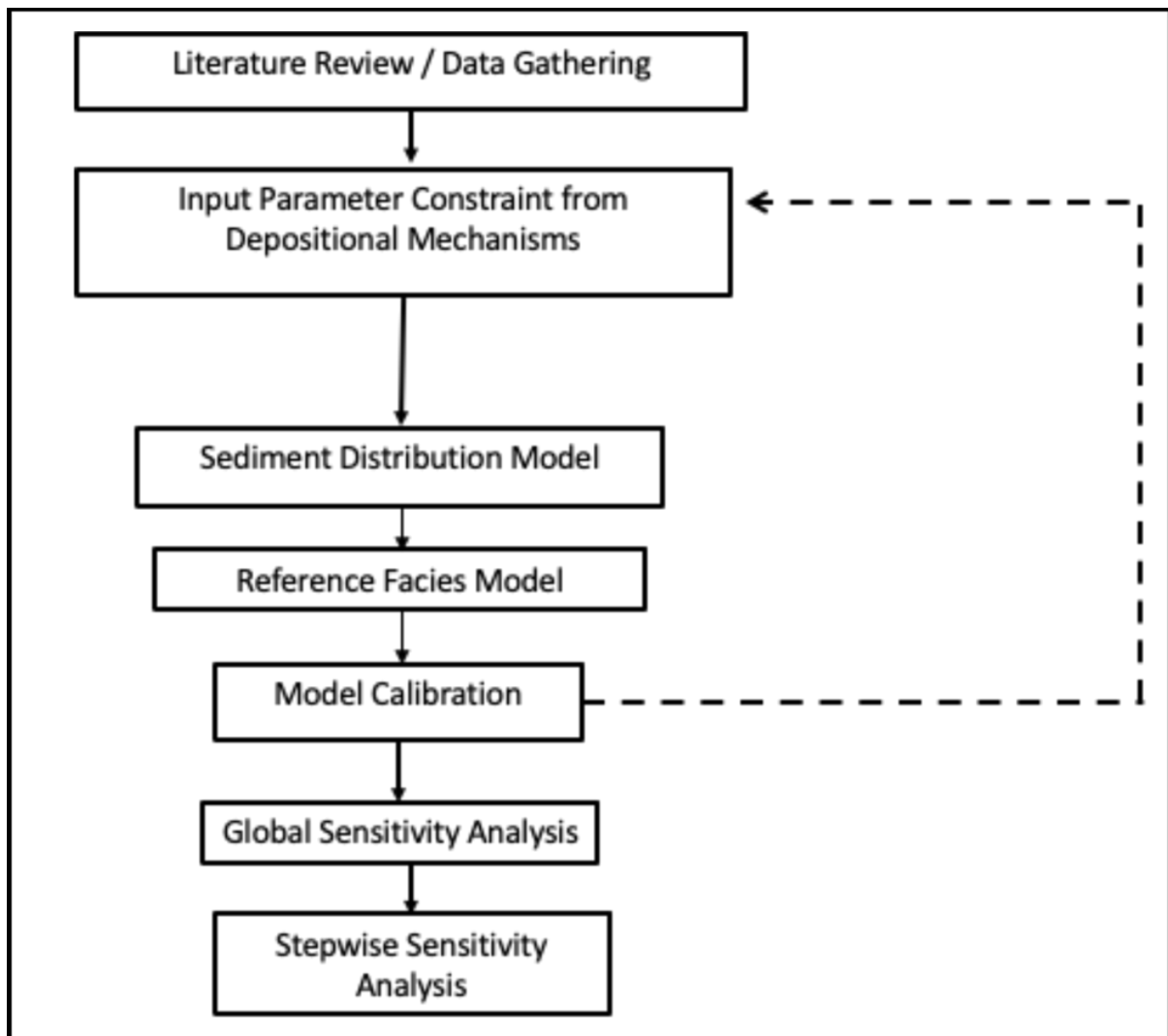
Figure 2.3: Summary of the modelling process

Table 2.1: Summary of modelling parameters

Parameters	Values
Model size	1444 km^2
Cell dimension	200 × 200 m
Number of cells	192 × 189
Total simulation time	2 myr
Time step	20 kyr
Subsidence rate	5 m Ma^{-1}
Wave base	20 m
Maximum wave energy flux	225 kW m^{-1}
Diffusion coefficient	Reworked grains 0.005 km^2 ka^{-1}; carbonate muds 0.05 km^2 ka^{-1}; dish corals 0.0005 km^2 ka^{-1}; massive corals 00001 km^2 ka^{-1}; rhodalgal 0.005 km^2 ka^{-1}

Table 2.2: Characteristics of the modelled sediment classes

Modelled sediment class	Maximum production rate (m Ma^{-1})	Wave energy flux (kW m^{-1})	Diffusion coefficient (km^2 a^{-1})	Transformation rates (m Ma^{-1})
Rhodalgal	400	≤20	0.005	50
Reworked grains	300		0.005	0
Carbonate mud	300	≤30	0.05	0
Dish corals	800		0.0005	100
Massive corals	1000	≥30	0.0001	100

Two kinds of sensitivity analyses were carried out on the model: a global sensitivity analysis in COUGAR which varies multiple parameters simultaneously and generates multiple simulations, as well as a stepwise sensitivity analysis that varies one parameter at a time in DIONISOS. In the global sensitivity analysis, multiple parameters were subjected to simultaneous sensitivity tests using the Latin hypercube sampling method (Gervais et al., 2016, 2018), with the aim of determining the most influential parameters on the model geometry and their respective contribution. This method of multi-parameter sensitivity analysis leverages on the development of response surfaces from small number of simulations depending on the number of uncertain parameters selected (Agrawal et al., 2015). To create a response surface model from which approximations of the modelled stratigraphy can be made, a total of 16 simulations and 4 confirmation runs were made based on four parameter sets: wave impact, eustasy, carbonate production and initial bathymetry. Parameters for the

set of simulations were constrained as follows: (1) the initial bathymetric map was varied between a range of +20 m depth (2) all other parameters such as carbonate production rates were varied within +20% of their reference values. These ranges were used to keep the simulation scenarios within a small window of variability that adequately provides an overview of the sensitivity of the model to parameter variation. Results from the global sensitivity analysis were used in selecting the parameters varied in the stepwise sensitivity analysis, in which a single parameter is varied multiple times to observe its effect on the platform geometry. In the stepwise sensitivity analyses, we aimed at investigating how maximum carbonate production rates and initial bathymetry impact the amount (length) of basinward progradation.

Development of the Reference Model

Duration and time resolution of the model

The evolution of the Llucmajor Platform from late Tortonian to early Messinian was modelled over an interval of 2 My (8.5 Ma to 6.5 Ma). With such a time consideration, the time resolution of the model becomes a key parameter. The modelling objective was to reproduce cosets of sigmoids which typically have periods of about 100 ky (Pomar and Ward, 1994; Pomar et al., 1996). In order to sample the sea level cycles multiple times and create higher resolution cycles such as sigmoids, a high time resolution of 20 ka was used after several trials with lower resolutions (50 ka, 100 ka, 200 ka), and higher resolutions (10 ka, 5 ka,1 ka). The time step of 20 ky was sufficient for the model development as it produces a representative geometry of the Llucmajor platform by creating an adequate number of sampling points along the sea level curve and allows for relatively short processing run-times for multiple runs during the sensitivity analyses.

Initial bathymetry and domain dimensions

The initial bathymetric map (Figure 2.4) for the model domain was reconstructed from the stratigraphic and sedimentological interpretation of 70 water wells presented by Pomar and Ward (1995). The surface encompasses a 38x38 km grid and a maximum elevation difference of 1200m. Previous studies have shown that subsidence in the Llucmajor area did not change significantly during the evolution of the carbonate

platform (Pomar, 1991; Watts and Torne, 1992; Ginés et al., 2012; Capó and Garcia, 2019) and we applied a constant subsidence of 5m/My rate for our model after testing several values of subsidence rates. Modelled properties are held in regular grid cells of 200x200 m, a dimension chosen based on the aim of the simulation to reproduce cosets of sigmoids which could typically be about 100 m in thickness (Pomar and Ward, 1994), and computing time considerations. The 200 m cells interact with the 20 ka timesteps to sufficiently sample the depositional cycles. By testing cell sizes of 100x100 m, 200x200 m and 300x300 m, we observed that a cell resolution of 200x200 m is sufficient to reproduce the desired model detail for the subsequent sensitivity analysis. A cell size of 100x100 m significantly increases computational time for each model run and would not have been feasible taking into account that we ran several hundred simulation runs in total.
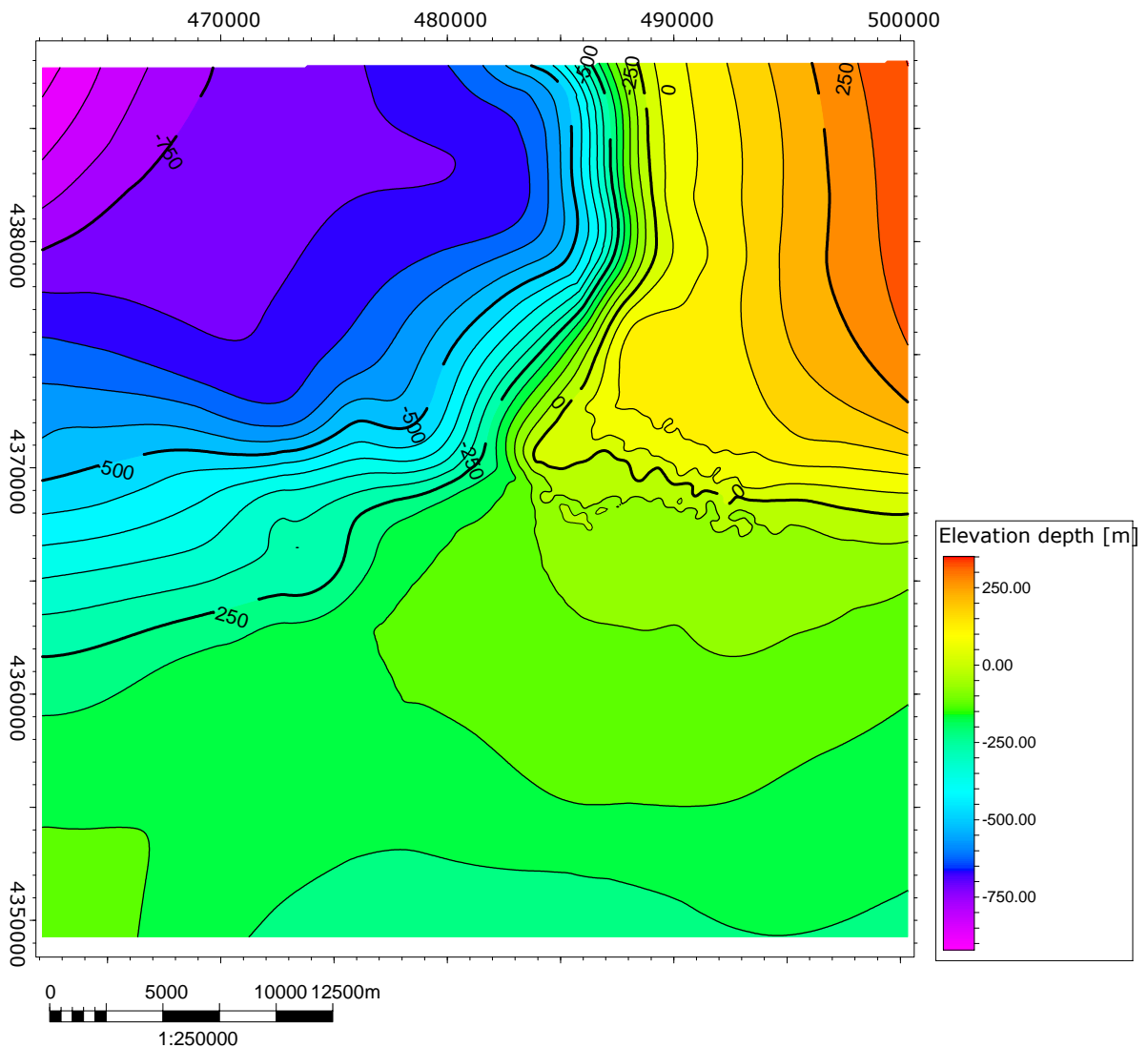
Figure 2.4: A map of the initial bathymetry used for the reference model (Pomar and Ward 1995).

Variation in accommodation space

The accommodation space in DIONISOS is modelled based on the interplay between eustatic sea level variations, subsidence, sediment accumulation, reworking and redistribution. The eustatic sea level curve used in this study is a composite curve (Figure 2.5) of four user-defined sinusoidal curves of varying periods, amplitudes and phases (Hüssner et al., 2001) constrained to the outcrop generated reef crest curve of Pomar and Ward (1995). This curve determines the time resolution of the model as the time-step for the model must be less than the period of the highest frequency curve. The composite curve has an amplitude of 25m and a period of 20 ky to capture the sigmoidal depositional units which approximately correspond to sets of sigmoids within the cosets (Pomar and Ward, 1995). Sets of sigmoids are stacks of basic sigmoidal units, reflecting sea level fluctuation of 20m to 30m amplitude and hundreds of meters of reef progradation (Pomar and Ward, 1999).

Carbonate production

Carbonate production (Figure 2.2) in our model is based on the biotic and reworked sediment components observed and interpreted from outcrops of the reef complex (Pomar et al., 1996). For our modelling purpose, we simplified these different biotic carbonate production and physical reworking processes into modelled sediment classes (Figure 2.2a), which were defined by water-depth and diffusivity or tendency of the sediments to be reworked by wave energy and/or gravity, expressed as diffusion coefficients. Diffusion coefficient (K) is measured in Dionisos by assuming that sediment flux (Qs) across a slope (S) is proportional to the slope, as given by the following equation (Granjeon and Joseph, 1999):

$$Qs = KS \hspace{4cm} (1)$$

Higher diffusion coefficients translate into higher tendency for the sediments to be moved by wave action above wave base, or gravity processes in the slope areas. The diffusion coefficients used in this model were selected after several experimental runs with different sets of diffusion coefficients. We defined five modelled sediment classes:

1) the massive corals: this is a simplified representation of the upper euphotic production from sea level to a maximum water depth of 30 m and a low diffusion coefficient of 0.0001 km^2/kyr (Figure 2.2b, Table 2.2). With production depth-curve developed from the model of Bosence et al. (1994), the massive corals were

constrained in the model to grow in highly agitated environments with a minimum wave energy flux of 30 kW/m. Wave agitation results in the erosion of some of the produced corals into grains and muds at a rate of 100 m/My (Table 2.2). The transformation rates used in this model were obtained from series of experimental runs in which several rates were tested.

	Period (Ma)	Amplitude (m)	Period (°)
Curve 1	0.4	15	0
Curve 2	0.1	15	40
Curve 3	0.023	5	10
Curve 4	0.08	5	2.5
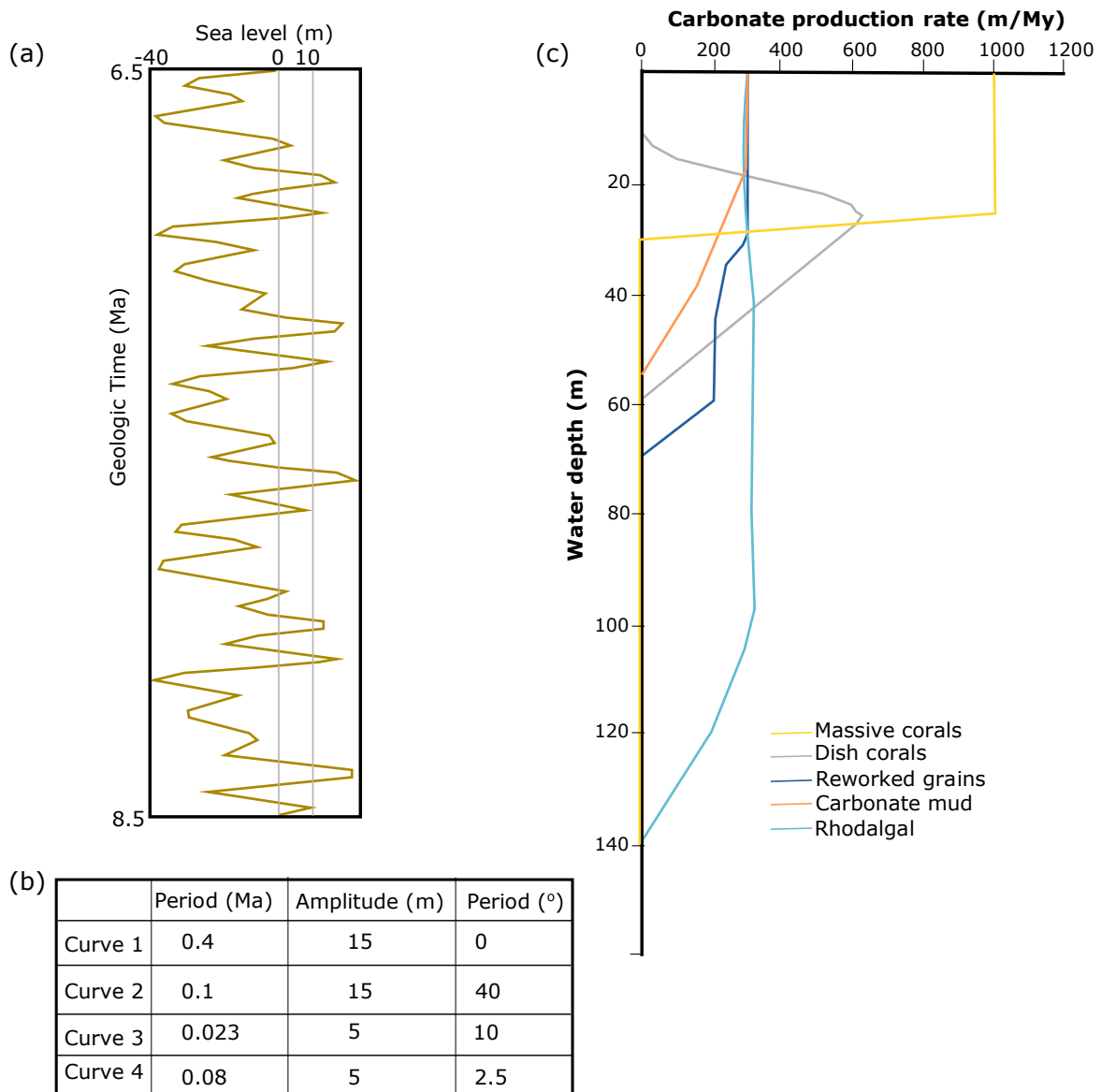
Figure 2.5: The input parameters for the model development: (a) the composite sea-level curve through the simulation time 8.5–6.5 Ma (Hüssner et al. 2001); (b) properties of the individual sinusoidal curves superposed to form the composite curve; and (c) the production-depth profile of carbonate production of each modelled sediment class.

2) the dish corals: this class represents the lower euphotic production restricted to between 10 m to 60 m of water depth (Figure 2.2b) and a diffusion coefficient of 0.0005 km^2/kyr (Table 2.2). The class is defined by a transformation rate of 100 m/Ma. Its production-depth curve was developed as a deeper extension of the massive corals.

3) the rhodalgal class: this class represents oligophotic production in the model. Production in the class reaches down to 140 m water depth (Figure 2.2b) and could be transported deeper with a diffusion coefficient of 0.005 km^2/kyr (Table 2.2). Development of the production-depth curve follows the method of Schlager (2003) who defined the production rate of cool water systems as a fraction of tropical systems. The modelled sediment class is defined by a transformation rate of 50 m/Ma and are produced only in quiet environments with a maximum wave energy flux of 20 kW/m.

4) the reworked grains: the class represents reworked sediments which are mostly produced from the physical reworking and redistribution of sediments of the massive coral, dish coral and rhodalgal classes. The class is defined by a relatively high diffusion coefficient of 0.005 km^2/kyr (Table 2.2) which by implication means that the sediment can be moved for a longer distance along the platform from their origin. This rate ensured that reworked grains increase towards the slope but decrease toward the open shelf. Grains classified as reworked grains have a grain size of about 1 mm.

5) carbonate muds: they also represent reworked and redistributed fragments of particles from the massive coral, dish corals and rhodalgal classes, but with grainsize of about 0.04 mm. They were defined in the model to be deposited in quiet environments with a maximum wave energy flux of 30 kW/m (Table 2.2) and are easily transported throughout the platform profile due to a high diffusion coefficient of 0.05 km^2/kyr despite their depth range of production (Figure 2.2b).

The production-depth profiles which set the bathymetric response of each modelled sediment class (Figure 2.5c) were inferred from the studies on the growth characteristics of corals and rhodalgals (Adey and Vassar, 1975; Davies and Hopley, 1983; Matsuda, 1989; Montaggioni, 2005; Hongo and Kayanne, 2011; Schäfer et al., 2011) as well as field observations on the Llucmajor Platform (Bosence et al., 1994; Pomar and Ward, 1995; Pomar et al., 1996, 2012a). The reworked grains and carbonate muds are disintegration products of primary sediments such as the massive

corals, dish corals and rhodalgal sediments. Their production rates therefore are essentially dependent on the erosion of these primary sediments, thereby leading to a reduction in bathymetry of the coral production rates below the "creation rates" for sand and mud in a cell.

Environmental constraints and sediment transport

To constrain the production of corals and the development of a backreef region of the platform, it was necessary to consider the influence of waves. Waves impact the platform geometry by eroding less rigid sedimentary particles from their production sites (Bourrouilh-Le Jan and Hottinger, 1988; Lüdmann et al., 2012; Betzler et al., 2013; Busson et al., 2019). This impact is however restricted to the wave base, assumed for this study as 20m (Table 2.1) based on the production depth of the massive corals.

The mobility of the produced sediment is a function of the competence of transport processes and the efficiency of down-slope sediment transport is quantified by the diffusion coefficient (Seard et al., 2013; Granjeon, 2014). Modelled sediment classes which are resistant to wave redistribution (e.g., massive corals and dish corals) are assigned low diffusion coefficients, while less-resistant classes are constrained by higher diffusion coefficients as numerically defined in Table 2.2.

Facies definition

On the Llucmajor platform, four main depositional facies have been identified on outcrop sections and well data with detailed description of their sedimentological and biofacies characteristics (Pomar and Ward, 1995; Pomar et al., 1996) which were parameterised for defining the facies of the reference model. The facies were defined by bathymetry, proportion of massive coral and rhodalgal components, wave energy and slope angle (Table 2.3, Figure 2.2a). The backreef lagoon represents shallow horizontal units with at least 20% mud proportion. The reef core facies represent shallow areas of the platform with a minimum of 50% massive and dish coral sediments. The forereef facies correspond to areas with maximum rhodalgal sediments restricted to water depths of 20m to 150m, while the open shelf facies represent the deeper domains with maximum rhodalgal sediments production and at least 7% carbonate muds and 16% reworked grains.

Table 2.3:Facies definition parameters

	Open shelf	Forereef slope	Reef core	Backreef lagoon
Bathymetry (m)	≥60	20–150	≤100	≤60
Corals % (massive + dish)			≥50	≤50
Reworked sediments (mud + grains) (%)	≤20	≥20		≥50
Rhodalgal (%)	≥70	≤70		
Slope (m km^{-1})			≥20	0 – 20
Wave energy flux (kW m^{-1})			≥30	≤30

The reference model was validated through a series of qualitative analysis of the convergence between geometry of the model and published outcrop data combined with evaluation of the facies distribution of the model platform and the outcrop. These tests were the basis for fine-tuning the input parameters to obtain a best-fit model that represents the observed geometries.

Published cross sections, maps and core logs from water wells in the study area (Pomar and Ward, 1995) served as reference to evaluate the quality of the model and were used to visually compare model pseudo-well logs to the corresponding water well data (Figure 2.6). Facies proportions and thickness distribution of the reference model could thus be qualitatively calibrated in detail across the platform. A systematic depth correction of the pseudo-wells for well-top matching between model results and published data was not performed due to the lack of an automated workflow in Dionisos. Manual depth correction of the model results is time and labour-intensive and impractical with respect to the amount of model runs needed for the sensitivity analysis. The model calibration was thus performed using the relative thicknesses of the published logs rather than the actual z-coordinates. This approach proved to suffice in developing the reference model.
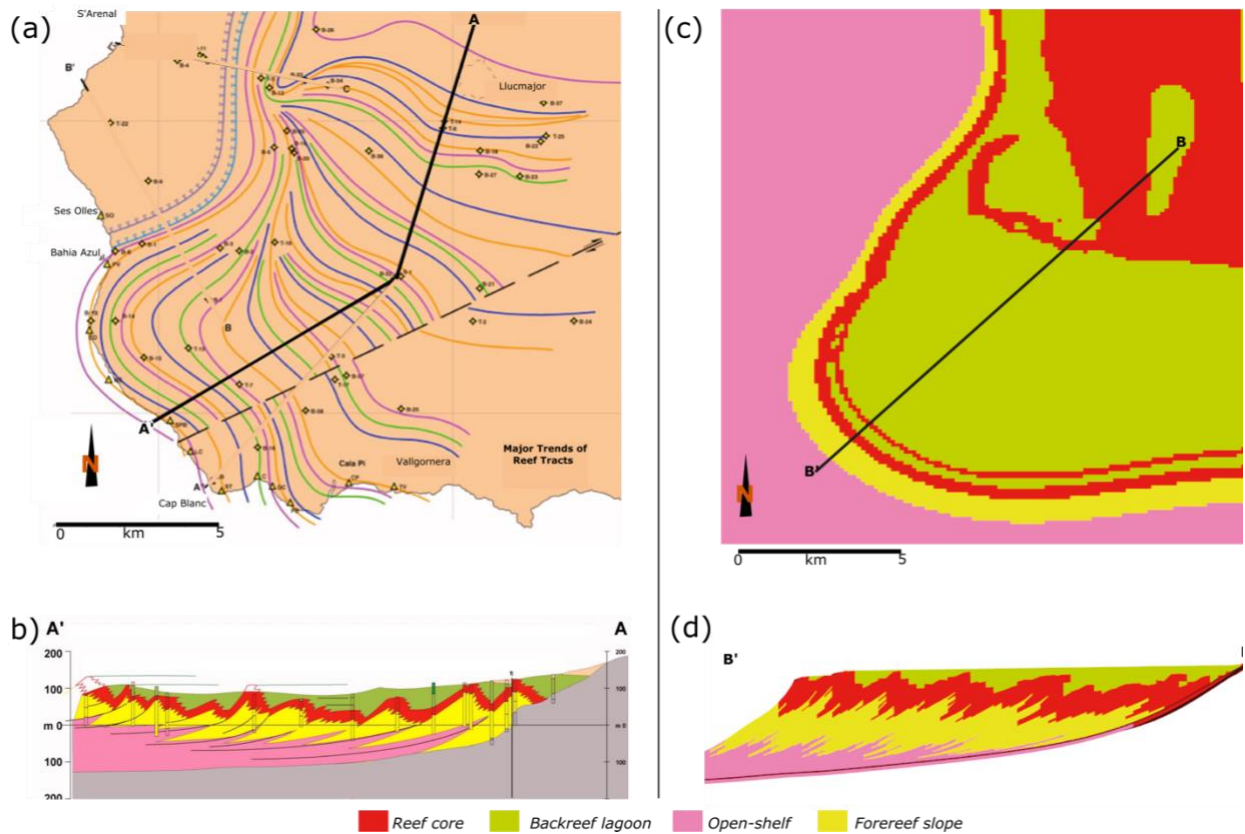
Figure 2.6: Comparison of the facies distribution and geometry of the model with the water-well-derived depositional model of Pomar et al. (1996): (a) the map of the reef tract trajectory as derived from water wells showing the line of section A–A′; (b) a cross-section running along line A-AI; (c) map view of the model platform showing the line of section B-BI; and (d) a section from the model along line B-BI.

RESULTS

Reference model: geometry and facies distribution

The reference model was qualitatively compared with outcrop description of the Llucmajor platform (Pomar, 1991). Figure 2.6 shows cross sections along the progradation direction of the forward model and the published outcrop/well model, giving a good match with the geometry and facies architecture of the platform. The model shows a basinward progradation of 20.6km in the southwestern direction, which compares well to the approximately 20 km measured progradation of the Llucmajor Platform (Pomar et al., 1996). The simulation responses to sea level variation compares well to observations made on outcrops and well data as shown in the juxtaposed cross sections from well data along line AA′ (Figures 2.6a and 2.6b) and along line BB′ from the model (Figures 2.6c and 2.6d).

The variation of accommodation through the simulation time created the development of cyclic accretion, progradation and erosion of the platform model leading to an overall basinward migration of the facies (Figure 2.7). This cyclic accretion and progradation of the platform are illustrated by the development of sigmoids consisting of the four facies representing a single time unit, or time-step (Figure 2.7a). Each sigmoid corresponds to a time unit of 20 Ky (the temporal resolution of the model) and shows the lateral distribution of facies from proximal backreef lagoon, reef core, forereef slope to distal open shelf. An exception are lowstand wedges, marked by the absence of backreef lagoon facies and which form during the initial phases of platform progradation (Figure 2.7b). Aggradation occurs as sigmoids build up in response to sea level rise (Figure 2.7c). The facies develop because of the interplay of sea level changes with the substrate for sedimentation, so that carbonate producers respond with shifts toward sites of favourable conditions. Figure 2.7d shows four main episodes of sea level flooding which led to the development of extensive backreef lagoons.

Distribution profile of the modelled carbonate sediment classes

Massive corals:

The massive corals in this model are the wave-resistant reef-builders which thrive in high-energy conditions. Their abundance ranges from about 30% in their deeper limits to about 100% production close to the sea level (Figure 2.8). Significant aggradation of the massive corals occurs at the platform margin during sea level rise which leads to the development of a backreef low energy region protected from the impact of waves. Thus, the model shows a high sensitivity of the massive corals to sea level variations, with reduced sedimentation rates of this factory in the backreef regions.

Dish corals:

The coral morphological zonation of the reef margin in the model imparts natural depth profiling to different reef-building corals. The growth of the dish corals is depth-restricted to a few meters immediately below the massive corals (Figure 2.8). This modelled sediment class directly overlies and interfingers with the underlying rhodalgal class. The dish corals production, like the massive corals, is significantly dependent on light penetration and occurs in the deepest part of the euphotic zone. This corroborates the moderately high (approximately 60 to 80%) abundance of the dish
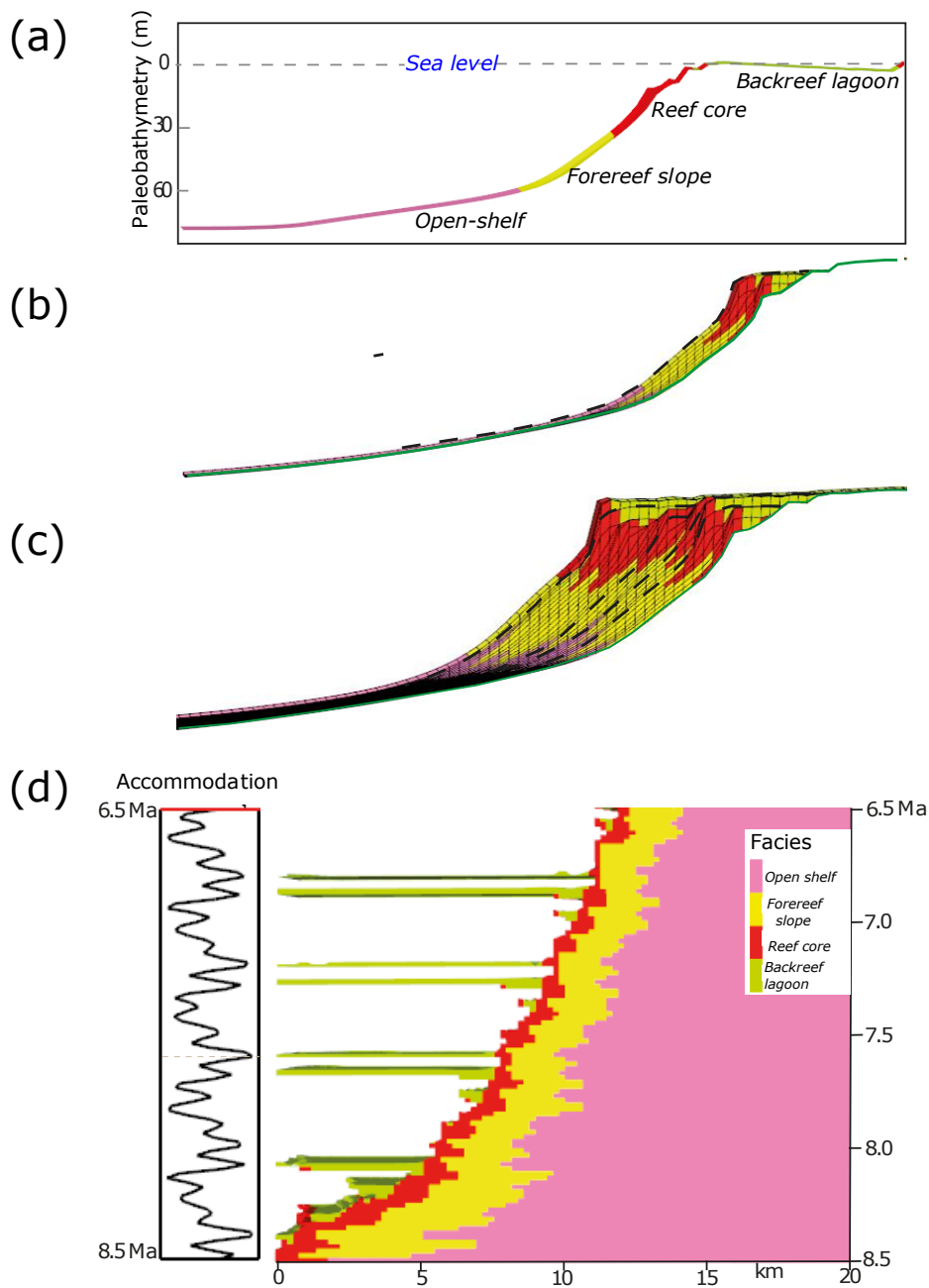
Figure 2.7: The sigmoidal building block of the model platform. (a) A single sigmoid illustrating the transition from proximal lagoon to reef, forereef slope and the distal open-shelf facies; (b) partially preserved sigmoidal units that form wedges of facies as the sea level falls and erosion takes place; (c) aggrading sigmoids formed subsequent to sea level rises; and (d) the temporal evolution of the basinward shift of facies over the simulation time and the extensive development of backreef lagoons during episodes of sea-level rise. Note that this is a series of time slices and does not represent facies proportions.
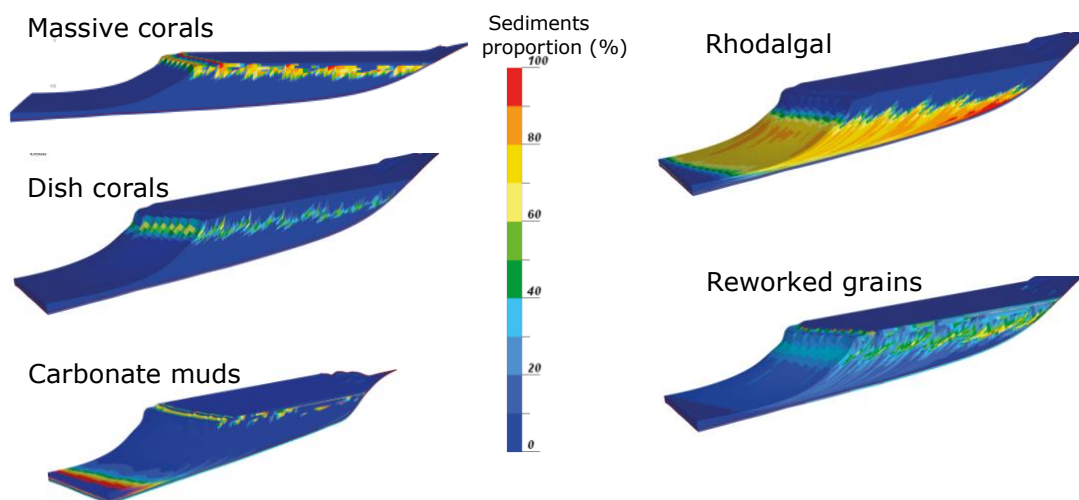
Figure 2.8: Distribution of deposits from the five modelled sediment classes.

corals in the platform as they are restricted to the deeper parts of the photic zone.

Rhodalgal:

Deposits of the rhodalgal class (Figure 2.8) are dominant in the deepest parts of the model grid and form the structure on which the platform progrades. The production is significant in the oligophotic zone (below 40 m) dominated by Heterostegina which thrive more under low light conditions and low wave energy (Hallock and Glenn, 1986; Pomar, 2001b). The class ability to extend to more distal sites during sea level fall, and accrete vertically during sea level rise, is an indication of its affinity for depths below wave impact with relatively low light penetration.

Reworked grains:

The model creates reworked grains which follow transport and distribution constraints imposed by high diffusion coefficients. Although the creation of the reworked grains was restricted to a maximum water depth of 70 meters, (Figures 2.4 and 2.7), the particles from this group are redistributed throughout the model bathymetric range due to their relatively high mobility.

Carbonate Muds:

Like the reworked grains, the presence and abundance of the carbonate muds is

linked to the reworking and redistribution of other modelled sediment classes into muds (Figure 2.8). However, their transport is characterised by high diffusion coefficients and deposited under low wave energy conditions such as in the backreef and deep open shelf environments which can be observed in the reference model (Figure 2.8).

Carbonate production and platform sequence stratigraphy

The facies-accommodation relationship is illustrated in the model through the development of progradation/aggradation patterns as sea level oscillates. This relationship produced stratigraphic sequences, each further subclassified into systems tracts (Pomar and Ward, 1999) identified by the stacking pattern of the sigmoidal units, the nature of the surfaces bounding them and the growth direction of the reef core facies (Figure 2.9). The initiation of the platform, starting from 8.5 Ma to 8.38 Ma, was during an episode of relative sea level fall with the development of laterally extensive open shelf and forereef/slope facies, and limited reef core facies (Figure 2.9a). Extensive lowstand systems tracts (from 8.38 Ma to 8.12 Ma) form between lowest sea levels and the onset of sea level rise (Figure 2.9b). During this time, there is a lateral proliferation of corals over earlier formed rhodalgal deposits, leading to the development and progradation of reef cores and the absence of or very restricted development of the backreef lagoon. The upper boundary of this lowstand systems tract (black dashed line in Figure 2.9b) is a sub-horizontal to gently undulating surface which truncates the wedged sigmoids beneath it and dips towards the basin. During rising sea level from 8.12 Ma to 8.04 Ma, an aggradational systems tract develops with characteristic vertical growth of the reef core deposits, the development of a significant backreef lagoon and fully preserved sigmoids with the presence of all four facies (Figure 2.9c). The upper boundary surface forms at the end of flooding of the backreef lagoon when vertical reef growth ceases (white dashed line in Figure 2.9c). At the highest point of each sea level cycle when vertical reef growth is at its maximum, a highstand systems tract develops with a basinward progradation of thin reefs that are mostly attached to the basin-facing wall of the reefs of the previous aggrading systems tracts. At this point (from 8.04 Ma to 7.96 Ma), the backreef lagoon is filled and consequently, reef growth shifts basinward (Figure 2.9d). Offlapping systems tracts form during falling sea levels with extensive basinward progradation of thinned reefs. Here, the facies grow laterally rather than vertically. There is also no development of

backreefs in this tract (Figure 2.9e) and amount of basinward progradation is dependent on the rate of sea level fall.
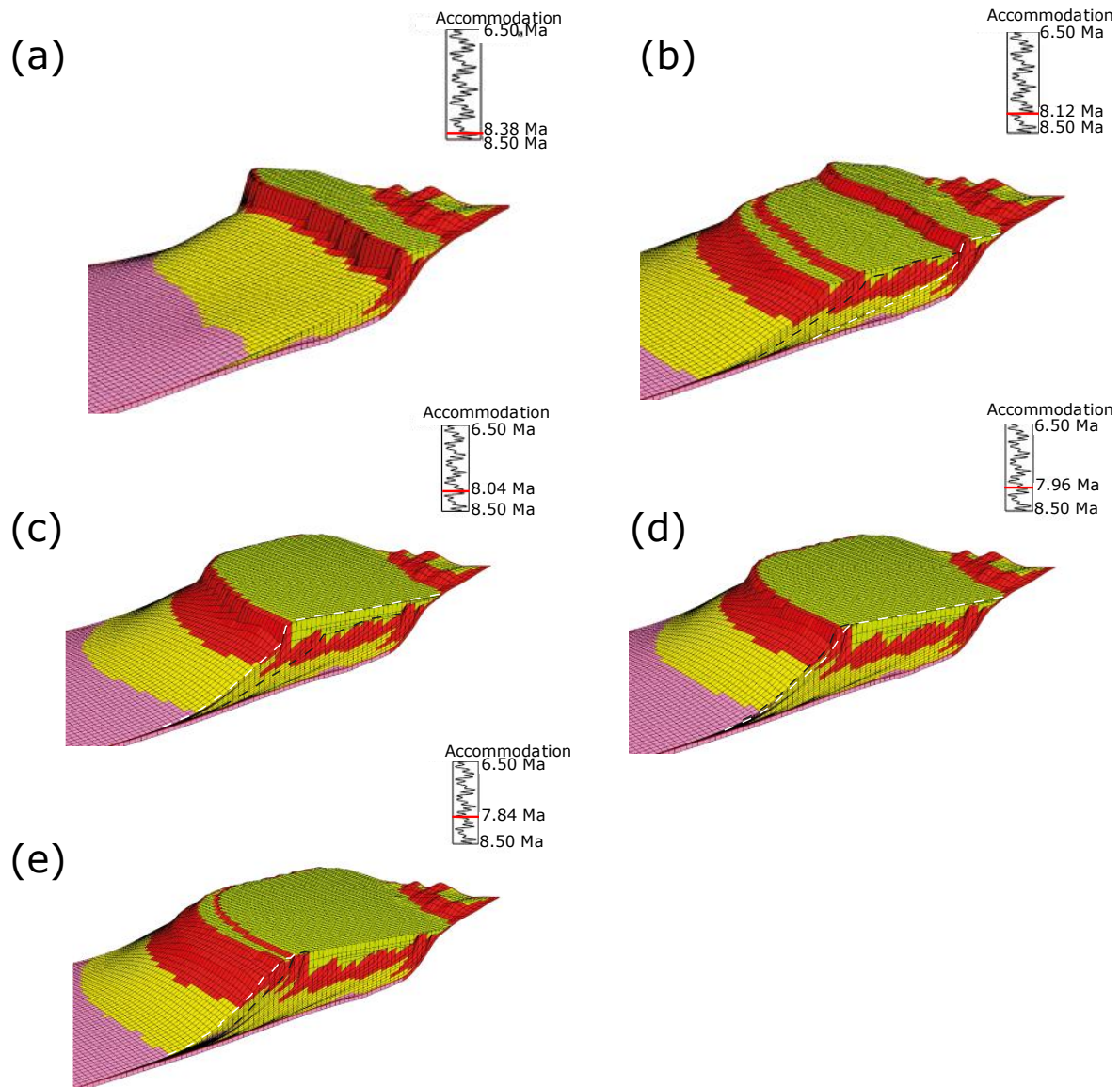
Figure 2.9: The development of systems tracts and key stratigraphic surfaces according to the model: (a) the initiation of the model platform; (b) a lowstand systems tract; (c) an aggrading systems tract; (d) a highstand systems tract; and (e) an offlapping system tract

Global Sensitivity Analysis

The aim of the global sensitivity analysis was to assess the effect of each of the input parameters on the resulting platform geometry and rank the influence of each parameter. All input parameters relating to accommodation, carbonate production, transport and oceanic conditions were subjected to the global sensitivity analysis to

allow for the multi-simulation process independently determine the influence of these parameters. The result of the sensitivity test is restricted to only parameters with at least 1% contribution to the variation of the mean thickness within a defined zone of interest in the platform model. This zone of interest (Figure 2.10a) was selected based on the presence of all four depositional facies in a vertical stacking at a point which represents the latest stages of platform progradation in the model, such that thickness variation of the zone in different scenarios of parameter variation is sufficiently captured in the sensitivity analysis. Carbonate production variation with depth has the highest percentage contribution to the variation of the platform geometry followed by initial bathymetry, maximum carbonate production rate and wave base at the initiation of the model (Figure 2.10b). Lower depths (shallowing) in the initial bathymetry led to progressively thinner models (Figures 2.9c). An opposite response is observed for deepening bathymetries. This observation is explained by the depth dependence of the carbonate production whose rate and subsequent accumulation are favoured in depth-zones with good light penetration. Increasing the carbonate production depth profile for each modelled sediment class increases the production interval within the model domain as the sediment production is able to catch up with increasing accommodation. Increasing the carbonate production rate increases the mean total thickness of the platform in the model.

A total of 16 simultaneous simulations (Figure 2.10d) were run with the parameters varied within the defined range and the response of each simulation with respect to the mean thickness at the zone of interest (Figure 2.10a) was plotted as bars (Figure 2.10e). Nine of these simulations have responses that are close to the mean thickness value as the simulator maintained a balance in the individual variation of the parameters. For example, simulation 6 with a shallow bathymetric variation factor of 0.57 (Figure 2.10c and 2.9d) is balanced by a carbonate production depth reduced to a variation factor of 0.14 and combined with the reference production rate constrained by a deepened wave base (22.9 m). However, simulations 10 to 16 reflect responses produced by biases towards specific parameters being varied. Simulation 16, for example, is biased towards carbonate production rate and wave base while keeping the reference values of bathymetry and carbonate production depths. The maximum variation factor of the production rate was combined with a reduced wave base of 16 m. From these observations, carbonate production and bathymetry were determined

as the parameters to be tested for their individual influence and how they affect the platform geometry.

(a)

(b)

(c)

(d)

Simulation	Bathymetry at 8.5 ...	CarbProd_Depth	CarbProd_Time	Wave 1.waveBa...
1	0.429	0.571	0.857	18.857
2	0.143	-0.714	-1.000	19.429
3	0.714	-0.286	-0.143	18.286
4	-0.571	-1.000	0.286	22.857
5	-0.143	0.143	0.571	17.143
6	0.571	-0.143	0.000	22.286
7	0.286	1.000	-0.714	20.000
8	-1.000	0.286	-0.429	16.000
9	0.857	0.429	-0.571	21.714
10	1.000	-0.429	-0.857	21.143
11	-0.429	0.000	0.143	20.571
12	-0.857	-0.857	0.429	17.714
13	-0.286	0.857	1.000	16.571
14	-0.714	0.714	-0.286	24.000
15	0.000	-0.571	0.714	23.429
16	0.000	0.000	1.000	16.000

(e)

Figure 2.10: Results of the global sensitivity analysis: (a) a map showing the position of the zone of interest in which the global sensitivity analysis was performed; (b) the most impactful parameters with an effect contribution of more than 1%; (c) the range of variations of the impactful parameters v. mean total thickness; (d) the simultaneous variations of the parameters used in the simulations; and (e) thickness variations for 16 models with parameter variations described in (d).

Stepwise Sensitivity analysis

Bathymetry and progradation

The most prominent response of the platform to changes in bathymetry is the amount of basinward progradation in the SSW direction (Figure 2.11a). Several initial bathymetries were tested to observe the response of the model in relation to lateral and vertical sediment production. Bulk shifting the initial bathymetry map step-wisely between 50 m shallower and 50 m deeper reveals that deeper initial bathymetries produce less basinward progradation compared to shallower initial bathymetries (Figure 2.11b). The interdependence between initial bathymetry and rate of progradation follows a linear trend which slightly increases the rate of progradation until a threshold of 30m shallower bathymetry (relative to the reference model) is reached. Beyond this point, progradation increases significantly and eventually exceeds the model boundary.

Carbonate production rate and platform progradation

In order to test the sensitivity of the model to changing carbonate production, all other parameters were kept at their reference values, while the carbonate production rates for the five modelled sediment classes were varied by a uniform factor of the carbonate production rate in the reference model. The responses of the platform model to the changes in carbonate production is in the platform geometry and basinward progradation (Figure 2.12a). Compared to the reference model, halving the carbonate production rate for all the modelled sediment classes resulted in less basinward progradation and reduces the margin steepness, while doubling these rates produces more basinward progradation with steeper margin slopes than the reference model. This response of the model was consistent over a range of carbonate production rates as illustrated in Figure 2.12b which was plotted by measuring the amount of progradation along the eastern edge of the domain compared with the reference model. Since the rate of accommodation change remains constant for all the model, increasing the carbonate production rates for all five classes produces a basinward progradation that allows for the continued production of the sediments, shifting the production and accumulation loci basinward as available accommodation is used up.
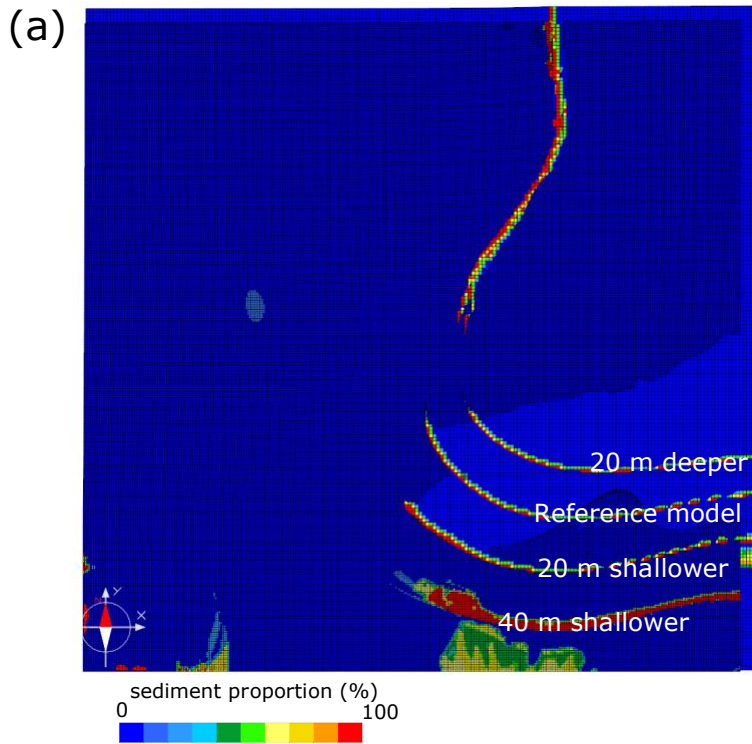
Figure 2.11: Impact of initial bathymetry on platform progradation: (a) plan view of multiple superposed models of different initial bathymetries showing the extent of basinward progradation of each model relative to the reference model; and (b) a plot of progradation v. bathymetric change relative to the reference model.

(a)

- – – Reference model   – – – Production rate twice the reference rate
- – – Production rate half the reference model

(b)

Effect of variation in carbonate production on progradation
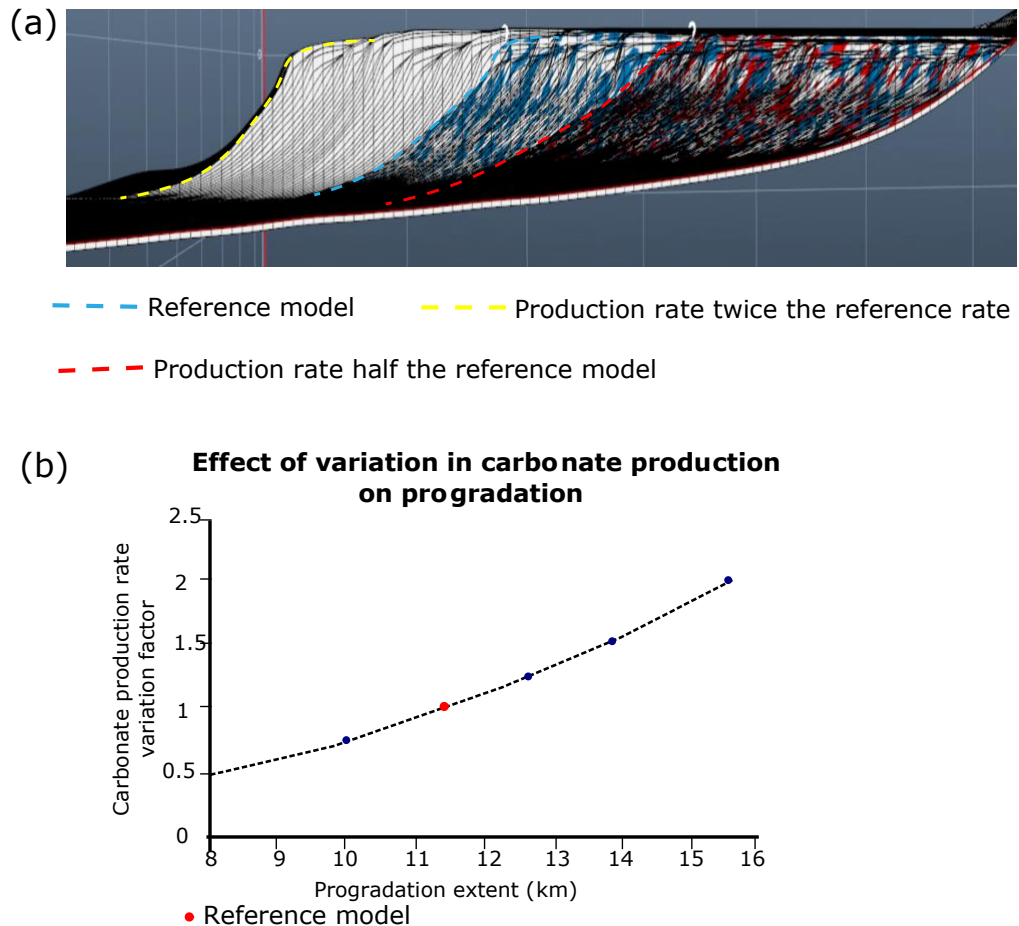
● Reference model

Figure 2.12: Impact of carbonate production on platform geometry: (a) three models, including the reference model, display different amounts of progradation and platform slope resulting from differential carbonate production rates; and (b) a plot of the progradation

Erosion and platform geometry

The rate of platform accretion is influenced, not only by the amount of carbonate sediment supplied but also by sediment erosion and redistribution. To examine if erosion of a highly productive euphotic coral system devoid of rhodalgal production could produce the required substrate volume for the platform to prograde upon, we tested multiple scenarios of changing wave bases (as a proxy for wave energy flux) and diffusion coefficients (as a proxy for frame rigidity). Figure 2.13 presents the reference model (panel I) and six experiments (panels II to IV) to compare effects of differential erosion on the platform geometry, specifically the extent of progradation and the slope steepness. Panel IIa is a model developed by reducing the wave base of the reference model to 5 m, resulting in faster progradation as the rhodalgal sediments quickly fill up the accommodation space due to lower wave agitation in the

euphotic zone. This also led to a significant reduction in coral production arising from a shallowing of the wave energy propagation depth thereby increasing rhodalgal production in shallower environments, which consequently increased the substrate volume for platform progradation. In contrast, panel IIb shows a model with a much deeper wave base of 40 m which resulted in reduced platform progradation, as coral production is now restricted to the shallowest areas. This is consequent to deepening wave energy propagation thereby unsettling the conditions necessary for rhodalgal production. As the rhodalgal sediments are unable to sufficiently accumulate vertically, the water column becomes too deep for coral production, leading to restricted marginal coral growth. The models in panels IIIa and IIIb examine responses to varied rigidity of the sediments produced. In panel IIIa, the diffusion coefficients of all the sediment classes were reduced by two orders of magnitude to increase the rigidity of the sediments. This did not change the model geometry significantly compared with the reference model (panel I). On the other hand, panel IIIb is a model with diffusion coefficients increased by two orders of magnitude as the reference model, thereby increasing the ease of sediment redistribution by wave, gravity, and water current which consequently resulted in very rapid platform progradation. The responses of panels IIIa and IIIb are due to the impact of looseness or rigidity of the sediments. Loose sediments are more susceptible to transport by waves and currents and are unstable under gravity. This process of reworking redistributes sediments into deeper sections, thereby creating substrates for more corals to prograde upon. In reality, however, this could lead to an unstable platform incapable of building rigid frameworks necessary for rim construction such as in the Llucmajor platform as the coral sediments are washed basinward as soon as they are produced. In the absence of rhodalgal production, doubling the maximum production rates of the corals and reworked sediments (panel IVa) resulted in reduced platform progradation accompanied by steepened slopes. In addition to the previous two sets of models testing the likely effect of erosion and sediment redistribution, we also examined the impact of the interplay of erosion of coral sediments by doubling the coral and reworked sediment production rates with no rhodalgal production, but with diffusion coefficients of the sediment classes increased by two orders of magnitude from the reference values (panel IVb). This led to increased platform progradation with coral sediments redeposited on steep slopes. These models indicate that the rate of
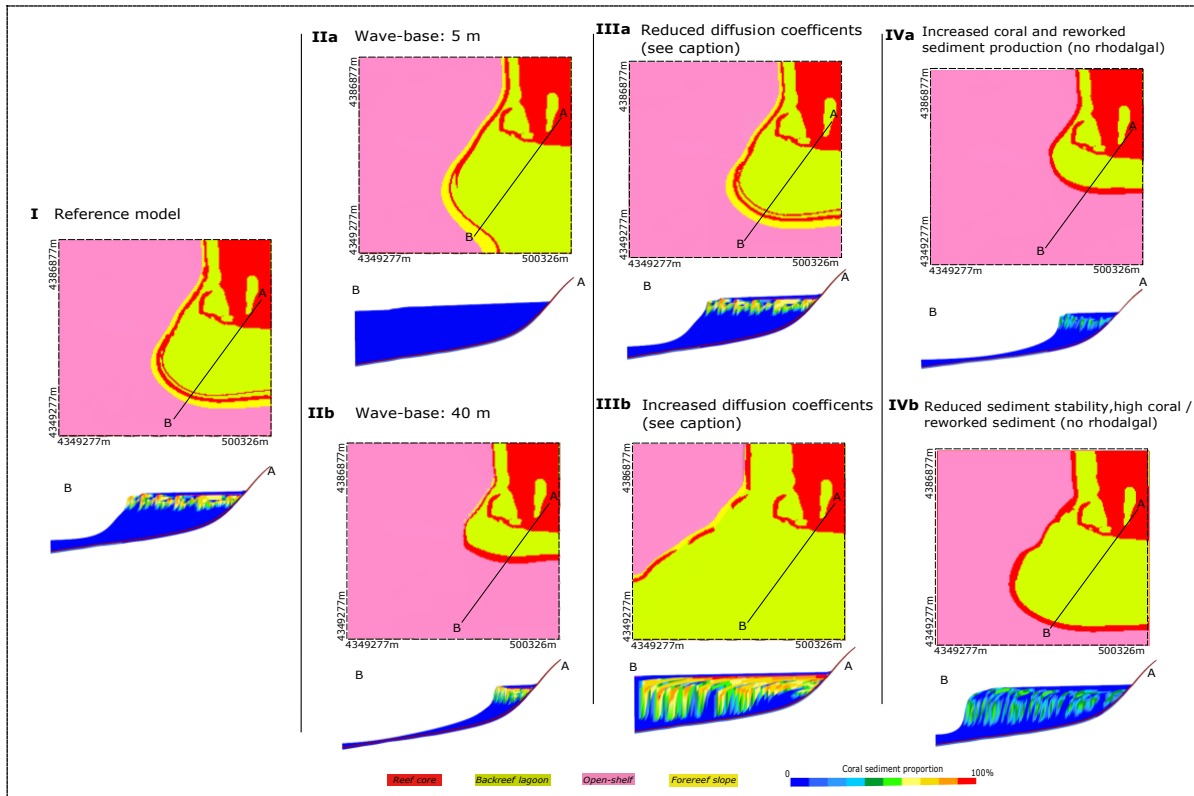
Figure 2.13: Testing how the erosion of sediments impacts platform progradation. (I) Reference model, (IIa) modelled with a wave base of 5 m, (IIb) modelled with a wave base of 40 m, (IIIa) modelled with diffusion coefficients lower than the reference values by two orders of magnitude, (IIIb) modelled with diffusion coefficients higher than reference values by two orders of magnitude, (IVa) reference parameters without rhodalgal production but doubled maximum production rates for corals and reworked sediments, (IVb) parameters the same as in IVb but with diffusion coefficients increased by two orders of magnitude above the reference values.

progradation would be impacted by erosional processes and framework stability. However, comparing these models with the reference model (panel I) reveals that a Llucmajor-type geometry requires a balanced interplay of euphotic and rhodalgal production. Models in which platform progradation was initiated through reduced wave base (panel IIa) or increased sediment redistribution (panel IIIb) are characterised by steeper slopes than the reference model (panel I), with coral production either too low (panel IIa) or too high (panel IIIb).

Oligophotic versus euphotic production.

Models of differential maximum production rates of one modelled sediment class against the other modelled sediment classes were compared with the reference model (Figure 2.14). The responses of the geometry to such changes were distinguishable

in the shapes, sizes and progradation extent of the models. Decreasing the massive coral production rates (Figure 2.14) by half of the reference rates did not create a significant change in the size and shape of the platform. Doubling the massive coral production rates alone without increasing the rhodalgal rates also caused no significant change in the platform size, shape or progradation. On the other hand, reducing the production rate of the rhodalgal class independently by half the reference value, caused a decrease in the platform size by causing a progradation that is less than the reference model. The resulting platform was also less steep than the reference model. However, doubling the rhodalgal production rates increased the basinward progradation of the platform by about 20% of the reference model but with less steep margins.

Changing the maximum production rates of the rhodalgal class independently in the absence of the massive corals also impacted the geometry of the model (Figure 2.14). These models without the euphotic corals, built no distinct slope breaks like in the reference model but rather displayed gently dipping ramp geometries. The size and shape of these models vary with the rates of rhodalgal production. Reducing the rhodalgal rate by half the reference value maintained the extent of progradation as in the reference model.

Independently varying the production rate of the massive corals in the absence of the rhodalgal significantly changed the geometry of the platform (Figure 2.14). The results show that in the absence of rhodalgal production, coral growth will be restricted to the shallowest photic zone with minimal progradation. Although the models without the oligophotic biota did not prograde much, they have very steep margins.

Sea level curves and model development

To determine the impact of sea level curves used in the model, two of the sea level curves tested are presented in the Figure 2.14. The model developed with the global sea level curve (Haq et al., 1988) shows consistent platform progradation with the development of a very limited backreef lagoon from the initiation to 7.58 Ma followed by the gradual erosion of the formed backreef lagoon with continued progradation. By 7.08 Ma of the simulation when the sea level falls sharply, intense erosion of the earlier formed platform dominated the system till 6.74 Ma, after which there was a widespread

development of flat-lying sediments. The overall model does now well reproduce observed geometry of the Llucmajor platform.

Results applying the Miller et al. (2005) curve showed some similarities with the reference model in its overall geometry but the relationship between the reef core areas and the backreef lagoon development does not fully reproduce the observed geometry of the platform. The reference model was developed with a synthetic curve which represents reef crest curves measured directly from the outcrops of the Llucmajor (Pomar and Ward, 1995; Hüssner et al., 2001).
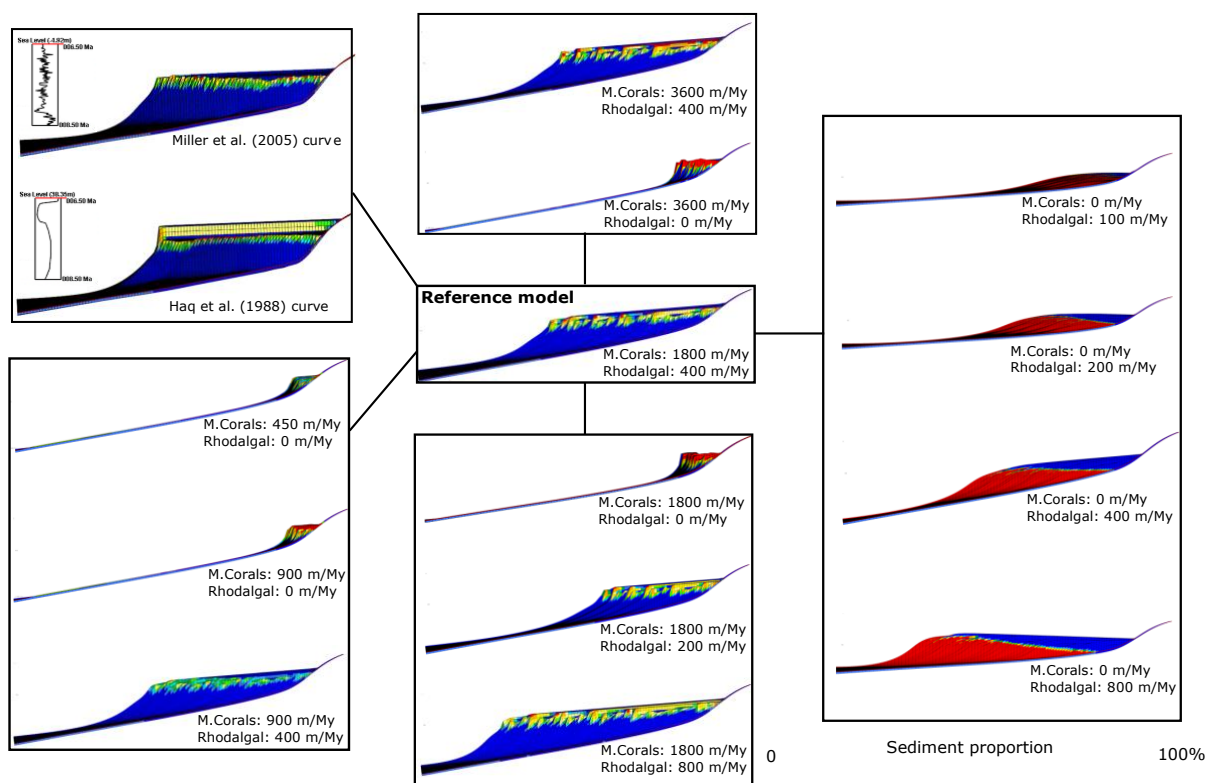
Figure 2.14: Sensitivity of the model to differential production rates for the rhodalgal and massive coral deposits. The legend illustrates the sediment proportion in each model. . Models to the right of the reference model display the proportion of rhodalgal sediments. All other models (including the reference model) display the proportion of massive corals (M.Corals).

DISCUSSION

Based on the global sensitivity analysis, the most influential parameters were determined from a modelling perspective to be the carbonate production parameters (depth profile and maximum production rate) and the position of the initial bathymetry

which determines the amount of accommodation space available at the initiation of the platform. The latter determines the available accommodation space at the onset of platform evolution and interlinks with the carbonate production depth profile, thus constraining production efficiency of the modelled sediment classes spatially. The superimposed sea level fluctuations during simulation have consequent significant impact on the available platform area on which carbonate production can be initiated. The stepwise sensitivity analysis provided detailed information about how the modelled sediment classes interact in the available accommodation space and how these factors influence the Llucmajor platform geometry.

Sensitivity of carbonate production to variation in accommodation

The results of the variation of the initial bathymetry in the models represent platform responses to the amount of accommodation space at the initiation of the platform through variation in the efficiency of the different modelled sediment classes to produce sediments. We found a threshold of accommodation (30 m shallower than the reference model) above and below which there is a change in the sensitivity of the classes to subsequent fluctuation in sea level (Figure 2.11). Carbonate production becomes increasingly sensitive to sea level fluctuation for shallower initial bathymetry as it becomes easier to flood the shallow platform during sea level rise and rapidly shed excess sediments into the deeper basin (Figure 2.11). Since the depth to the basin floor is shallow, there is increased light penetration which in turn increases the area over which the oligophotic sediment production can occur (Jones and Desrochers, 1992; Handford and Loucks, 1993; Pomar, 2001b; Warrlich et al., 2002; Sarkar, 2017), thus increasing the progradation of the platform (Figure 2.11). This implies that for the platform to prograde, sediment needs to be produced at greater depths than where the corals thrive in order to provide the shallow substrates necessary for coral growth. These deeper sediments can be significantly supplied by the rhodalgal biota. This is consistent with observations from outcrop studies of the Llucmajor platform where westward progradation towards the Palma basin is largely limited by the deep and steep bathymetric gradients of the area, whereas there is extensive southward progradation due to the shallowness and low bathymetric gradients in the southern area (Pomar and Ward, 1995; Pomar, 2020). The carbonate production in the eastern section is very efficient due to the shallowness of the area and can shift the platform south-westward as sea level varies (Figure 2.10).

Carbonate production rate and platform progradation

The results of 16 simulations with uniform variation of the overall carbonate production rates for each modelled sediment class show that although accommodation and carbonate production rates are important controls on platform geometry, the variation of the production rates of the classes with depth must be adequately understood for improved geological plausibility of carbonate platform models (Figure 2.9). The production-depth profile of each modelled sediment class determines how much sediment is produced at a given depth (Figure 2.4c). This variation interacts with the accommodation space which determines the depth of the water column. When the accommodation is too high, the depth production window of each modelled sediment class will not be attained, thus resulting in a sediment-starved system. Lower accommodation space as observed in Figure 2.10 provides the optimal depth window for maximum production of carbonate sediments. This explains why the shallow models prograded more than the deeper models as there is a coeval occurrence of the maximum production for all the modelled sediment classes. In addition to proving numerically that carbonate production rates (Figure 2.12) have strong controls on platform development (Jones and Desrochers, 1992; Pomar, 2001b, 2001a; Williams et al., 2011; Seard et al., 2013; Li et al., 2020), our multiple simulations (Figure 2.10) show that the variation of carbonate production rates with depth for each factory intensely influence the interaction between biota and accommodation to produce sediments and modify the platform geometry.

Increasing production rates affect the progradation of the platform by rapidly filling the available accommodation space (Figure 2.12). Thus, accommodation is a strong limiting factor that determines how carbonate particles and facies are distributed within the basin. Systems with low rates of accommodation creation but high carbonate production will result in more progradation compared to higher accommodation (subsidence and/or eustatic sea level rise) systems. Comparing models with the same initial bathymetry (same accommodation variation) but with different carbonate production rates show that increased carbonate production rate increases progradation without any intense change in the aggradation. This suggests that increased supply of carbonate sediments increases the basinward shift in facies while vertical growth of the platform is a function of accommodation change (Schlager, 1993; Schlager et al., 1994). This numerically supports the field interpretation of the

Llucmajor platform being a supply-dominated platform characterised by extensive progradation resulting from rapid filling of the shallow accommodation (Pomar and Haq, 2016). This, again, emphasises the need for understanding the impact of sediment input in modelling carbonate systems in exploration activities.

The role of euphotic (corals) and oligophotic (rhodalgal) biota in platform evolution

The impact of carbonate production on platform progradation is due to the capacity of oligophotic rhodalgal sediments to build out into the basin (Figure 2.14). Therefore, higher oligophotic production rates allow the platform to prograde more than lower rates of oligophotic production. In fact, coral sediment production does not make a significant contribution to the progradation. Pomar et al. (1996, 2012a) have hypothesized based on field observations that in the Llucmajor platform progradation is enhanced by the significant development of the oligophotic factory during sea level lowstands. Our modelling results confirm this hypothesis (Figure 2.14).

The sensitivity analysis of the impact of the rhodalgal production rate on the platform geometry revealed a range of possible platform types (Figure 2.14). The model response to the absence of rhodalgal production was a platform with coral growth restricted to the coastline, forming fringing reefs and very minimal platform progradation as there is little shallow substratum for coral growth, thus, limiting platform development to the shallow fringes of the shelf instead of the barrier rimmed shelf that characterizes the reference model. Our model also suggests that the reason for these restricted reefs is the abrupt transition of water depth from shallow to deep due to the absence of oligophotic deposits on which the reefs could have prograded. This affirms that the production rate of the rhodalgal sediments, which can grow at relatively greater depths, is key in platform development, progradation and geometry (Figure 2.14). This is a numerical proof of concept on the impact of carbonate sediment type on the geometry of Mediterranean platforms (Pomar et al., 2012a).

The production rate of the rhodalgal sediments, although very significant in the generation of the Llucmajor platform geometry, needs a proportionate interaction with shallow water corals to generate such a geometry. Turning off the coral modelled sediment classes, such that only the rhodalgals are produced, resulted in a geometry that is better described as a distally steepened ramp geometry (Figure 2.14). As the production rate of both the rhodalgal and the corals are varied between these two end-

members, a spectrum of possible geometries are produced, ranging from rhodalgal-starved rimmed platform with fringing reefs to rhodalgal-dominated ramps. Thus, the generation of any type of platform geometry is significantly influenced by the proportion of rhodalgal (oligophotic) versus coral (euphotic) production at play. This is consistent with numerical investigations on the role of euphotic versus oligophotic carbonate production in the determination of platform geometries, where euphotic production results in the formation of steep margin platforms, while oligophotic production leads to the formation of ramps (Williams et al., 2011; Sultana et al., 2021). The Miocene Menorca, Ragusa and Latium-Abruzzi ramps of the Mediterranean present field scale examples of geometrical significance of oligophotic production (Canals and Ballesteros, 1997; Pomar et al., 2002; Brandano, 2003; Ruchonnet and Kindler, 2012a).

Impact of erosion and sediment redistribution

Combined with the production-depth profiles of carbonate sediment classes and their production rates, erosional processes also drive changes in the platform geometry (Figure 2.13). Several researchers have identified sediment erosion and redistribution as significant factors in the evolution of carbonate geometries through the modification of facies patterns and slope angles (Droxler and Schlager, 1985; Schlager and Camber, 1986; Pomar, 1991; Schlager, 2000; Pomar et al., 2002, 2012b; Wunsch, 2017). However, our models suggest that in the development of the Llucmajor platform the main controls on the platform geometry include the complex dynamics of coral versus rhodalgal interaction with each other and changing sea level. Figure 2.13 reveals that while erosion and redistribution of coral sediments could produce a highly prograding carbonate platform, the distribution of different sediments and nature of platform slopes observed on the Llucmajor platform require significant production of rhodalgal sediments. Evidence of the need for an active rhodalgal base in the development of the Llucmajor platform has been recognised by earlier researchers from the shallow depths of frame-building wave-resistant corals of the platform, (Esteban, 1979; Pomar, 1991; Pomar and Ward, 1995; Pomar et al., 1996), as well as the abundance of rhodalgal sediments in the forereef slope to open shelf environments which are usually below wave agitation (Pomar, 1993; Scheibner et al., 2007; Pomar and Kendall, 2008b; Pomar et al., 2012a; Michel et al., 2018).

Does sea level curve matter?

In developing the reference models, two of the other sea level curves that we used for the model development include Haq et al. (1988) and Miller et al. (2005). In both cases, the observed geometry and facies relationships of the Llucmajor platform were not adequately reproduced mainly because of differences in frequencies of the sea level curves and the observed facies cyclicity of platform. This is because the biotically-driven stratigraphy of the Llucmajor Platform is controlled by a specific temporal variation of the sea level over the evolution period, a phenomenon which is not uncommon in studying local sedimentary systems (Miall, 1992). Local trends in sea level variation deduced from local stratigraphic records could be used to refine global sea level curves (Betzler et al., 2018; Grant et al., 2019). The Llucmajor platform is an example of such sedimentary systems with local variations in sea level preserved in the reef crest (Pomar and Ward, 1995), characterised by some deviations from global sea level curves.

Implications for petroleum geology

Stratigraphic forward modelling (SFM) can be a valuable tool in petroleum geoscience. In appraisal stages with generally sparse well data, SFM can be used as reference tool for geological concept testing (Granjeon and Joseph, 1999), improved understanding of stratigraphic uncertainties (Warrlich et al., 2008) and the development of multiple subsurface stratigraphic scenarios (Burgess et al., 2006). SFM also proves useful in exploration and production for its potential to serve as constraints for geostatistical models as well as in the prediction of depositional reservoir facies heterogeneities (Doligez et al., 1999; Burgess et al., 2006; Borgomano et al., 2014; Gervais et al., 2018). This is underpinned by the here presented stratigraphic models which provide detailed spatial facies patterns. This can directly be used to guide subsurface well-correlation, reservoir facies and petrophysical modelling. In particular the combination of SFM and petrophysical modelling of carbonate reservoirs received renewed attention in recent years (Huang et al., 2015; Hawie et al., 2017; Otoo and Hodgetts, 2021). Thereby the modelling of early diagenetic effects on reservoir properties can be assisted by SFM results due to better constraints of subaerial exposure times of the carbonate sequences and related hydrogeological regimes (Whitaker et al., 1997; Berra et al., 2016). Carbonate systems are additionally frequently affected by early deformation and syndepositional

fracturing. Geostatistical modelling of syndepositional fractures, which may constitute long-lasting fluid flow pathways is particularly challenging as these fractures do not necessarily follow regional tectonic stress fields but are also controlled by the morphology and geometry of the carbonate platform (Berra and Carminati, 2012; Nolting et al., 2018). It is therefore a complex task to obtain quantitative data on syndepositional fracture characteristics as outcrop analogues are only of limited use and fractures are predominantly below seismic resolution. However, (Frost and Kerans, 2010) established a relationship of syndepositional fracture density and intensity with the progradation/aggradation (P/A) ratio of a given carbonate platform. Syndepositional fracture orientation can be deduced by reef-crest trajectory, where fractures develop normal and parallel to the reef-crest (Frost and Kerans, 2009; Nolting et al., 2018). Our simulation results show that these sets of parameters can be generated from detailed SFM models. The P/A ratio is a function of the sea-level curve and zones of different P/A episodes can be deduced from the modelling results which may then guide the fracture modelling workflow. The Llucmajor platform would constitute an ideal case study to ground-truth and investigate SFM-derived fracture network models as platform trajectories (see Figure 2.12a) and episodes of rapid progradation followed by aggradation can be modelled in detail (Frost and Kerans, 2010; Moore and Wade, 2013a).

This study gives insights into the role of bathymetry in impacting the geometries of carbonate systems and provides an enhanced understanding of the role of euphotic and oligophotic production variation on platform geometry. Nevertheless, more research and detailed stratigraphic forward modelling of additional carbonate platforms with similar biotic components, as typical for the Miocene of the Mediterranean, but different spatial and vertical distribution is needed to provide further insights on how these complex interactions of the carbonate producing biota shape carbonate platform geometry and their stratigraphic architecture.

CONCLUSION

The process-based modelling employed in this study has used current understanding of the Llucmajor platform as a conceptual framework to investigate the possible responses of the carbonate platform to changes in bathymetric profiles, overall change in carbonate production rates and differential variations in production rates of euphotic

and oligophotic biota. The reference model, which was developed to simulate the spatial and temporal variation of carbonate production in the Llucmajor platform by five modelled sediment classes, was qualitatively validated by comparing the geometry and facies of the model with published data. The sensitivity analysis reveals that the evolution of a Llucmajor-type platform is strongly impacted by carbonate production rates as sea-level-controlled-accommodation fluctuates through time, by the bathymetry of the basin and the interplay among different modes of biogenic carbonate production. Key inferences from these results are as follows:

1. Progradation is strongly influenced by the interplay of the bathymetric profile of the basin and variation of carbonate production alongside accommodation. Given these types of carbonate production processes and provided all other conditions (e.g. turbidity, salinity and temperature, etc.) for carbonate sedimentation are fulfilled, shallower depositional areas will tend to produce more basinward progradation than deeper areas under similar conditions (Warrlich et al., 2002). Carbonate production reaches peak efficiency when the accommodation space and basin floor geometry provide optimal conditions for the ensemble of production-depth profile of each carbonate-producing class. Changes of one production-depth profile will affect the entire interaction and balance of the carbonate system and result in significant different platform geometries as shown in the stepwise sensitivity analysis. This provides numerical evidence that the role of carbonate producing biota and their interplay in space and time has a substantial influence on carbonate platform geometry.

2. The main biotic driver of progradation in this case study is the oligophotic production of rhodalgal sediments. Increased production rate of the rhodalgal sediments resulted in increased progradation of the platform, whereas reduced rhodalgal production rate resulted in the opposite response. While changing the production rate of the euphotic corals caused very limited change in the amount of progradation of the platform, decreasing the production rate of the rhodalgal sediments resulted in a reduction in the progradation of the platform. This highlights two key observations: (i) each carbonate producing class in the SFM model encompasses a specific role with respect to platform evolution and overall geometry and (ii) variation of carbonate production depth profiles not only affects overall progradation but also the internal geometry of the platform.

3. Carbonate-producing biota types determine the type of carbonate system that develops. The here presented results show that platform geometry and internal architecture varies significantly according to the interaction of the predominant carbonate producing biotas. These findings need to be considered in stratigraphic forward modelling studies of carbonate systems. The input parameters for this study are based on well-understood Miocene carbonate biotas which are however not necessarily suitable for carbonate systems of different ages where other age-specific biogenic systems are at play. It is crucial that each carbonate producing class is modelled explicitly within the simulation run and not averaged with one carbonate production-depth profile. This is particularly of importance in carbonate subsurface exploration studies based on stratigraphic forward models. While the overall platform geometry may be approximated through calibration runs and constrained by seismic surveys and wellbores, the internal architecture is likely to be over-simplified. Thus, an in-depth understanding of the target carbonate system and transfer to forward modelling parameters is needed to predict platform architecture and consequently reservoir geometry.

ACKNOWLEDGMENTS

Chapter 3
TESTING SEA-LEVEL AND CARBONATE PRODUCTION EFFECTS ON STRATAL ARCHITECTURE OF A DISTALLY STEEPENED CARBONATE RAMP (UPPER MIOCENE, MENORCA): A 3D FORWARD MODEL APPROACH

ABSTRACT

Although distally steepened carbonate ramps have been studied by numerous researchers, the processes that control the development of these carbonate systems, including tectonics, differential carbonate production along the ramp profile, or antecedent physiography of the slopes, are an ongoing discussion. We use a stratigraphic forward model to test different hypotheses to unravel controls over distally steepened ramp development, referenced to the well-known Upper Miocene Menorca carbonate ramp (Spain). Sensitivity tests show that distally steepened ramps develop under complex interaction among accommodation, carbonate production and sediment transport parameters. Ramp slope initiation is favoured by still stands and falls of sea-level, in a setting with high-frequency sea-level fluctuations with amplitude between 20 m and 40 m. Low-frequency and higher amplitude sea-level fluctuations of about 115 m tend to form models with no significant slope development. The impact of antecedent slope on the geometry of ramps is determined by the paleoslope inclination, with flat to subhorizontal paleosurfaces resulting in ramps that mirror the antecedent slope. In contrast, steeper paleosurfaces tend to result in ramps with well-defined slopes. Our models, therefore, show that the ramp profile becomes more influenced by the depth constraints on the carbonate sediment producers than by the geometry of the underlying topography as the inclination of the paleosurface increases. The presented models also show that seagrass-dominated shallow carbonate production tends to result in steep slopes due to the low-transport characteristic imposed by seagrass trapping. This steepness can, however, be altered by the introduction of high transport sediment grains from deeper carbonate producers, which fill the slopes and more distal sections of the ramp profile.

Keywords: forward model, distally steepened ramp, sea-level fluctuation, sensitivity analysis, sediment transport, carbonate production, grain association.

INTRODUCTION

Ahr (1973) introduced the term carbonate ramps to indicate low gradient depositional systems without clearly defined slope breaks. Carbonate ramps are swept by wave and current activities in response to fair-weather and storm wave base and impacted oceanographic conditions such as winds, storms, and tides (Wright, 1986; Burchette and Wright, 1992). The interaction between carbonate production processes and mechanisms that cause their redistribution may result in differential physical accommodation across the depositional profile (Pomar and Kendall, 2008a). Read (1982, 1985) differentiated carbonate ramps as either homoclinal, characterised by uniform gentle dips, usually less than 1° (e.g., Elrick and Read, 1991; Burchette and Wright, 1992; Pomar, 2001b), or distally steepened, characterised by a change in dip in their distal areas. The processes resulting in the steepening of the distal slope and clinoform development have been attributed to tectonic controls such as inherited slope physiography (Olsson, 1988; Choi and Simo, 1998; Elvebakk et al., 2002), differential subsidence or faulting (Kershaw and Guo, 2006; Resor and Flodin, 2010; Rinke-Hardekopf et al., 2018), carbonate sediment production, either as differential carbonate production across the ramp profile (Pedley and Carannante, 2006) or the continuous supply of carbonate sediments in the oligophotic zone accompanied by sediment shedding from the inner ramp (Burchette and Wright, 1992; Schlager et al., 1994; Pomar, 2001b, 2020), or to eustatic control through protracted sea-level still stand (Pedley and Grasso, 2006). These processes may interact, but as investigating these processes is usually based on modern analogues, outcrops or seismic data, the information is limited by the nature of the data sets resulting in limited spatial extent or resolution. This leads to limitations in the quantitative assessment of processes and their impacts on the ramp geometries and internal facies organisation. These limitations can be reduced by integrating qualitative and quantitative data from carbonate systems from modern settings and the geological record, using stratigraphic forward modelling (SFM) techniques (Bice, 1988; Granjeon and Joseph, 1999; Burgess, 2012). Due to its potential to integrate ecological, physical, and oceanographic parameters, SFM has been a versatile tool to test stratigraphic

concepts, eliminate geologically implausible scenarios, and develop and advance new ideas of stratigraphic and sedimentological evolution of carbonate systems. Since the work of Bice (1988), SFM has been incorporated in basin studies to examine the controls of individual variables of sediment supply, sediment transport, tectonic subsidence and eustasy on sedimentary systems (Aurell et al., 1998; Granjeon and Joseph, 1999; Boylan et al., 2002; Warrlich et al., 2002; Burgess, 2012; Seard et al., 2013; Lanteaume et al., 2018). Although the deterministic results of SFM are non-unique, they provide numerical quantification of the impact of individual and multiple controls on sedimentary systems (Aurell et al., 1998; Warrlich et al., 2002; Williams et al., 2011; Burgess and Prince, 2015; Sultana et al., 2021; Tella et al., 2022b).

Therefore, this paper aims to discuss the outcomes of multiple forward modelling experiments as results of the interaction between biogenic carbonate production processes, sediment transport parameters and antecedent slope topography in the development and evolution of distally steepened carbonate ramp geometries. In particular, as carbonate systems are not only subjected to changes in physical accommodation but also ecological dynamics (Pomar, 2001a), this paper will differentiate biogenic carbonate production processes according to differential production zones across the depositional profile. As a reference model, the Upper Miocene Menorca ramp, which has hitherto not been studied via numerical modelling, has been chosen. The Menorca ramp is a suitable carbonate system for this research as it presents i) a well-studied distally steepened ramp, with copious information on the depositional environments, the biogenic carbonate producers and their production depth zones which can be adequately related to Holocene systems, ii) a distinct distribution of multiple grain associations across the ramp profile with a defined relationship to fair-weather and storm wave bases, and iii) the presence of platform-parallel dunes in the middle ramp as evidence of high energy regimes (Obrador et al., 1992; Pomar et al., 2002; Brandano et al., 2005; Mateu-Vicens et al., 2008; Asprion et al., 2009; Sàbat et al., 2018; Pomar, 2020), (iv) deposition at a time when sea-level curves are well constrained. The obtained models focused on contrasting the role of sea-level fluctuation versus carbonate sedimentation on the steepening of carbonate ramp slopes and examining the impact of sediment transport parameters on the ramp geometry.

THE MENORCA DISTALLY STEEPENED CARBONATE RAMP

General geologic setting

The models presented in this study focused on the Lower Tortonian carbonate ramp of Menorca (Pomar et al., 2002; Pomar, 2020), the northernmost Balearic Island in the western Mediterranean (Figure 3.1a). The Upper Miocene deposits of the Balearic Islands, including the Menorca ramp, are post-orogenic and overlie older deformed sedimentary and basement rocks of Palaeozoic and Mesozoic age (Obrador, 1970; Pomar et al., 2002; Sàbat et al., 2018). These islands form the NE-SW trending emergent part of the Balearic Promontory, which was affected by regional thinning and extension in the Mesozoic, with the Cenozoic being an interval of compressional and extensional tectonic regime (Sàbat et al., 1994, 2011a; Doglioni et al., 1997). The Upper Miocene units are primarily restricted to the southern part of Menorca Island (Figure 3.1a), where they have been only affected by slight late Neogene to middle Pleistocene tilting and flexure (Pomar et al., 1996; Pomar, 2001a; Sàbat et al., 2018). The Menorca carbonate ramp was deposited during the lower Tortonian and is mainly composed of Heterozoan biotas (Obrador et al., 1992). The ramp deposits are overlain by an upper Tortonian-lower Messinian flat-topped platform, including Messinian oolites and stromatolites (Figure 3.1b).

Facies and depositional systems of the Menorca ramp

The Lower Tortonian ramp is a distally steepened ramp rich in red algae and foraminifera (Figure 3.1c), which has been the subject of numerous outcrop studies (Pomar et al., 1983, 2002; Obrador et al., 1992) and divided it into inner, middle, ramp slope, with well-developed upper ramp slope and lower ramp slope rich in in situ rhodoliths., and outer ramp depositional environments.

The inner ramp environment comprises primarily mollusk-foraminifera packstones and wackestone with some minor grainstones, strongly bioturbated, baffled and trapped by seagrass in the euphotic zone (Pomar et al., 2002). The inner ramp environment is characterised by the co-occurrence of the large benthic foraminifera Amphistegina and Ammonia, which indicate the dominance of warm conditions during Tortonian times in the region (Calvo et al., 1993; Mateu-Vicens et al., 2008). Epiphytic foraminifera also contributes sediments in the inner ramp. The carbonate grain association in the inner ramp environment is primarily dominated by seagrass meadows in the euphotic zone,
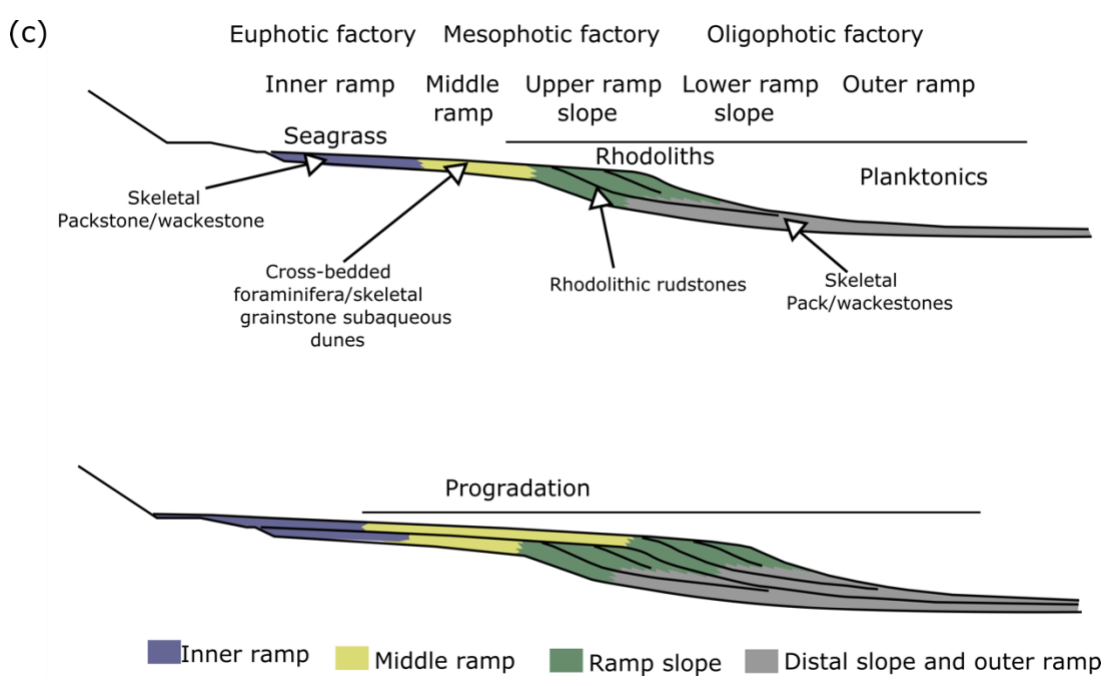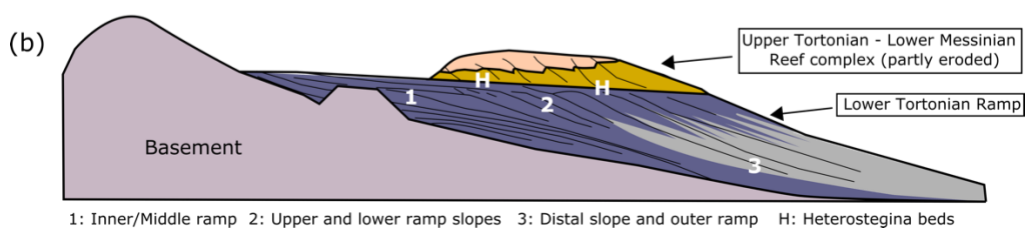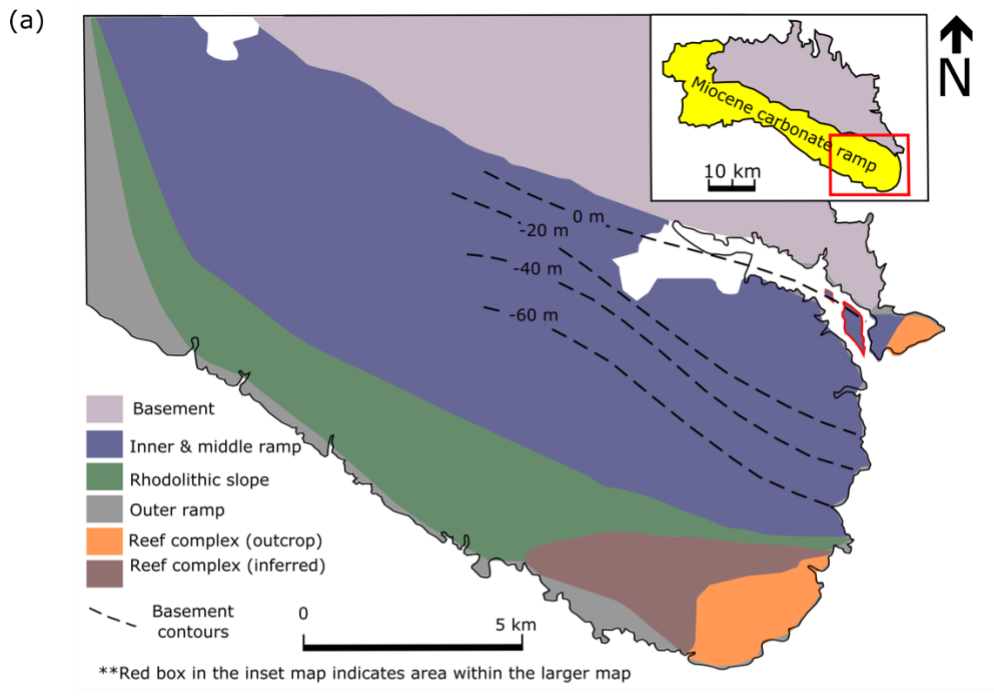
Figure 3.1: A) Geologic map of Menorca showing the distribution of the Upper Miocene ramp facies over Mesozoic basement (modified from (Pomar et al., 2002). B) A cross-section showing the stratigraphic relationship between the Menorca ramp and the overlying reef complex. The depositional

environments in the ramp show transition from foreshore deposits in the proximal area to the outer ramp environment (modified from Pomar et al., 2002). C) biogenic carbonate production along the Menorca ramp profile. Epiphytic seagrass production is dominant in the euphotic zone, with high sediment accumulation in the ramp slope due to an effective oligophotic production. The bottom illustration shows how the ramp responds to sea level fall by progradation due to a basinward shift in the carbonate production loci (Pomar, 2020).

providing a suitable biotope for a wide variety of carbonate producers such as epiphytic organisms and sediment dwellers (Mateu-Vicens et al., 2008).

The middle ramp is characterised by cross-bedded grainstones with large benthic foraminifera, such as Amphistegina and some Heterostegina, with other benthic foraminifera such as Ammonia, Textulariia, and bolivinids in the mesophotic zone (Pomar et al., 2002; Brandano et al., 2005). The middle ramp also includes scattered skeletal rhodolithic components and fragments of red algae, echinoids and mollusks. The red algal components comprise Melobesioids, Mastophoroids, Sporolithaceans and Lithophyloids families ((Brandano et al., 2005).

The ramp slope depositional environment is subdivided into upper and lower ramp slope settings (Pomar et al., 2002; Mateu-Vicens et al., 2008). Mateu-Vicens et al. (2008) described the upper ramp slope as consisting of grainstones forming 15o – 20o inclined strata and rhodolithic rudstone beds that alternate red algal grainstones (Bosellini and Ginsburg, 1971; Bosence, 1983; Brandano et al., 2005). The lower ramp slope (Mateu-Vicens et al., 2008) mainly consists of reworked cross-bedded grainstones/packstones rich in large benthic foraminifera, epiphytic foraminifera and red algae. There are also skeletal fragments of echinoids, mollusks, bryozoans and serpulids. The high ratio of Melobeiosioid to Mastophoroid components suggests that the lower ramp slope environment was characterised by a water depth range of 70 m to 100 m (Brandano et al., 2005).

The most distal part of the ramp profile is the outer ramp depositional environment (Pomar et al., 2002; Brandano et al., 2005; Mateu-Vicens et al., 2008). The outer ramp is characterised by fine-grained wackestones to packstones composed mainly of in situ planktonic foraminifera, mollusks and echinoids, with some transported shallow-water remains of organisms such as epiphytic foraminifera, large benthic foraminifera, filter feeders, red algae and other foraminifera (e.g., Buliminidae, Ammonia, etc.) (Mateu-Vicens et al., 2008).

In addition to in situ carbonate sedimentation by the grain associations described in the settings above, (Mateu-Vicens et al., 2008) also described sediment components

accumulated ex situ in the distal part of the inner ramp, middle ramp, ramp slope and outer ramp settings. These sediments include transported epiphytic foraminifera, Ammonia, Textularia, large benthic foraminifera, filter feeders and coralline algae.

DATA AND METHODOLOGY

The depositional model of the Menorca ramp, which served as a reference for this numerical study, is the cross-section (Figure 3.1b) and 3D synthetic model (Figure 3.2) developed from field studies by Pomar et al. (2002).
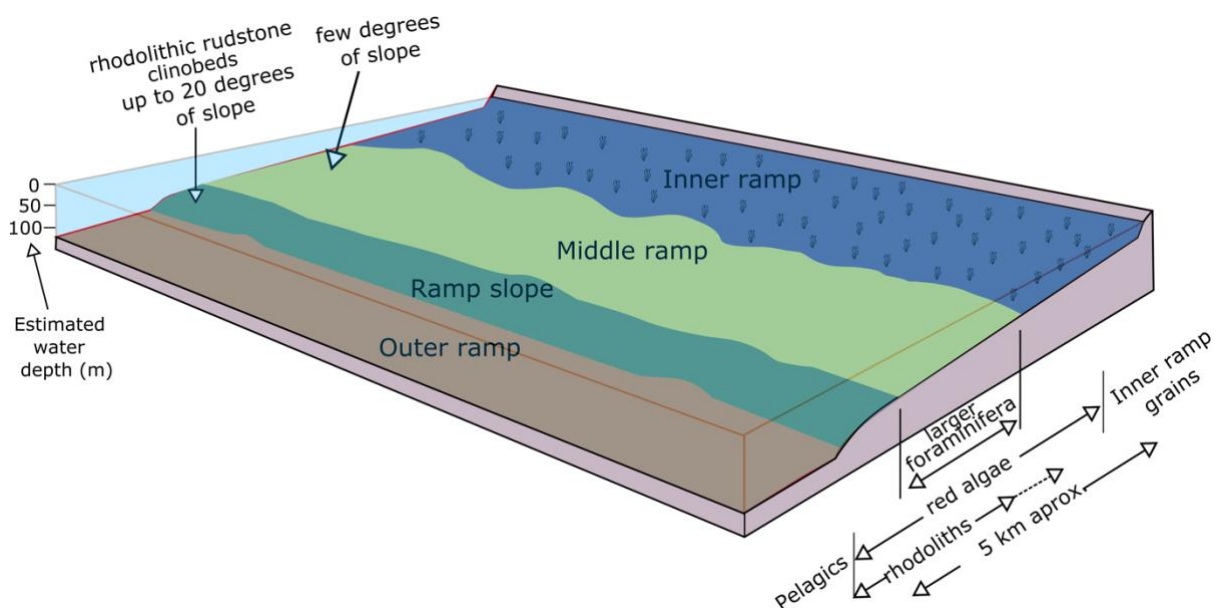
Figure 3.2: A depositional model of the Menorca ramp illustrating the bathymetric range and grain association defining the inner ramp, middle ramp, ramp slope and outer ramp depositional environments (modified from Pomar et al., 2002).

Stratigraphic forward modelling using the DionisosFlow creates digital stratigraphies by mathematically synthesising time-limited interplay of geological processes such as accommodation creation and reduction through eustasy and tectonics, carbonate sediment production, accumulation, and preservation, as well as sediment transport by waves and gravity (Granjeon and Joseph, 1999). Sediment production parameters are essential inputs for developing stratigraphic models, and for carbonate systems, sediments are produced in situ according to water depths and then subject to reworking and redistribution through wave energy and gravity processes. Dionisos simulates this transport through a diffusion equation (Granjeon, 1996; Granjeon and Joseph, 1999), which relates sediment flux (Qs) to the slope (S) by a diffusion coefficient (K) as follows:

$$Q\_s = K * \text{Wave Energy} * S \tag{1}$$

Table 3.1: Initial parameters of the reference model

Parameter	*Parameter description*	*References*
Grid	Dimension: 50.4 km x 35.8 km	
	Grid size: 200 m x 200 m	
	Initial bathymetry: Figure 3.3b	Pomar et al. (2002; Mateu-Vicens et al. (2008)
Simulation Time	Model duration: 2.6 My	Pomar et al. (2002)
	Time step: 50 ky	
	Display interval: 7 Ma to 11.6 Ma	
Carbonate production	— Euphotic class: Figure 3.4 — Water depth range: 0 - 40 m	Brown (2005); James et al. (2009)
	— Mesophotic class: Figure 3.4 — Water depth range: 40 - 70 m	Mateu-Vicens et al. (2008); Morsilli et al. (2012)
	— Oligophotic class: Figure 3.4 — Water depth range: ≥ 22 m	James and Bone (1991; Sultana et al. (2021)
	— Muds/Pelagics: Figure 3.4 — Water depth range: ≥ 22 m	Cita et al. (1978); Scholle et al. (1983)
	— Rhodoliths: Figure 3.4 — Water depth range: 70 - 110 m	Kinsey (1978)
Sea level curve		Miller et al. (2005)
Wave base	20 m	Coe et al. (2003)

where K is higher for loose sediments than for bioconstructions.

The development of the Menorca ramp forward model required inputs including (1) an initial bathymetric map that represents the initial paleosurface over which carbonate sediments are deposited with respect to water depth variation, (2) accommodation variation through sea-level fluctuation and tectonic subsidence, and (3) carbonate sediment production as a function of bathymetry. These input parameters are derived from published studies (Kinsey, 1978; Cita et al., 1978; Scholle et al., 1983; James and Bone, 1991; Pomar et al., 2002; Brown, 2005; Miller et al., 2005b; Mateu-Vicens et al., 2008; James et al., 2009; Morsilli et al., 2012; Sultana et al., 2021). In applying these previous studies in the development of the Menorca model, several assumptions

were made, as summarised in Table 3.1. Hydrodynamic assumptions for the model include a wave base of 20 m (Figure 3.3a), which is considered a general average for carbonate platforms (Coe et al., 2003). To simulate carbonate production in the model, carbonate production-depth profiles are required to represent biogenic carbonate sediment production by different biotic associations. The development of carbonate production-depth profiles was constrained to reflect production at different depth zones along the depositional profile (Kinsey, 1978; Cita et al., 1978; Schlager, 2000; Strasser and Samankassou, 2003; Brown, 2005). The initial bathymetry was developed with a gentle slope following approximations from the basement contours of Pomar et al. (2002), creating a relief of approximately 150 m across the model domain. Based on facies description from outcrops (Obrador, 1970; Pomar et al., 2002; Brandano et al., 2005; Mateu-Vicens et al., 2008), sediment transport was defined as relatively low in the inner ramp due to sediment trapping by sea-grass, higher in the middle ramp, low in the upper ramp slope and high in the outer ramp environments. The model was run from 10.95 Ma to 8.35 Ma to reflect the time of evolution of the Menorca ramp in the lower Tortonian.

Initial bathymetric map

The distribution of foraminifera and red algal species in the Menorca ramp provides insight into the variation of palaeowater depth across the ramp profile (Pomar et al., 2002; Brandano et al., 2005; Mateu-Vicens et al., 2008). Based on these studies, the initial bathymetric map used for this study has a relief of 150 m (Figure 3.3b). The map covers an area of 1700 square km representing the south of Menorca down to offshore areas with a uniform dip of 0.15º, an inclination inferred from the basement contours of Pomar et al. (2002).

Accommodation variation

The Menorca ramp was deposited during a period of high frequency and moderate amplitude sea-level fluctuations during the lower Tortonian (Haq et al., 1988; Pomar et al., 2002). Accommodation variation is modelled as an interaction between sea-level oscillation and subsidence. As there is no evidence of significant subsidence variations during the ramp system's evolution, the model development relied on different Miocene sea-level curves at different resolutions (Haq et al., 1988; Miller et al., 2005a, 2020; Haq, 2014).
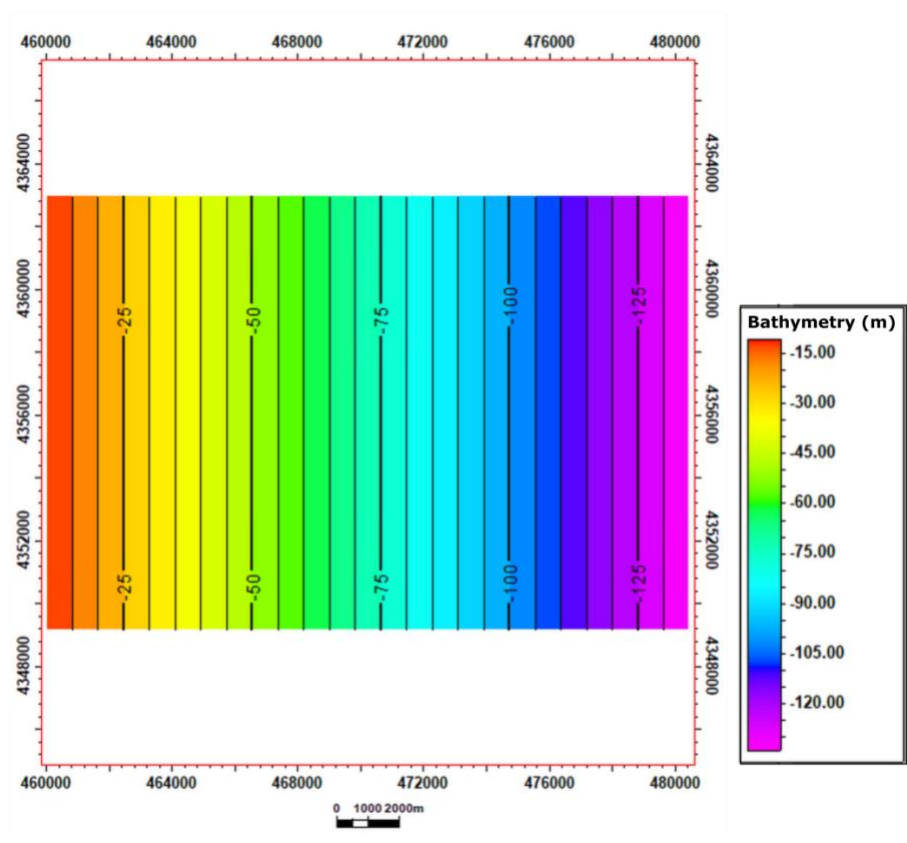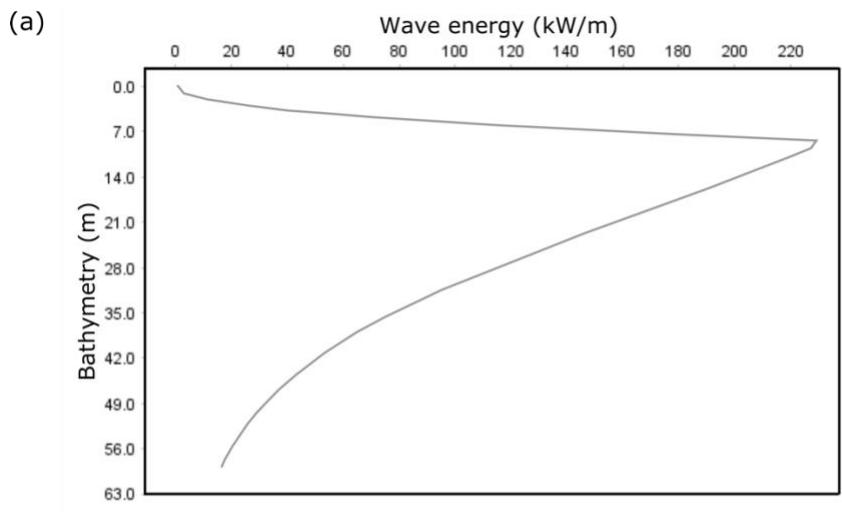
Figure 3.3: Modelled parameter inputs A) Simulated hydrodynamic pattern, which influences carbonate production and transport. B) Initial bathymetry" of the modelled sedimentary system (map visualisation from Petrel software).

Carbonate sediment production and transport

Carbonate sediment production in Dionisos is based on the bathymetry-dependent attenuation of sediment production rate influenced by processes such as accommodation change, wave energy flux, climatic changes, etc, through geologic time, which determine the amount and type of sediment produced (Schlager, 2005;

Wright and Burgess, 2005). This means that carbonate production is simulated through a series of production versus depth curves which produce carbonate sediments at rates that are a fraction of pre-set maximum production rates.

For our model, we defined five sediment classes: euphotic class, mesophotic class, oligophotic class, muds/pelagics and rhodoliths (Figure 3.4a). These sediment classes represent the quantification of the depth-dependent production of the grain associations (Figure 3.4b) in the five described depositional environemnts. Each of these classes is defined by varying hydrodynamics (Equation 1, Table 3.1). It should be noted, however, that the biogenic carbonate production of the Menorca ramp is characterised primarily by Heterozoans carbonates (Pomar et al., 2002), and the terms euphotic, mesophotic, oligophotic and aphotic in this study are therefore based on the relative depths of occurrence of different biota as described by (Mateu-Vicens et al., 2008), rather than strict biological classification based on the components (Kindler and Wilson, 2012).

Euphotic class: Sediment production in the euphotic class reflects the high rate of carbonate sediments production in the inner ramp depositional environment described in section 2.2. Carbonate production is characterised by low diffusion coefficients of 0.0001 km2/kyr (Table 3.2) to withstand the high wave energy flux as in a seagrass environment. Production occurs down to about 40 m water depth, with sediment production declining from 20 m (Figure 3.4b). The decline of the euphotic production is set at the chlorocline, which represents the deepest occurrence of green algae and usually coincides with the lower limit of seagrass growth (Ros et al., 1985; Mateu-Vicens et al., 2008; Morsilli et al., 2012). The maximum carbonate production rate is set at 15 m/My, which is within calculated rates of carbonate sediment production within seagrass-dominated environments by earlier studies (Brown, 2005; James et al., 2009).

Table 3.2: Carbonate production and sediment transport coefficients of model sediment classes

Modelled sediment classes	Maximum production rate (m/My)	Wave energy flux (kW/m) constraints	Diffusion coefficients (km^2/m)
Euphotic class	15	40 to 230	0.0001
Mesophotic class	10	—	0.01
Oligophotic class	15	0 to 100	0.001
Lime muds/Pelagics	7	—	0.1
Rhodoliths	12	—	0.0001
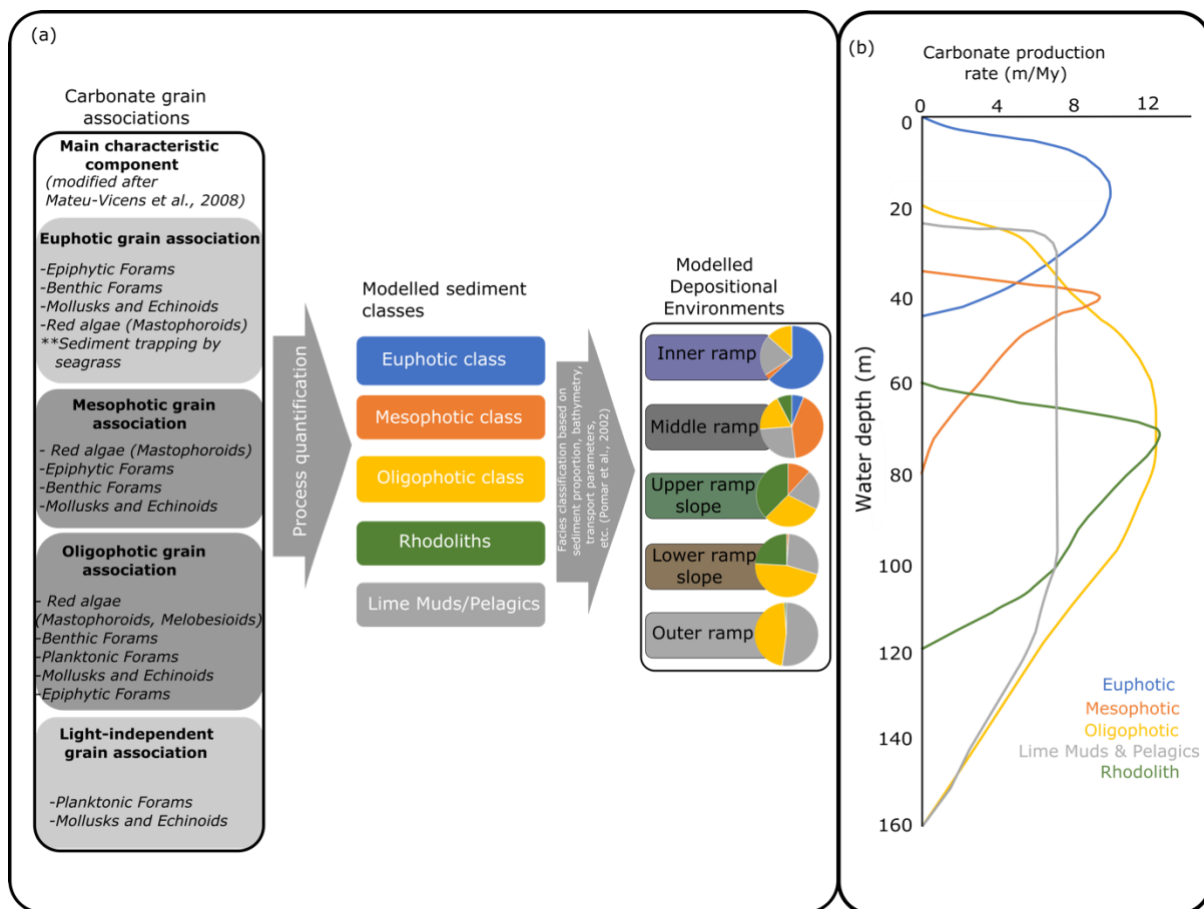
Figure 3.4: A) Summary of biogenic carbonate associations at different depth zones in the Menorca ramp and their conversion to forward model sediment classes, as well as the translation of these model sediment classes to facies in the reference model. Pie charts represent the average proportion of each sediment class in the model facies. B) Production-depth profile of the model sediment classes.

Mesophotic class: This class corresponds with the grain association in the middle ramp. Sediment production in the mesophotic class ranges from about 40 m to 80 m with a maximum carbonate production rate of 10 m/My. The sediments in this class are more prone to reworking by wave agitation as they are not trapped by seagrasses and therefore include a wave diffusion coefficient of 0.01 km2/kyr (Table 3.2).

Oligophotic class: This class corresponds with in situ red algal and ex-situ (e.g., epiphytic foraminifera) grain association across the ramp profile. Sediments produced in this class are more prone to be redistributed by waves, with production occurring down to 160 m water depths (Figure 3.4). The production of the oligophotic grains follows the depth-dependent growth profile of rhodalgal systems (James and Bone, 1991; Schlager, 2003; Sultana et al., 2021), with a maximum production rate of 12

m/My. Sediments in the oligophotic class are defined by diffusion coefficients of 0.001 km2/kyr (Table 3.2).

Rhodoliths: This class corresponds with the grain association in the ramp slope. We modelled rhodoliths by defining them as carbonate accumulations occurring from 50 m to 100 m (Figure 3.4) with a maximum production rate of 12 m/My which is within the range of rates calculated for coralline red algae (Kinsey, 1978; Halfar et al., 2001; Bosence and Wilson, 2003). The sediment class is characterised by a low wave diffusion coefficient of 0.0001 km2/kyr (Table 3.2).

Lime muds and Pelagics: This class represent suspended sediments/particles deposited across the ramp profile but dominating sediment accumulation in the outer ramp environment (Figure 3.4). With a maximum accumulation rate of 7 m/My (Cita et al., 1978; Scholle et al., 1983), muds and pelagics were produced in the simulation from depths of 20 to 160 m with accumulation and preservation dependent on the wave energy regime. The suspension and settling of lime mud and planktonic foraminifera were modelled in the lime muds and pelagic sediment class with a diffusion coefficient of 0.1 km2/kyr (Table 3.2).

Facies definition

The modelling results were analysed based on post-processing "facies" which were defined by the distribution of the model sediment classes and other environmental parameters such as wave energy flux and bathymetry (Table 3.3), following the outcrop facies description of Pomar et al. (2002). Five depositional environments were defined, representing aggregate sediment accumulation and prevailing environmental conditions (Figure 3.4): 1) The inner ramp depositional environment is defined by model sediment association in the shallowest water depths down to 40 m with euphotic sediment proportion of 60% or more; 2) the middle ramp depositional environment represent the modelled sediment association between 40 to 70 m bathymetry, with a minimum mesophotic sediment proportion of 40%; 3) the upper ramp slope represent sediment association between bathymetry of 70 to 90 m, with rhodolith proportion of 15% or more; 4) the lower ramp slope defines sediments from 90 m to 110 m, with rhodolith proportion of 15% or more and 5) the outer ramp defines sediments deposited in water depths greater than 110 m, with a minimum Lime mud/pelagics proportion of 52%.

Table 3.3: Postprocessing parameter constraints for the definition of model depositional environments

	Inner ramp	Middle ramp	Upper ramp slope	Lower ramp slope	Outer ramp
Bathymetry (m)	0 to 40	40 to 70 m	70 to 90	90 to 110	≥ 110
Euphotic class (%)	≥ 60	—	≤ 1	—	—
Mesophotic class (%)	—	≥ 40	—	—	—
Rhodoliths (%)	—	—	≥ 15	≥ 15	—
Oligophotic class (%)	—	—	—	—	—
Lime muds/pelagics (%)	—	≥ 20	—	—	≥ 52
Wave energy flux (kW/m)	≥ 70	≥ 70	—	—	—
Slope angles (degrees)	≤ 2	—	—	—	—

RESULTS

The reference model

The reference model (Figure 3.5a) is defined by five depositional environments which correspond to the conceptual model of Pomar et al. (2002) (Figures 3.1b and 3.2), namely inner ramp, middle ramp, upper ramp slope, lower ramp slope and outer ramp. The model's geometry is defined by a gradient in which the inner and middle ramp areas are flat-lying to subhorizontal and transition into a steep ramp slope area, transitioning into subhorizontal outer ramp areas.

The inner ramp is dominated by highly transport-resistant euphotic sediments that are abundant in the model's high wave energy domains (Figure 3.6). Euphotic sediment proportion in the inner ramp ranges from 100% in the shallowest portions of the model, where they are most protected by seagrass baffling, to 30% in the area close to the middle ramp. Wave energy distribution defining the inner ramp ranges from 80 kW/m in distal sections close to the middle ramp to 230 kW/m in proximal areas. Mesophotic sediments are less abundant in the inner ramp, where they are present only as wave-swept components of the inner ramp, especially during sea-level rise, with proportions ranging from 0% to about 25%. Muds/pelagics proportion in the inner ramp ranges from about 20% to 45%, like oligophotic sediment proportion, which ranges from about 19% to 45%. Rhodoliths are not significant sediment contributors in the inner ramp.

The inclination of the inner ramp profile is generally low, ranging from 0.02° in the proximal areas and increases basinward to 1.3°.

The middle ramp (Figure 3.5b) is defined by a slightly more inclined slope than the inner ramp. It interfingers with the inner ramp in a cross-sectional view, illustrating the basinward and landward shift of the ramp system as sea-level fluctuates. Gradients of the middle ramp range from less than 2° in the proximal areas to about 7° in the more distal areas. Wave energy in the middle ramp is moderate to low, progressively decreases with depth, and ranges from 15 kW/m distally to about 80 kW/m in the proximal areas. Here, the sediment components (Figure 3.6) are dominated by mesophotic grains with proportions ranging from 35% to about 50%. Oligophotic grains are also abundant in the middle ramp, with proportions ranging from 27% to 39%. Muds/pelagics, which are expected to increase with depth, are generally low in the middle ramp environment, ranging from about 17% to 29%, as they are more exposed to bottom currents and the absence of seagrass baffling effect. The middle ramp shows early onset of rhodoliths, albeit in a low proportion ranging from 0% to 32%. Euphotic sediment proportion in the middle ramp is generally about 0% in most parts, with streaks of euphotic grains reaching 30% in the shallow middle ramp areas.

The ramp slope in the model is classified into two depositional environments – upper ramp slope and lower ramp slope (Figure 3.5a). The upper ramp slope is characterised by a high inclination ranging from 8° in proximal areas to about 22° distally. Sediment accumulation in the upper ramp slope is dominated by rhodolithic floatstone to rudstones and oligophotic grains (Figure 3.6). Rhodolith sediment proportion ranges from 32% to 39%, while oligophotic grain proportion ranges from 29% to 40%. Muds/pelagic sediment proportion plots below 20% due to high gravitational processes occurring on the slope. Deposition of mesophotic grains on the slope is only significant during episodes of sea-level fall where mesophotic sediment proportion could rise to about 20%, otherwise, sea-level rise shifts the deposition of mesophotic sediment to the middle ramp. Expectedly, euphotic grains form an insignificant component of the ramp slope.
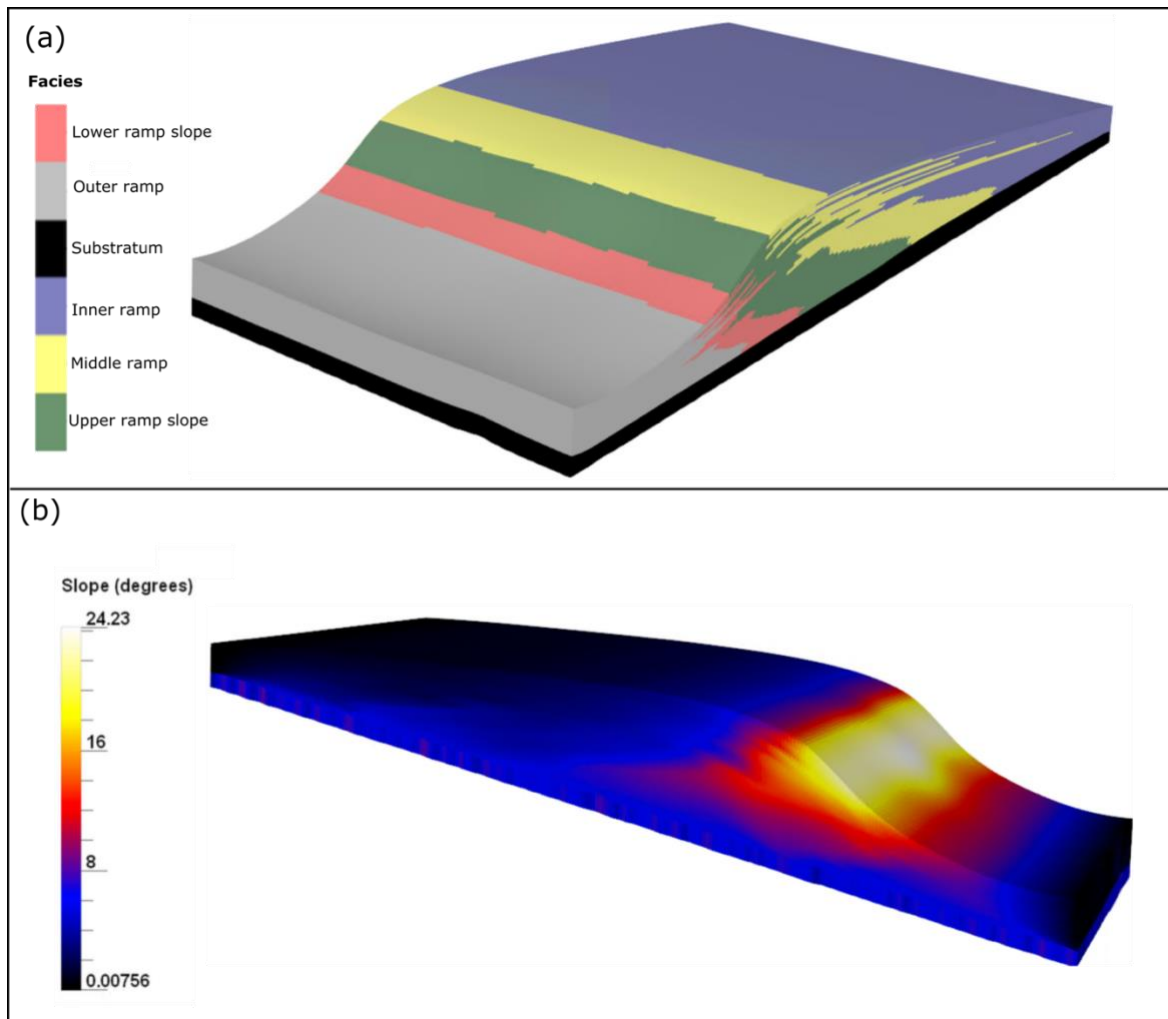
Figure 3.5: A) The reference model with five facies subdivision. B) Slope gradients along the profile of the reference model.

The lower ramp slope (Figure 3.5a) occurs below the upper ramp slope, characterised by a gradual decrease in the gradient from about 22° in upper sections to about 7° in deeper areas. Most of the lower ramp slope sediments have been gravitationally redeposited from the upper ramp slope or eventually transported by bottom currents. Rhodolith sediment proportion (Figure 3.6) falls from about 30% in areas bounding the upper ramp slope, to about 15% in deeper sections. Oligophotic grains representing coralline algal accumulation are significant sediment contributors in the lower ramp slope, with the comprising at least 40% oligophotic grains sediment proportion. Along the lower ramp slope, the sediment proportion of muds/pelagics increases with depth, ranging from about 20% in shallower areas to 31% in the deeper areas. Mesophotic and euphotic grains, however have very low sediment proportion in the lower ramp slope (Figure 3.6).
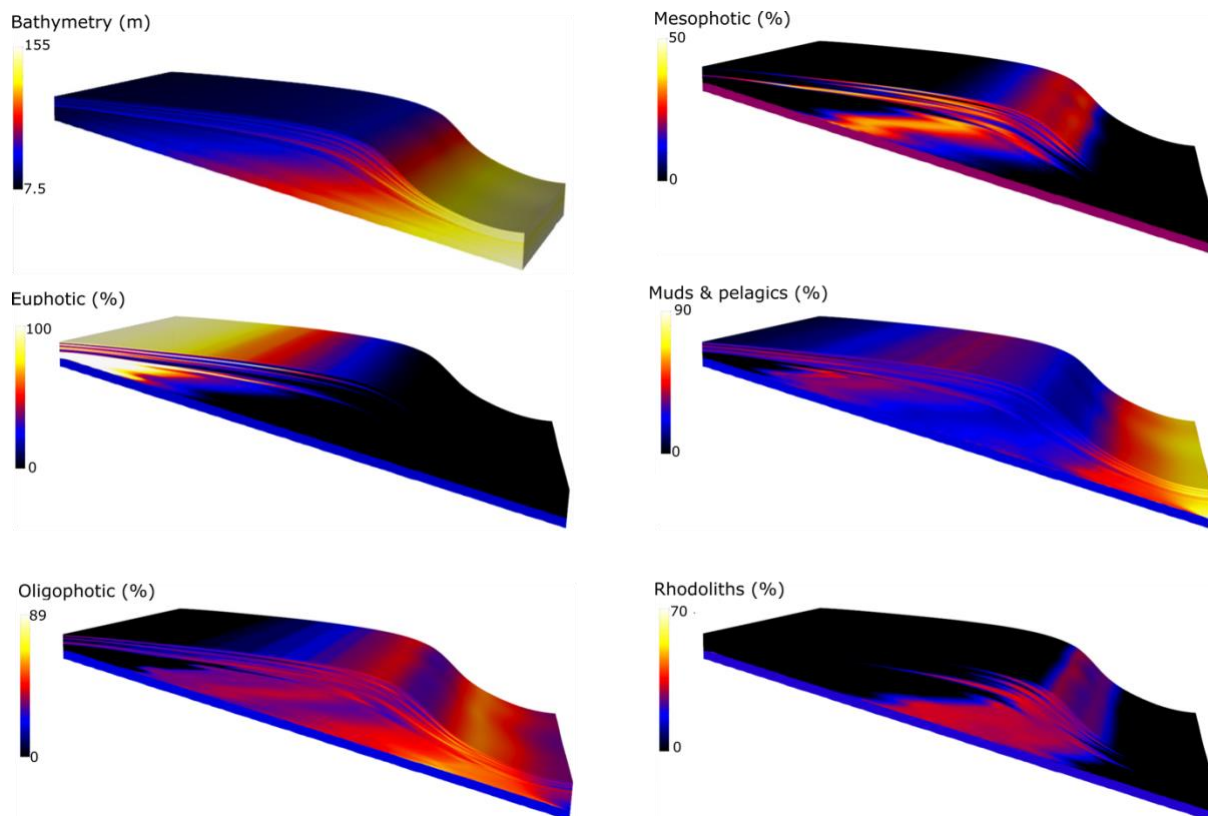
Figure 3.6: Properties of the reference model, including bathymetry and sediment proportion of the model sediment classes along the model profile.

The outer ramp represents the deeper-water environment (Figure 3.5a), mainly constituted by the muds/pelagic sediment class with sediment proportion (Figure 3.6) ranging from 33% at the contacts with the lower ramp slope, to above 90% in deeper areas. Oligophotic grains, which are mostly reworked from shallower depths, are abundant at the contact with the lower ramp slope, where they have sediment proportion up to 60%, which quickly decreases to about 20% at greater depths. Specks of rhodoliths, with a low sediment proportion of 12%, occur in the proximal portion of the outer ramp. The outer ramp interfingers with the lower ramp slope, in response to the sea-level fluctuations and gravity impacting the ramp profile. Sediments in the outer ramp environment are mainly deposited as flat-lying units with slopes mostly less than 4º.

The Menorca ramp was deposited under high frequency, moderate amplitude cyclic sea-level fluctuations (Pomar et al., 2002) and these high-frequency cycles were modelled using a timestep of 50 ky on the (Miller et al., 2005) sea-level curve. The model records response of the ramp to sea-level fluctuations through progradation, aggradation and weak retrogradation patterns of the main facies belts. Specifically, intervals of sea-level still stands (e.g., from 10.3 Ma to 9.85 Ma) are characterised by

progradation (about 8.9 km/My) with increased sedimentation in the ramp slope, while the inner ramp slowly shifts basinward (Figure 3.7a). As sea-level falls (e.g., the interval between 9.65 Ma and 9.5 Ma), rapid progradation of the ramp occurs (up to 50 km/My), with inner ramp and middle ramp developing on earlier slopes (Figure 3.7b). Episodes of sea-level rise result in aggradation in the inner ramp with resultant vertical accretion and steepening of the ramp slope related to a local progradation (Figure 3.7c). Evidence of sea-level fluctuation is best recorded along the ramp profile, especially in the ramp slope where there is an alternation of shallower and deeper environments at the slope margins (Figure 3.7d).

Net "facies" ratios (the ratio of lateral spread of each depositional environment to the total depositional environments deposited) for each time step were calculated and plotted with the sea-level variation from 10.75 Ma to 8.35 Ma (Figure 3.8). Periods of sea-level still stands and sea-level fall are associated with the dominance of the inner ramp depositional environment as the ramp progrades. Episodes of sea-level rise are accompanied by increased middle ramp proportion, decreased slope facies proportion, and increased outer ramp proportion.

Sea-level change and ramp slope development

The impact of different sea-level amplitudes and frequencies on the model was tested using different sea-level curves developed at different temporal resolutions. Specifically, in addition to the Miller et al. (2005) curve used to develop the reference model (Model SL1), Models SL2, SL3 and SL4 were run with the Haq et al. (1988) long-term sea-level curve, Haq et al. (1988) short-term sea-level curve and Miller et al. (2020) sea level curve respectively (Figure 3.9). Model SL1 was simulated with the Miller et al. (2005) sea-level curve, providing a much higher frequency of sea-level fluctuation during the Miocene, with an amplitude of about 30 m in the simulation interval. Model SL1 shows an overall progradation of the ramp in the first 1 My of the simulation, a period characterised by a general low sea-level still stand. High-frequency sea-level fluctuation resulted in significant development of the ramp slope during alternating episodes of sea-level falls and rises. The internal facies architecture also shows an interfingering relationship between proximal and distal facies. Model SL2 was run with the Haq et al. (1988) long-term sea-level curve, which is characterised by a near-linear relative sea-level fall of 38.5 m over the simulation interval (10.95 Ma to 8.35 Ma). This translated into a ramp model in which sediment
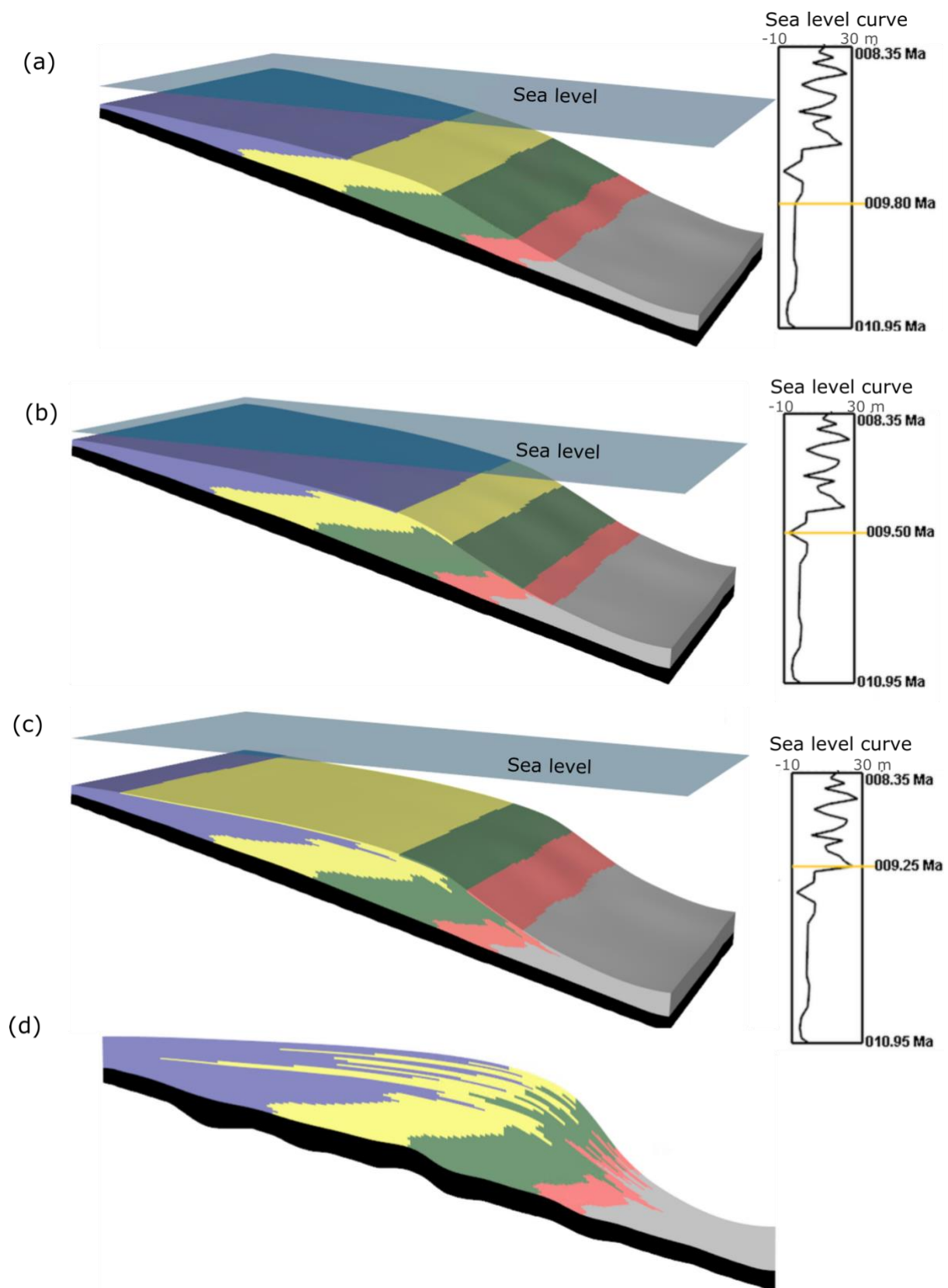
Figure 3.7: Facies development with sea-level changes: A) facies progradation and slope initiation during sea-level still stands. B) Ramp progradation during sea-level rise. C) Ramp aggradation and landward facies shift during sea-level rise. D) A model cross section showing the overall ramp development and facies architecture.
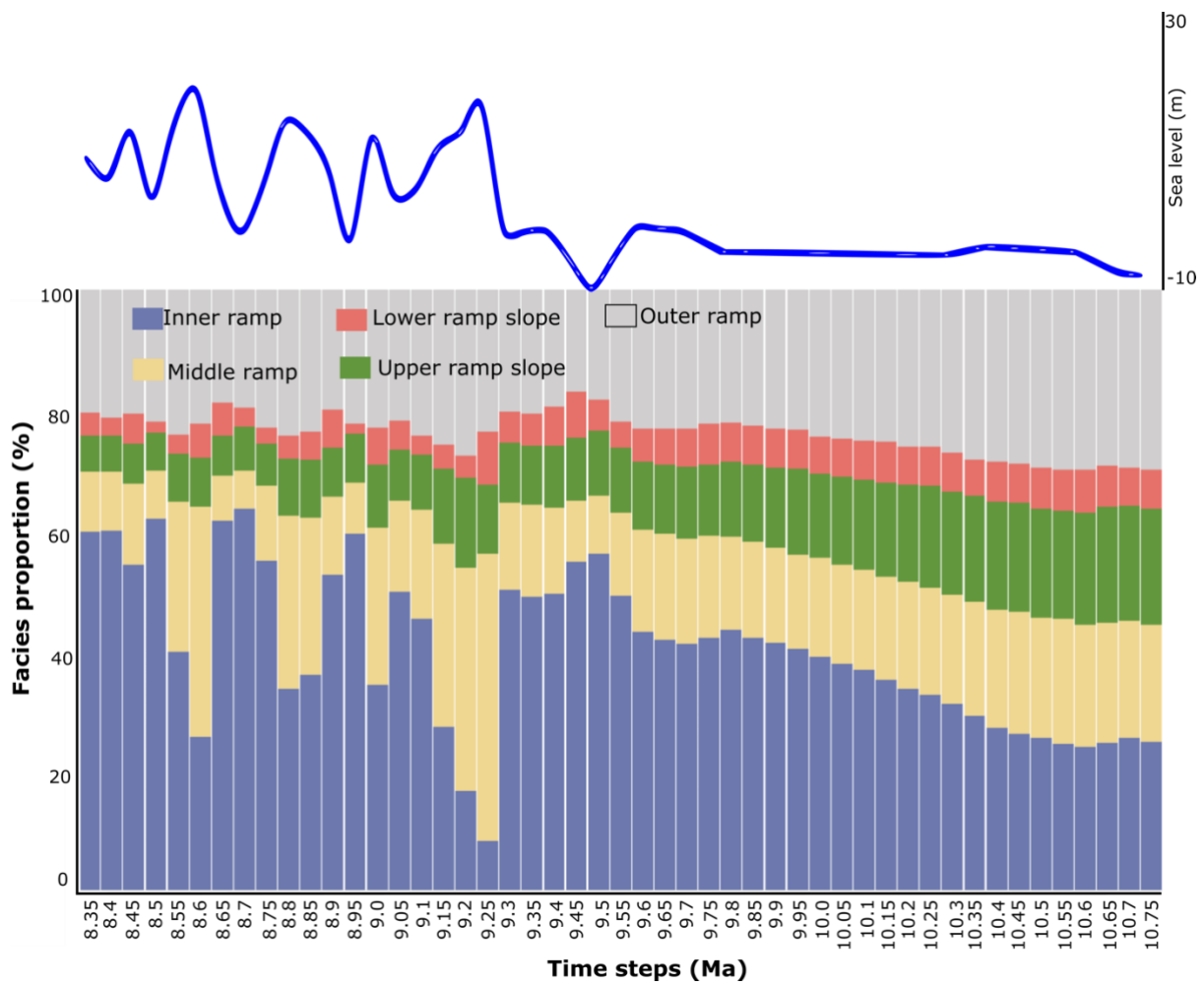
Figure 3.8: Relationship between facies development and sea-level fluctuation.

accumulation sites progressively shift basinward. Dissolution/erosion of the earlier shallower deposits occurs from 9.65 Ma of the simulation due to subaerial exposure as sea-level falls below accumulated sediment thickness, leading to a modification of the ramp geometry in the proximal areas. The consistent basinward shift of carbonate production resulted in high sediment accumulation beyond the gentle ramp slope, resulting in thick distal units without a well-defined slope development. The internal facies geometry of Model SL2 reflects a simple continuous distribution with low heterogeneity. Model SL3 was run with the Haq et al. (1988) short-term sea-level curve to test how higher frequency sea-level changes could influence the ramp model. The most significant impact of this higher frequency sea-level curve is due to the rapid sea-level fall of about 100 m between 10.7 Ma to 10.6 Ma, leading to an abrupt shift
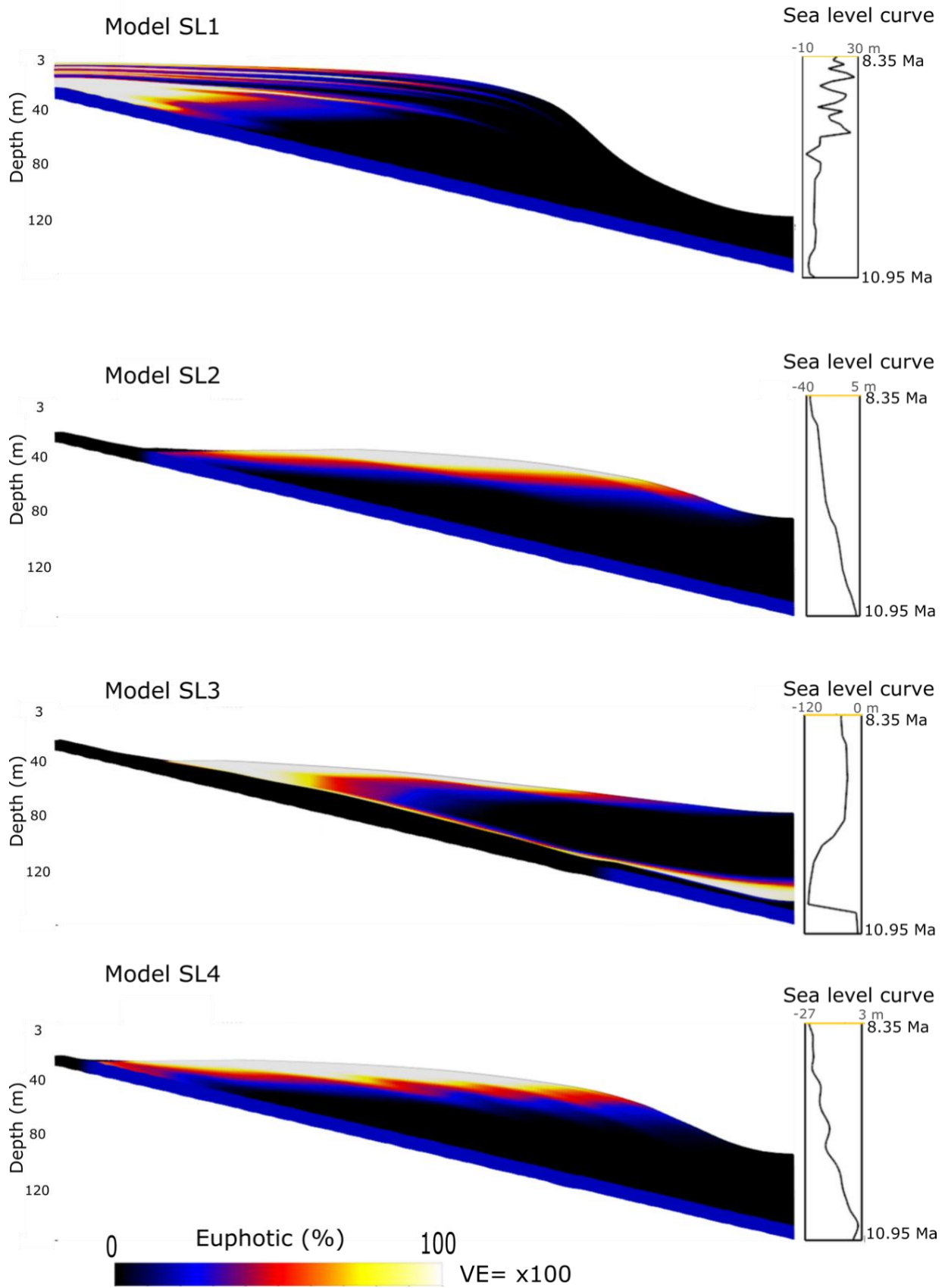
Figure 3.9: Sensitivity analyses testing the influence of sea-level fluctuation patterns.

in sediment production and accumulation locus to the deepest parts of the model domain. The subsequent rise in sea-level from 10.6 Ma to 9.6 Ma did not lead to a significant recovery of sediment accumulation in the shallow areas of the model domain. The progradation arising from the next sea-level still stand was insufficient to develop a ramp slope but rather enhanced the distal thickening. Model SL4 was run with the Miller et al. (2020) sea-level curve, which is also characterised by an amplitude of approximately 30 m in the simulation interval (10.95 Ma to 8.35 Ma), but with a much lower frequency and a near-linear fall in sea-level throughout the simulation interval. The long-term sea-level fall in Model SL4 led to an overall progradation of the ramp, with the development of a distal slope. The basinward part of the slope is, however rapidly filled as the locus of carbonate production shifts basinward in successive timesteps throughout the simulation interval. Although Models SL1 and SL4 share similarities in their overall ramp geometry, their internal geometries differ. While Model SL1 shows a continuous distribution of facies, the facies in Model SL4 show a shingled layer stacking (Read, 1998). The margin of Model SL1 also shows steeper slopes than in Model SL4.

Antecedent slope, initial bathymetry and wave energy

The impact of the antecedent slope and initial bathymetry on the development of the ramp profile was tested using multiple scenarios of bathymetric configuration while keeping carbonate production rates and sea-level curves constant (Figure 3.10). An initial bathymetric setup characterised by a horizontal surface with a uniform water depth of 50 m in Model S1 resulted in a corresponding flat-lying carbonate ramp dominated by euphotic grains (> 60%) and muds/pelagics (> 30%) in the upper 30 m; and mesophotic grains (> 30%), muds/pelagics (>30%) and oligophotic grains (>20%) below 30 m water depth. This bathymetric configuration does not support the accumulation of the rhodolith class, which is produced mainly in water depths greater than 50 m. Increasing the depth of the initial bathymetry to 100 m without an increase in the inclination in Model S2 (Figure 3.10b) did not significantly change the results as in Model S1. A bathymetric configuration of 100 m water depth and a slightly increased slope of 0.001° (Model S3) resulted in the deposition of flat-lying sediments dominated by oligophotic grains, rhodoliths and muds/pelagics at all model timesteps with no accumulation of euphotic grains and less than 15% mesophotic sediment proportion in the shallowest water depths up to about 70 m. Due to the deep initial bathymetry

slope = 0°, depth = 50 m — Model S1

slope = 0.001°, depth = 100 m — Model S2

slope 0.001°, depth = 100 m — Model S3

slope 0.07°, depth = 28 m to 88 m — Model S4

slope 1°, depth = 31 m to 907 m — Model S5

slope 0.15°, depth = 16 m to 147 m — Model S6

Euphotic (%) 0 — 100
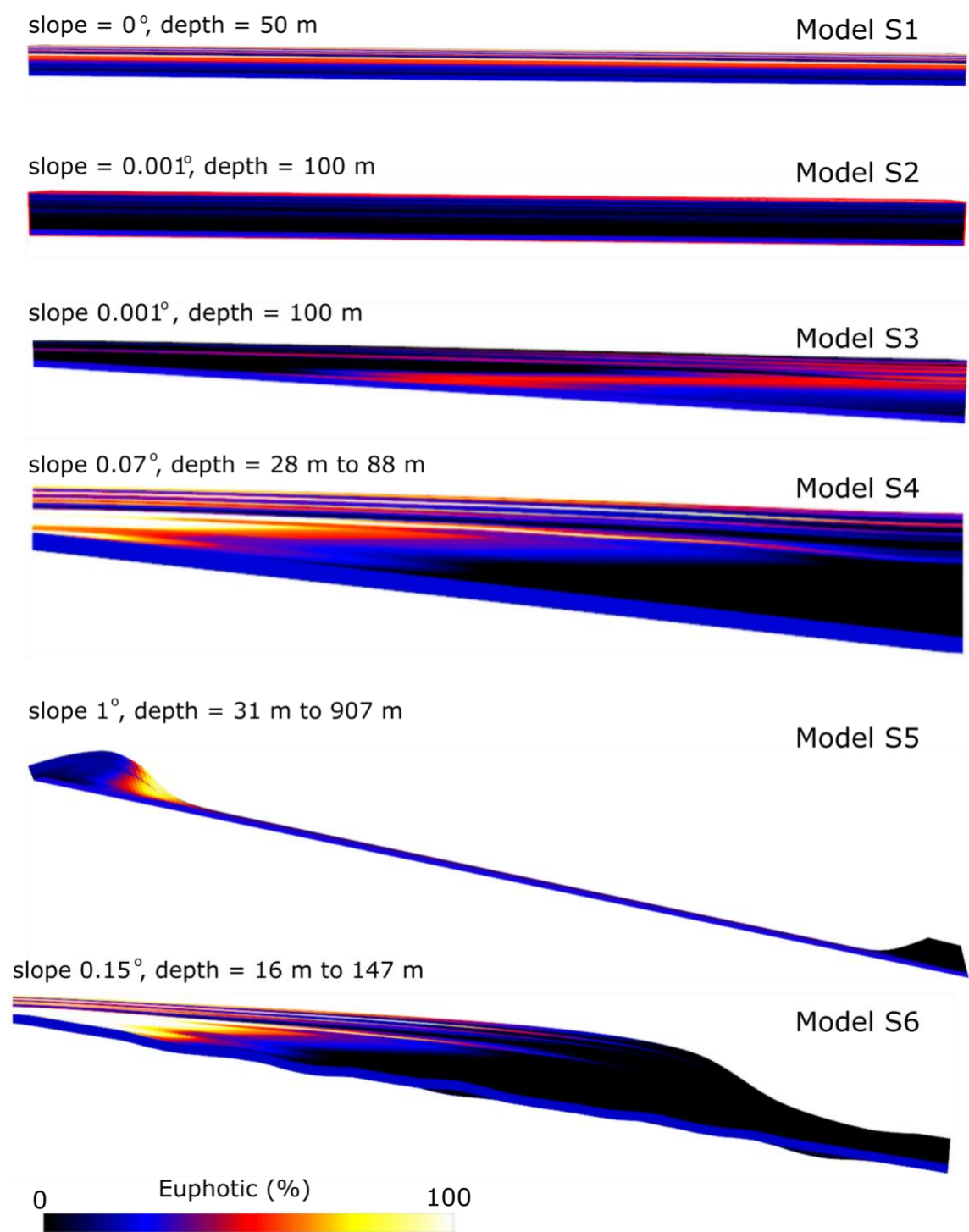
Figure 3.10: Sensitivity analyses testing the influence of the configuration of the initial bathymetry.

across the model domain, accommodation space is created faster than carbonate sediment production in the euphotic and mesophotic zones. Increasing the slope inclination of the initial bathymetry to 0.07° with a relief of 80 m resulted in Model S4, characterised by an internal facies organisation in which euphotic grains developed an interfingering relationship with mesophotic grains as observed in the inner to middle

ramp facies of the Menorca ramp. However, there is no development of a distal slope steepening that is a marked feature of the Menorca ramp. Rhodoliths are also deposited in the deepest part of the model, indicating that slope steepening may develop if the basin has sufficient lateral extent. An initial bathymetry with a steeper slope of 1o created a relief of 876 m across the Model S5 domain. This resulted in the restriction of the ramp development to the shallowest parts (up to 145 m) of the model, with the accumulation of mud/pelagic sediments and minor reworked oligophotic sediment in the deepest parts of the model. Between the shallow accumulation of euphotic grains, mesophotic grains, oligophotic grains and rhodoliths at shallower depths, and the deeper mud/pelagic and reworked oligophotic grains sediment accumulation, there is an extensive zone of non-accumulation of sediment arising from the down-slope transport of sediments. An optimal facies organisation and geometric development of the ramp model was obtained from a slope of 0.15o with a relief of 131 m in Model S6, in which the gentle rate of basin deepening led to a depth of about 150 m in the deepest areas of the model domain. This resulted in the creation of adequate water depths for the accumulation of each model sediment class.

The relationship between wave energy distribution along the ramp profile and the development of the ramp was studied by testing two end member wave bases of 10 m and 40 m, as well as an intermediate depth of 20 m. Model WB1 was developed with a wave base of 10 m (Figure 3.11), in which oligophotic grains accumulated up to the shallowest parts of the model where the maximum wave energy flux is lower than 12 kW/m, thereby creating quiescence in which many coralline red algal organisms thrive. In this condition of shallow wave base, euphotic production is significantly reduced as oligophotic grains dominate the entire ramp profile. Deepening the wave base to 40 m in Model WB2, however, significantly modifies the geometry of the ramp model because of increased wave transport of euphotic grains and the restriction of oligophotic grain production to the deepest areas of the model where wave energy is relatively reduced. In this high wave energy regime, rhodolith production thrived with a sediment proportion in the ramp slope being as much as 90%, despite which there is no significant development of slope steepening owing to the basinward transport of mesophotic grains which fill up the distal part of the rhodolith because of lack of adequate resistance to the increased wave energy, unlike the euphotic grains. However, a wave base of 20 m in Model WB3 resulted in a more representative ramp profile as described in the reference model.

Wave base = 10 m

Model WB1

Wave base = 40 m

Model WB2

Wave base = 20 m

Model WB3

0   Oligophotic (%)   100
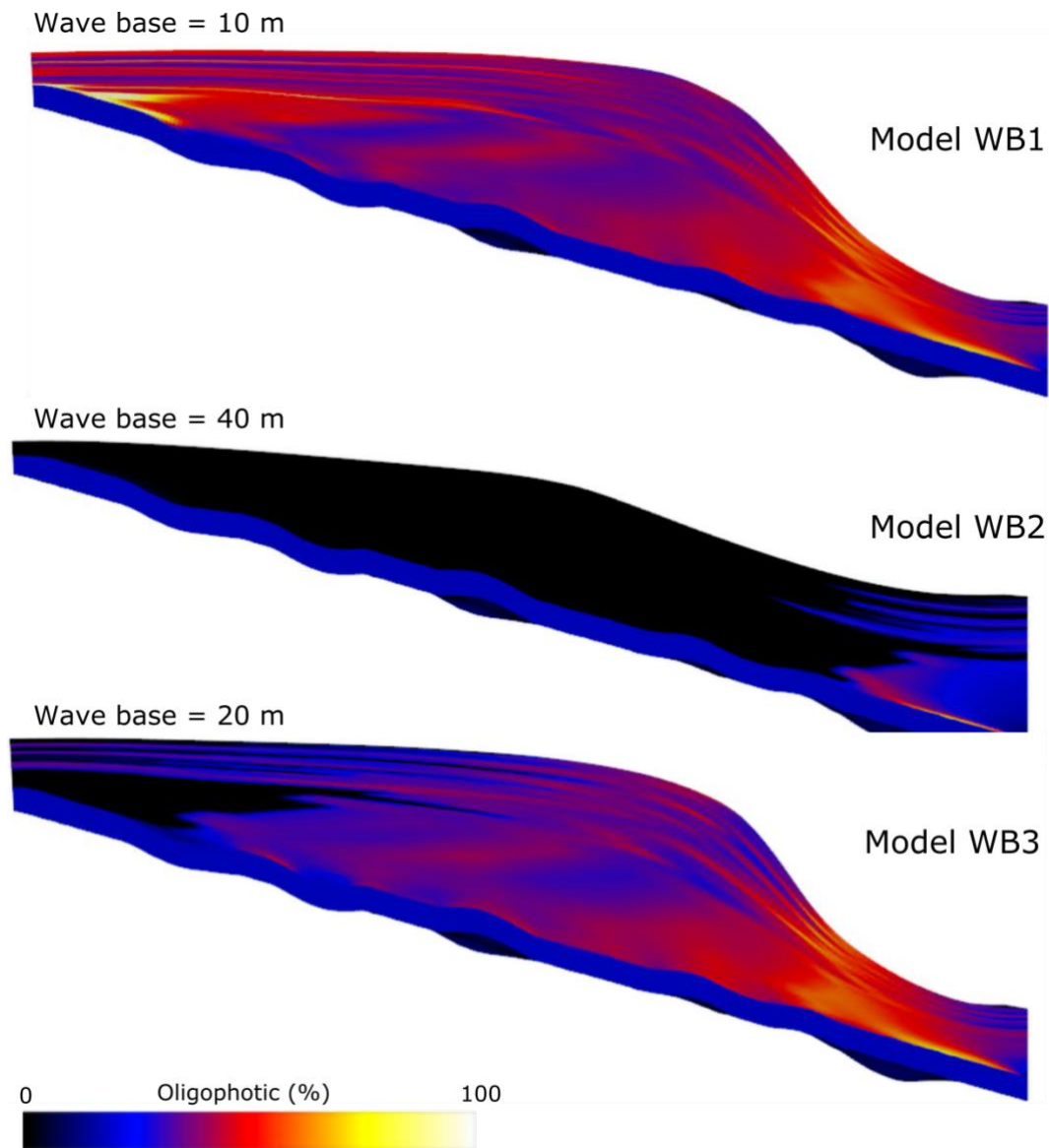
Figure 3.11: Models testing different wave bases.

Carbonate production and sediment transport

The role of differential carbonate production along the ramp profile in ramp development and the slope steepening was tested (Figure 3.12). Model CP1 involved creating higher carbonate production in the deeper facies by significantly reducing carbonate production in the shallow environments by 90% of the reference production rates. This was done by downscaling the production-depth profile of the euphotic, mesophotic grains and rhodolith sediment classes, while retaining the reference production-depth profile of the oligophotic and muds/pelagics classes (Figure 3.11). This carbonate production configuration produced a model dominated by non-rigid high-transport oligophotic grains, which tend to be readily transported along the ramp

profile, and consequently impact the ramp geometry by developing gentle dips from shallow to deep environments. The resultant model is characterised by a gentle transition from the middle ramp to the deeper sections without significant slope development. In contrast, Model CP2, in which deeper carbonate sediment production rates (oligophotic and muds/pelagics classes) are trimmed by 90% of the reference production-depth profile, resulted in much higher gradients from the middle ramp to the ramp slope. Here the gradients transition sharply from 4.5° in the middle ramp to 18° in the ramp slope. Both models contrast with the relatively moderate gradient transition of the reference model from 5° in the middle ramp to 7° in the upper margin of the ramp slope.

To test the possibility of the development of a distally steepened ramp such as in the Miocene of Menorca through significant basinward transport of euphotic dominated carbonate sediments, wave and gravity-driven sediment diffusion in Model CP3 and Model CP4 were increased by one and two orders of magnitude respectively while retaining the parameters of Model CP2, leading to a decrease in the inclination of the ramp slope compared to the reference model (Figure 3.6). Model CP3, however, shows limited sediment accumulation in the distal areas beyond the slope as sufficient sediments are not transported basinward from shallower areas. The increased transport parameters in Model CP4 mode sufficient sediment downslope with an associated decrease in slope inclination and reduced proximal sediment accumulation.

DISCUSSION

Relationship between accommodation variation and ramp geometry

Previous studies have suggested that the Menorca ramp evolved under a high frequency, moderate amplitude sea-level fluctuation (Pomar et al., 2002). This was numerically tested by developing models with varied eustatic sea-level curves. Since there is no field-based evidence of sediment exposure during ramp development (Obrador et al., 1992; Pomar et al., 2002), sediment loss due to subaerial exposure was not considered to impact accommodation changes. Our sensitivity analyses show that sea-level fluctuation, together with carbonate production along the ramp profile, is a main control in the development of the distally steepened ramp (Figure 3.9).
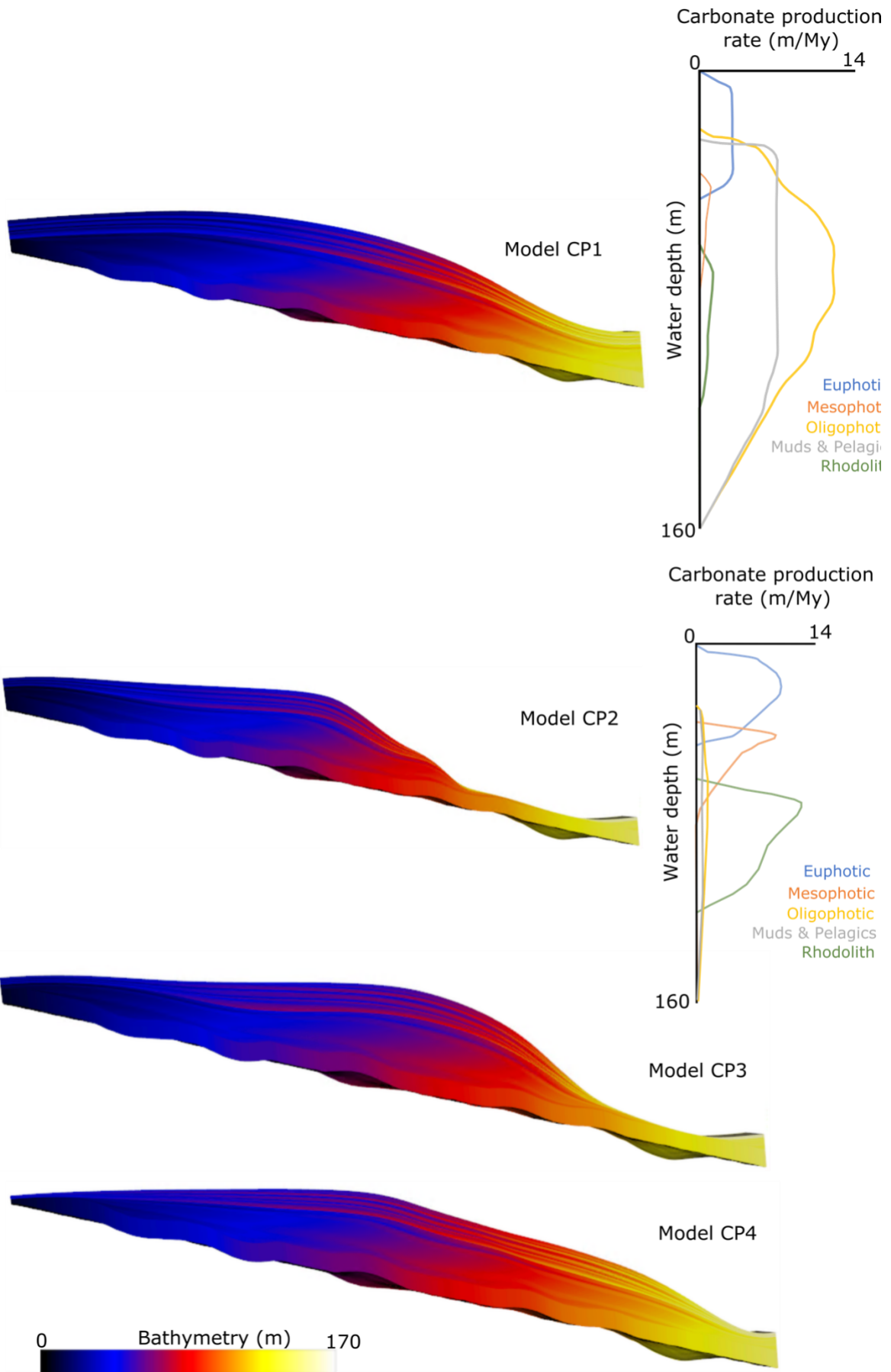
Figure 3.12: Models testing differential carbonate production along the ramp profile.

Models SL1, SL2 and SL4 were developed with sea-level curves characterised by amplitudes ranging between 30 m and 40 m during the simulation interval (Haq et al., 1988; Miller et al., 2005b, 2020). All three models show different degrees of slope development if compared with Model SL3, obtained using the short-term Haq et al. (1988) curve, where no significant slope developed during the considered time. Analysing each model per time step reveals that the development of steep slopes occurs in all three models (Models SL1, SL3 and SL4) at intervals of relatively long sea-level still stands, or periods of sea-level falls (Figure 3.9). This is due to the continuous progradation of the ramp and sediment accumulation on the slope as available accommodation is rapidly filled. This accommodation, however, does not reach up to sea-level (Figure 3.7) but relates to the concept of "shelf equilibrium profile", which illustrates the balance between sediment supply and the tendency of sediments to be mobilised by waves and currents (Swift and Thorne, 1991; Pomar, 2001a; Pomar et al., 2002; Pomar and Kendall, 2008a).

 The frequency of the sea-level fluctuation also influences sediment distribution along the ramp profile. The reference model (Model SL1) is characterised by a significant slope initiated during a low-frequency interval (between 10.3 Ma to 9.85 Ma) and enhanced by the high-frequency fluctuation from 10.6 Ma to the end of the simulation. Model SL1 is characterised by high facies cyclicity, especially in the proximal areas, which reflect high-frequency sea-level fluctuations. This response is typical of icehouse ramps (Read and Horbury, 1993; Read, 1998). The occurrence of ramp progradation and aggradation with clear ramp slopes reflect the balanced interaction between carbonate production rates and high-frequency sea-level changes (Pomar et al., 2002). This response can be linked to the presence of seagrass, which in a modern environment strongly impacts the interaction of the seafloor with hydrodynamics, influencing key processes such as sediment resuspension and particle trapping leading to high sediment accretion rates in shallow water areas (Hendriks et al., 2010; Potouroglou et al., 2017). Even on a Heterozoan ramp, such as the Upper Miocene of Menorca, the presence of seagrass contributes to sediment accretion in the euphotic zone, mimicking the depositional patterns commonly related to Photozoan carbonates.

Models SL2 and SL3 are characterised by low slope angles, low facies cyclicity and aggradational stacking, reflecting rapid filling of available accommodation due to high sedimentation rates. These characteristics are typical for low amplitude, low-frequency

sea level variations such as those described in greenhouse ramps (Goodwin and Anderson, 1985; Read and Horbury, 1993; Read, 1998). However, a lower frequency sea-level curve during the simulation interval presents a contrasting scenario with no slope development as sediment accumulation is sustained at relatively uniform rates over greater lateral extents for longer time intervals. Model SL3, simulated with the short-term Haq et al. (1988) sea-level curve, characterised by a rapid fall of 115 m within the first 0.5 Ma of the simulated interval, resulted in a basinward shift of all sediment-producing sites. The subsequent low-frequency sea-level fluctuation resulted in flat-lying deposits. However, the recovery of sedimentation along the ramp profile (Model SL3) may imply that steep slopes will eventually develop but at greater lateral distances beyond the model domain, leading to extensive inner and middle ramp facies. Model SL4, on the other hand, reflects a transitional ramp's characteristics by its intermediate slope angle and moderate facies cyclicity.

Closely related to the impact of sea-level variation on the ramp geometry is the configuration of the initial bathymetry (substrate physiography), a surface representing the inherited topography and paleo-water depth at the initiation of the ramp. Substrate paleoslope has been recognised as a significant control on some ramp facies evolution and development (Olsson, 1988; Franseen et al., 1997; Pomar et al., 2014), with its strong influence on the physical conditions at play during ramp development (Choi and Simo, 1998; Elvebakk et al., 2002; Williams et al., 2011). Our sensitivity models tested the impact of the depth and inclination of initial bathymetry on the development of ramp geometries (Figure 3.10), and the results indicate that the depth and inclination of the initial bathymetry influence the carbonate deposition in a system characterised by multiple grain associations like the Menorca ramp, which in turn influences the development of slopes (Pomar, 2020). Tests with varied initial bathymetric configurations indicate that the inclination and physiography of the substrate impact the geometry of the resultant carbonate ramp by modulating the amount of accommodation space available for biogenic carbonate production. Steeper initial bathymetries result in very high accommodation in which the lateral extent of the photic zone is minimal, thereby leading to a volumetrically low carbonate ramp development. The amount of accommodation created by horizontal to sub-horizontal initial bathymetries depends on water depth, with optimal water depths for light-dependent carbonate producers leading to a laterally extensive ramp development. An example of such an extensive and thin low-angle carbonate ramp is the Nisku Formation of the

West Canada Basin (Watts, 1987). The carbonate ramps of the Arabian Gulf further exemplify the development of extensive low-angle ramps over paleosurfaces characterised by the low inclination of much less than 1° (Walkden and Williams, 1998). Our models (Figure 3.10) further demonstrate that optimal geometric development of the ramp profile requires a balance between water depth and the inclination of the initial surface. As shown in Models S1 to S6, the inclination of the surface regulates the rate of basin deepening, which consequently determines the rate of transition from the depth zone of one sediment class (biogenic carbonate producer) to the other. Steep initial surfaces lead to a higher rate of accommodation creation than the biogenic producers can keep up with (Model S5. This suggests the impact of high relief along lateral accommodation stretch on the development of carbonate ramp geometries. Consequently, as most shallow marine carbonate producers are most productive in shallow environments, available accommodation for carbonate sediment accumulation is restricted to only a small shallow band. Williams et al. (2011), while providing insights into the roles of sediment transport in the evolution of carbonate systems geometries, demonstrated that transport-dominated ramps tend to reflect the geometry of the underlying topography. Our sensitivity tests advance this understanding (Williams et al., 2011) by showing that ramp geometries tend to reflect the antecedent topography provided that the paleoslopes are characterised by relatively low-angle. As the inclination gradually increases, such as from 0.07o in Model S4 to 0.15o in Model S5, the ramp profile becomes more influenced by the depth constraints on the carbonate sediment producers than by the geometry of the underlying topography. The inclination of the paleoslope also influences internal facies organisation as facies differentiate better with increasing inclination of the paleoslope.

Effects of carbonate production and transport on ramp geometry

The sensitivity tests we ran on the carbonate production attempted to provide an insight into how distally steepened ramps are impacted by differential carbonate production (Figure 3.12). Model CP1, which represents a system dominated by sediment production in oligophotic (relatively deeper) settings, shows that high transport biogenic sediment production concentrated in oligophotic settings tends to produce homoclinal or low angle ramps. This is the characteristic response of carbonate systems dominated by heterotrophic producers (Carannante et al., 1988; James, 1997; Pedley and Carannante, 2006; James et al., 2009; Mutti, 2019), in which

the main biogenic systems produce non-rigid sediments that are readily redistributed by waves, currents and gravity. Examples of such systems are the low-angle Lower and Middle Miocene ramps of Central Mediterranean, where sediments are mainly composed of bryozoan/algal rich rudstones, rhodoliths and hemipelagic marls (e.g., Franseen and Esteban, 1996; Mutti et al., 1997; Knoerich and Mutti, 2003; Benisek et al., 2009). Conversely, concentrating sediment production in the seagrass-controlled euphotic zone (Model CP2) shows a sedimentary response which tends toward rimmed shelf geometry. As noted by James et al. (2009) from their study of marine seagrass carbonate systems in southern Australia, the characteristic poorly sorted sediments in seagrass-dominated environments tend to remain trapped, which could lead to the vertical accretion of sediments in the shallow areas, thereby creating steep slopes as in Model CP2 (Figure 3.12). Therefore, for a distally steepened ramp to develop, such as in the Upper Miocene Menorca ramp, there is the need for an intricate balance between the multiple carbonate production components (Pomar, 2020). The oligophotic and light-independent components (muds/pelagics) are necessary for inhibiting the transition of the ramp into a flat-topped platform by creating sufficient sediments that balance up accumulation beyond the ramp slope.

Sediment transport processes also play an essential role in determining the geometry of ramps. Our models (Figure 3.12) illustrate how sediment transport processes could modify ramp geometries, whereby higher transport coefficients tend to push more sediments basinward. However, sensitivity tests (Figure 3.12) indicate that, as also shown by Pomar and Kendall (2008b), the evolution of distally steepened ramps involves a complex interaction between a highly productive, low-transport shallow carbonate production with a high-transport oligophotic production. The models in Figure 3.11 illustrate how the wave base tends to modify the ramp architecture. Wave base influences ramp development in two main ways: 1) it regulates the depth for the development of both euphotic grains and oligophotic grains by changing the energy dynamics within the basin; 2) it creates a change in sediment transport characteristics along the ramp profile. A steeper slope, therefore, tends to form where the wave base is shallow (Models WB1 and WB3), as more oligophotic sediments can accumulate in situ with less sediments being transported away from the inner/middle ramp areas. These results are consistent with the inferences of Pedley and Grasso (2006), who observed that basinward sediment transport from inner and mid-ramp areas caused the low-angle profile of carbonates in Sicily/Malta (Knoerich and Mutti, 2003). The

complex interplay of carbonate sediment production and sediment transport as modelled in the Menorca ramp is also observed in the Neogene carbonates of south-eastern Spain (Braga et al., 2006).

General implications of the model

Carbonate systems, particularly Photozoan carbonates, have been known to effectively preserve records of sea-level changes due to their depth dependence (Kendall and Schlager, 1981; Schlager, 2005; Kim et al., 2012). Provided sedimentation can keep up with the shelf equilibrium profile (Pomar and Kendall, 2008a, 2008b), lateral facies shifts track sea-level fluctuations (Handford and Loucks, 1993; Tucker et al., 2009a). However, Heterozoan carbonates are considered less reliable indicators (John and Mutti, 2005). Our model defined different facies with a significant relationship with sea-level fluctuation such that grainy facies (middle ramp and ramp slope facies) increase in proportion (Figure 3.8) during episodes of sea-level rise. The presence of seagrass contributes to sediment accretion in the euphotic zone, mimicking the depositional patterns commonly related to Photozoan carbonates, even on a Heterozoan ramp, such as the Upper Miocene of Menorca, and interplaying with different carbonate production along the ramp profile in response to sea-level fluctuations, is a main control in the development of the distally steepened ramp.

CONCLUSION

This paper approached the question of the impact of sea level amplitude and frequencies, carbonate production (dominated by Heterozoan biotas versus Photozoan biotas), as well as wave energy propagation and antecedent topography on the evolution of distally steepened ramps by developing a stratigraphic forward model referenced to the upper Miocene Menorca ramp.

Our sensitivity experiments show that sea-level amplitudes and frequencies play a significant role in the geometry of carbonate ramps. Carbonate ramps which develop during sea-level fluctuations characterised by a moderate amplitude (e.g., 30 to 40 m in our models) will tend to develop distally steepened sloped compared to ramps evolving in a higher amplitude sea level fluctuation scenario. The models show that a combination of moderate amplitude and high-frequency sea-level fluctuation offers a suitable condition for distally steepened ramp development.

The models also relate ramp geometry to the variability of Heterozoan versus Photozoan carbonate production. Even if the ramp is Heterozoan dominated, the presence of seagrass introduces a key, light-dependent component. Seagrass-dominated shallow carbonate production tends to result in steep slopes due to the low-transport characteristic of this sediment class. This steepness can, however, be altered by the introduction of high transport sediment grains from deeper carbonate producers, which fill the slopes and more distal sections of the ramp profile. This underscores the significance of seagrass sediment trapping in the development of ramp geometry, whereby accumulated sediments are protected from downslope transport, leading to the development of steep slopes.

Antecedent slope is a critical factor that influences the geometry of carbonate ramps. The steepness of the paleosurface impacts facies distribution along the ramp profile as the models show that flat paleosurfaces tend to produce facies which are simply differentiated vertically across the platform. Although previous studies have demonstrated that transport-dominated ramps tend to reflect the geometry of the underlying topography, our sensitivity tests show that this concept is valid only for relatively low-angle paleoslopes. The ramp profile becomes more influenced by the depth constraints on the carbonate sediment producers than by the geometry of the underlying topography as the inclination of the paleosurface increases. The optimal geometric development of the ramp profile requires a balance between water depth and the inclination of the initial surface.

ACKNOWLEDGEMENT

Chapter 4
INVESTIGATING BIOGENIC SEDIMENT THRESHOLDS REQUIRED FOR THE DEVELOPMENT OF STEEP MARGINS IN CARBONATE SYSTEMS THROUGH FORWARD MODELLING

ABSTRACT

The geometries of carbonate systems, which may range from homoclinal ramps to flat-topped platforms with steep margins, have been attributed to the dominant biogenic carbonate producers. Several examples in the geologic record and in modern systems show that Photozoan-dominated carbonate systems typically evolve as forms of rimmed platforms, while Heterozoan-dominated systems typically develop ramp profiles. This suggests that Photozoan sediment production is a necessary requirement for the evolution of rimmed platforms with steep margins. However, the minimum amount of Photozoan sediments in a system required for the development of significant slopes is not yet known. This study presents a novel approach by using stratigraphic forward modelling combined with automated sensitivity analysis to investigate the minimum threshold of Photozoan sediments required to form platforms with steep margins. We also extended this by examining the possibility of seagrass trapping of sediments in a Heterozoan-dominated system to enhance the formation of steep slopes. This was done by establishing two forward models representing a Photozoan-dominated flat-topped platform, and a seagrass-influenced Heterozoan distally steepened ramp. Sensitivity experiments were done on both models to determine the relationship between the geometry and proportion of Photozoan sediments and seagrass-influenced sediments. The models show that in a Photozoan-dominated environment, steep margins begin to develop as the proportion of Photozoan sediments becomes greater than a threshold of about 40%. Below this threshold, the amount of Photozoan sediments is not sufficient to develop steep margins. Above this threshold, there is a varied possibility of margin development. The models also suggest that margin steepness increases as the effectiveness of seagrass trapping increases. However, slope development in a seagrass-influenced Heterozoan environment would need to be stabilized in conjunction with adequate sediment fabric development or microbial binding. In the Photozoan-dominated system, the magnitude of slope steepness depends on the proportion of Photozoan

sediments in the system. This study presents an additional classification tool for carbonate systems based on their biogenic components, as systems with Photozoan sediment proportion below the threshold tend to not develop steep margins.

Keywords: Photozoan, Heterozoan, distally steepened ramp, slope, flat-topped platform, forward modelling, sensitivity analysis

INTRODUCTION

Carbonate systems represent a continuum of depositional profiles that range from flat-topped platforms with steep margins to homoclinal ramps with gentle uniform dips and a variety of forms in between these end members (Ahr, 1973; Burchette and Wright, 1992; Pomar, 2001b; Bosence, 2005; Pedley and Carannante, 2006). Factors considered to be responsible for these geometries include tectonics (Burchette, 1988; Bosworth et al., 1998; King et al., 2012), sedimentation rate (Smith and Kinsey, 1976; Schlager, 1993), sediment fabric (James and Mountjoy, 1983; Kenter, 1990; Kenter et al., 2005), and eustasy (Kendall and Schlager, 1981; Eberli and Ginsburg, 1989; Pomar and Ward, 1995; Cathro et al., 2003; Pedley and Grasso, 2006). Biological evolution trough time and the dominant type of biogenic carbonate sediments have also been recognised as significant determinants in the evolution of carbonate systems profiles (Pomar, 2001b). This is because most shallow marine carbonates are biogenic in origin (Tucker et al., 2009b). Biotic sediments in carbonate systems are contributed by organisms broadly grouped into Heterozoans and Photozoans (James, 1997). The Heterozoan biotic association represents carbonate-producing organisms such as coralline algae, bryozoans, molluscs, foraminifera, as well as echinoids and ahermatypic corals which often dominate environments characterised by cool temperatures (Halfar et al., 2004) and requiring little or no light penetration for survival (Pomar, 2001b; Schlager, 2005). In contrast, the Photozoan biotic association, which includes green algae, hermatypic corals, and ooids, is associated with warm tropical waters (Halfar et al., 2004), and requires high light penetration (Pomar, 2001b; Schlager, 2005). Each of these biotic associations is related to a specific spectrum of carbonate geometries (Schlager, 2005; Pomar, 2020). Flat-topped platforms generally result from the dominance of Photozoan biotas such as shallow water frame builders producing grainy bioconstructions (Wilson, 1975; Read, 1982; James, 1997). Ramps are often the result of Heterozoan sediments which are typically characterised by high

susceptibility to redistribution by waves and currents (James, 1997). Photozoan biotas in carbonate systems have been recognised to produce low-transport sediments which form rigid frameworks that can withstand high energy conditions (Montaggioni, 2005; Schlager, 2005). This implies that carbonate systems dominated by Photozoans develop steep margins with significant slope breaks (Carannante et al., 1988). On the other hand, Heterozoan biotas are unprotected from redistribution by waves and currents, and therefore tend to build high-transport carbonate ramps characterised by gentle gradients from proximal to distal areas (Pomar, 2001b, 2020).

The geologic record suggests that the proportion of Photozoan biotas in carbonate systems forms a spectrum of carbonate profiles, whereby low or insignificant Photozoan proportion results in ramp geometries and high Photozoan proportion results in well-developed margin slopes. This seems to suggest that Photozoans are a necessary requirement for the development of flat-topped platforms. For example, the Upper Tortonian – Lower Messinian Llucmajor platform is defined by significant steep margins and comprised a high abundance of Photozoan biotas strongly prograding over a Heterozoan base (Pomar, 1993; Pomar et al., 1996). The Albian rimmed platform in Gobea, western Apennines also illustrates the roles of Photozoans in creating steep margins on carbonate systems (Gómez-Pérez et al., 1999). Carbonate systems with low Photozoan sediments proportion develop some margin slopes which usually are not steep enough to be termed actual flat-topped platforms. This is exemplified by the geometric turnover from ramp to margin slope steepening in the Burdigalian Sedini Limestone, where the change in platform profile is attributed to the introduction of corals into the system (Benisek et al., 2012). Ramps are an end member of this spectrum where the absence or low proportion of Photozoans results in the preclusion of steep margin development. This is exemplified in ramps such as the Latium-Abruzzi ramp (Brandano et al., 2012), the Menorca ramp (Pomar et al., 2002; Mateu-Vicens et al., 2008) as well as in modern settings such as the Arabian Gulf (Walkden and Williams, 1998). This paper is therefore based on the hypothesis that, if Photozoans have been shown as essential in steep margin development in both modern and ancient settings, there should be a threshold of Photozoan proportion in a carbonate system required for steep margins to develop.

The aim of this research is to determine the minimum Photozoan proportion required for steep margin development in shallow marine carbonates by using a theoretical framework and analysis based on stratigraphic forward modelling (Bice, 1988; Boylan et al., 2002). Stratigraphic forward modelling presents an approach to quantitatively test different scenarios of carbonate system development. We believe this approach can give further quantitative insights into the role of Photozoans in carbonate systems development, which can then be matched with field investigation. Such investigations will advance the current understanding of the roles of carbonate production by different biotic associations. It will also provide an improvement in the classification of carbonate systems geometries based on their constituent biogenic sediments.

METHODOLOGY

Model development and initial parameters

Modelling for this study was done using Dionisos, a forward modelling software developed by Beicip Franlab. Dionisos simulates digital stratigraphies through the quantitative synthesis of sedimentary processes that were at play during the evolution of a sedimentary system. The simulation mathematically relates the processes of basin alteration through tectonics and sediment loading, sediment supply and transport, as well as accommodation variation effected by eustasy and subsidence (Granjeon and Joseph, 1999). Forward modelling of carbonate systems, therefore, requires inputs such as an initial substratum surface, in situ carbonate sediment production, sediment transport, sea level curves and subsidence data. This approach has been used in this study to develop models that spatially and temporally reproduce the architecture of carbonate systems under variable influences of sediment supply and transport regimes.

Carbonate sediment production in Dionisos is simulated through a depth-dependent variation of sediment production rate in relation to a maximum production rate (Bosscher and Schlager, 1992). The amount of sediments retained in a cell of the model is influenced by processes such as accommodation change, wave energy flux, climatic changes, and changes in other ecological stress etc, through geologic time, which determine the amount and type of sediment produced (Warrlich et al., 2002; Schlager, 2005; Wright and Burgess, 2005). This implies that in carbonate systems with multiple grain associations, carbonate production is simulated through a series of

production versus depth curves which produce carbonate sediments at rates that are a fraction of pre-set maximum production rates.

Carbonate production in the models is simulated based on the relationship of carbonate depositional profiles to the net carbonate accumulation (Pomar, 2020). The depth-dependent production of carbonate sediments allows the characterisation of carbonate biotas into euphotic, mesophotic, oligophotic and aphotic biotas (Pomar, 2001b). The dominance of each of these biotic categories determines the carbonate depositional profile (Pomar, 2020; Figure 4.1). Deeper water production of loose grains (curve A) will lead to a low-angle ramp. Distally steepened ramps will develop from a relatively shallower production of loose grains (curve B). Curves A and B are unable to fill the whole physical accommodation controlled by the wave energy which is higher above the wave base. Shallow water loose grains (c) will result in the development of open shelves as sediments accumulate above the wave base. Shallow water framework sediments fill the high-energy ecological accommodation to form steep margined platforms.
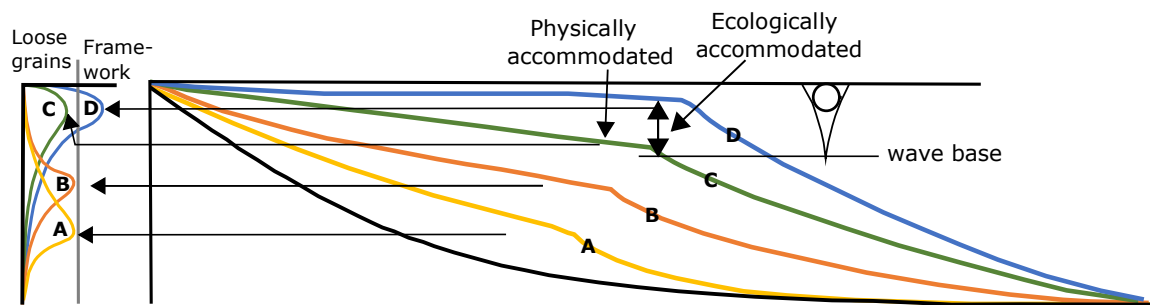
Figure 4.1: Carbonate depositional profiles as functions of sediment accumulation and bathymetry (modified from Pomar, 2020).

Sediment transport is a critical parameter in modelling carbonate systems as it defines the process of sediment entrainment in the model. Dionisos simulates sediment transport through an implicit function finite difference method that uses a modified diffusion formula stated as follows:

$$Qs = K * S \qquad\qquad (1)$$

where Q_S is the sediment flux, S is the topographic gradient and K is the diffusion coefficient in square meters per year. The implication of this is that the sediment transport rate at any given point in the model depends on the topographic gradient and the diffusion coefficient at that point (Granjeon and Joseph, 1999). Although

diffusion coefficients are poorly constrained for sedimentary systems, rigid sediments are generally characterised by lower diffusion coefficients than loose sediments (Williams et al., 2011; Tella et al., 2022b).

The numerical experiments in this study are designed based on sensitivity analyses carried out on two stratigraphic forward models representing a low transport flat-topped Photozoan platform (Reference A), and a high transport Heterozoan ramp (Reference B). The parameterization of these models follows the model specification in Tella et al. (2022b) for Reference A, and (Tella et al., 2022a) for Reference B, with parameters selected based on the range of values observed in natural systems. Reference A represents a flat-topped rimmed platform dominated by shallow Photozoan biota capable of building wave-resistant coral frameworks prograding over a Heterozoan base. Reference B represents a distally steepened ramp primarily constituted of Heterozoan biota with an effective shallow seagrass factory.

Modelling Approach for a low-transport flat-topped platform (Reference A)

Reference A runs on a 38 km long two-dimensional section (Figure 4.2a) defined by square grid cells which are 200 m in length. The model is characterised by a wave base of 20 m controlling wave energy flux per depth as shown in Figure 4.2b, which is the average wave base reported for shallow marine environments (Coe et al., 2003), and runs over an interval of 2 My and a constant subsidence rate of 20 m/My, with an initial surface characterised by a bathymetric range of about 250 m and a proximal slope of 2.3^{o} which passes basinward into a subhorizontal surface with a bathymetry of up to 250 m.

Carbonate sediment supply in Reference A (Figure 2c) is characterised into five classes. This assumes that carbonate sediment production across a flat-topped platform such as in the Llucmajor platform (Pomar et al., 1996) follows sediment production in different depth zones dominated by different biotas which produce sediments of different types and resistance to redistribution. These depth zones are summarised as follows:

Euphotic 1: represents carbonate production at the shallowest euphotic zone up to 30 m and is defined by low diffusion coefficients of 0.0001 km^2/kyr (Table 4.1) to simulate

the stability of sediments produced by this class. In typical shallow marine reefs, the Euphotic 1 class represents carbonate sediments produced in the reef crest.

Euphotic 2: represents Photozoan sediments produced in the euphotic zone corresponding to the reef wall in modern reefs. Sediment production in this class occurs at depths from about 15 m and declines to zero at a depth of about 60 m (Figure 4.2c). Sediment transport here is also very low and defined by diffusion coefficients of 0.0005 km^2/kyr (Table 4.1).

Figure 4.2: Model setup for Reference A: (a) Initial bathymetry for Reference A, Ø1 is 2.3°. (b) hydrodynamic simulation influencing carbonate production and transport (c) Carbonate sediment production versus depth curves (d) Reference A model showing the simulated environments and geometry (from Tella et al. 2022b)

Heterozoan class: This represents sediment production in the oligophotic zone and is characterised by higher sediment transport rates defined by diffusion coefficients of 0.005 km^2/kyr (Table 4.1). Carbonate production reaches depths of about 140 m and occurs in low-energy regimes (Figure 4.2c).

Table 4.1: Modelling parameters for the Photozoan model

Model	Initial Bathymetry	Duration	Subsidence Rate (m/My)	Carbonate Production Rates (m/My)					Diffusion coefficient (km2/kyr)				
				Euphotic 1	Euphotic 2	Heterozoan	Carbonate grains	Carbonate Muds	Euphotic 1	Euphotic 2	Heterozoan	Carbonate grains	Carbonate Muds
Reference A	Figure 4.2a	2 My	20	1000	800	400	100	450	0.0001	0.0005	0.005	0.005	0.05
Model A	Figure 4.2a	2 My	20	0	0	200	0	0	0.0001	0.0005	0.005	0.005	0.05
Model B	Figure 4.2a	2 My	20	62	50	400	6	28	0.0001	0.0005	0.005	0.005	0.05
Model C	Figure 4.2a	2 My	20	250	200	400	25	112	0.0001	0.0005	0.005	0.005	0.05
Model D	Figure 4.2a	2 My	20	500	400	800	100	450	0.0001	0.0005	0.005	0.005	0.05

Carbonate grains: represent sediment grains with high tendency of being transported by waves and current, such that though they are mostly produced at shallow depths (Figure 4.2c), they can be transported to deeper realms.

Carbonate muds: represent sediments deposited across the platform through suspension and are abundant in the deeper realms of the platform (Figure 4.2c).

The carbonate sediment production rates as given in Table 4.1 are from values estimated from modern analogues and from ancient platforms (e.g., Adey and Vassar, 1975; Davies and Hopley, 1983; Henrich et al., 1995; Montaggioni, 2005; Schäfer et al., 2011).

Reference A (Figure 4.2d) was modelled to reproduce four main environments, which are the backreef lagoon, reef core, forereef slope and open shelf.

Modelling Approach for a seagrass-influenced carbonate ramp (Reference B)

Reference B runs on a 50 km long two-dimensional grid (Figure 4.3a) with square grid cells 200 m in length. The total duration of the simulation is 4 My with a constant subsidence rate of 20 m, and an initial surface defined by relief of 135 m and a gentle homoclinal slope of 0.15^o. The wave base in Reference B is 20 m which is considered a general average for shallow water environments (Coe et al., 2003), and defines the vertical propagation of wave energy flux (Figure 4.3b).

Carbonate sediment supply is defined by five model sediment classes (Figure 4.3c) following the modelled sediment classes of Tella et al. (2022a) and are summarised as follows:

Euphotic (seagrass environment): this class simulates carbonate sediment production in the shallow areas characterised by seagrass trapping of sediments. Sediment production occurs in the shallowest areas of the model up to depths of about 40 m and is defined by diffusion coefficients of 0.001 km2/kyr (Table 4.2).

Heterozoan 1: this class represents carbonate sediment with maximum production at depths between 60 and 80 m and reaching as deep as 160 m. Sediment redistribution by gravity and current is common and defined by diffusion coefficients of 0.001 km^2/kyr (Table 4.2).

Heterozoan 2 (Rhodolith): this class (Figure 4.3b) represents sediments that are often accumulated as red algal nodules in ramp slopes. They are often the main
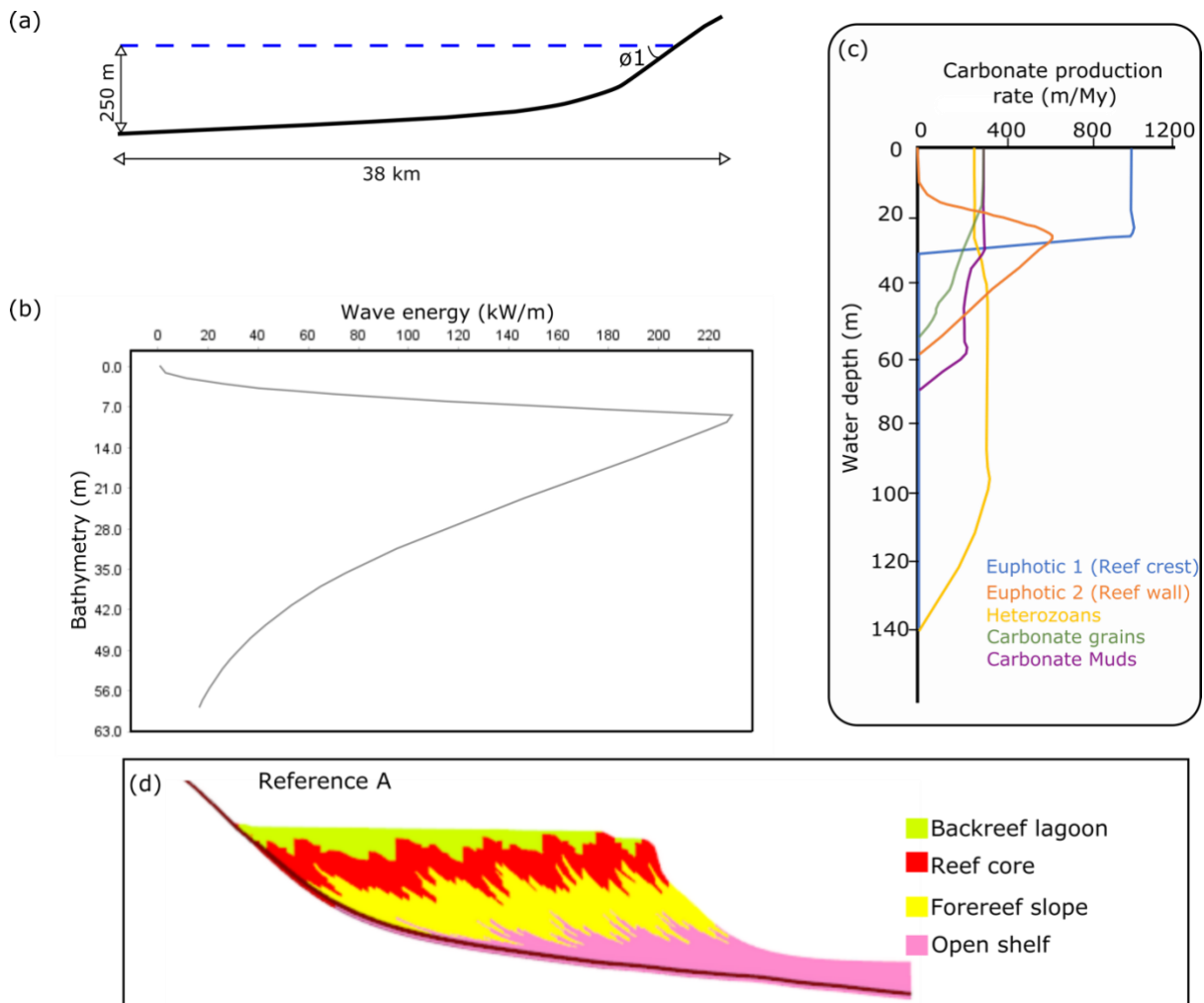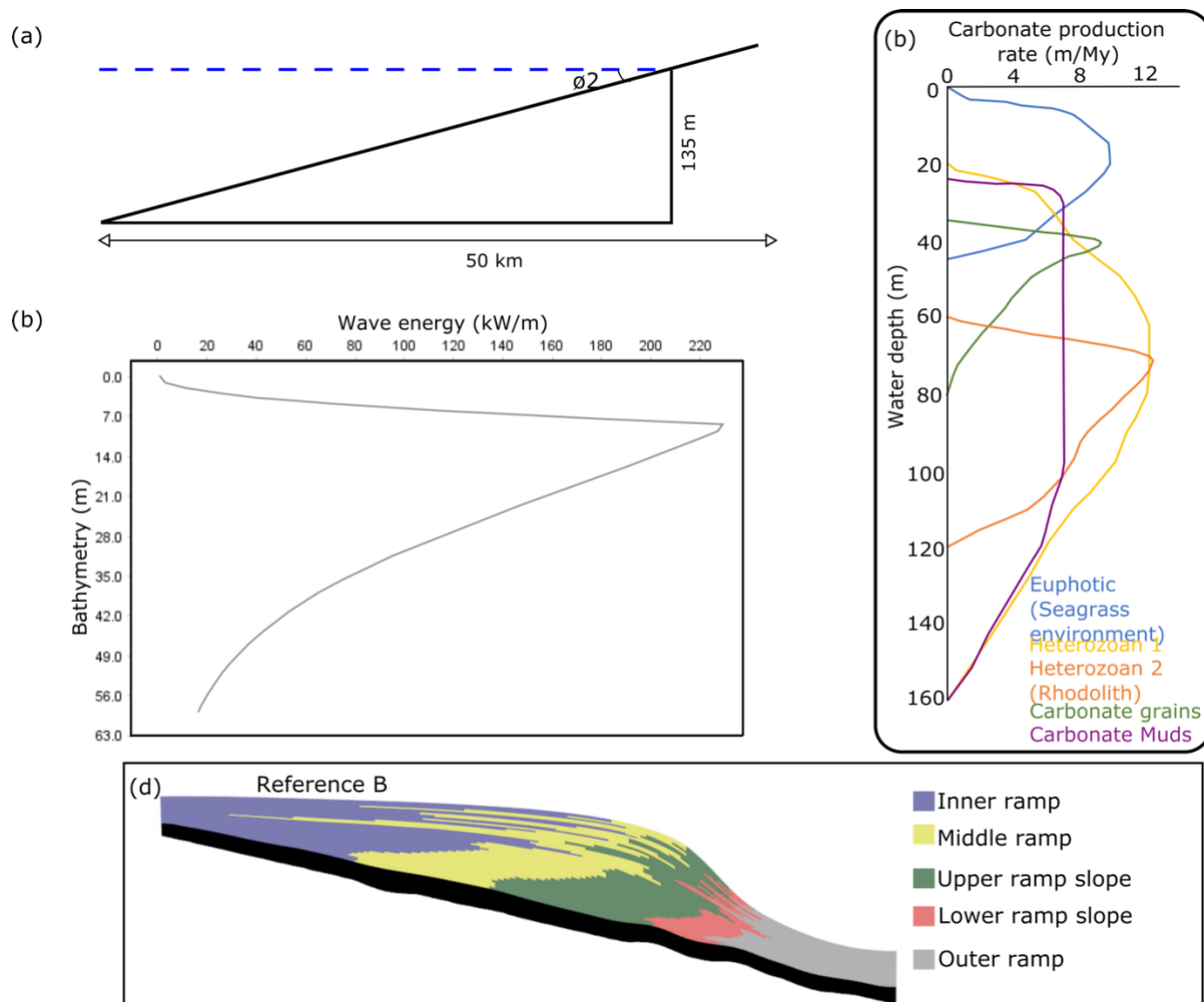
Figure 4.3: Model setup for Reference B (a) Initial bathymetry for Reference A, Ø2 is 0.15°. (b) hydrodynamic simulation influencing carbonate production and transport (c) Carbonate sediment production versus depth curves for the ramp model (d) Reference B model showing the simulated environments and geometry (from Tella et al. 2022a)

components that build steep margins in distally steepened ramps and thus are characterised by relatively low transport which is defined in Reference B by a diffusion coefficient of 0.0001 km^2/kyr (Table 4.2).

Carbonate grains: this class represents sediments produced in typical middle ramp environments. Production is from about 30 m to 70 m (Figure 4.3b) and is defined by a diffusion coefficient of 0.01 km^2/kyr (Table 4.2).

Carbonate muds: this class simulate sediments that are typically light-independent and thus can occur at all water depths. They are readily transported and are therefore defined by a diffusion coefficient of 0.1 km^2/kyr (Table 4.2).

Production rates of these classes are given in Table 4.2 and have been estimated from Heterozoan sediment production rates measured in modern analogues (Ros et

al., 1985; Brown, 2005) and inferred from the geologic record (Cita et al., 1978; Scholle et al., 1983; James and Bone, 1991).

Reference B is a distally steepened ramp model (Figure 4.3d) which is characterised by five main environments, which are the inner ramp, middle ramp, an upper ramp slope, an inner ramp slope and an outer ramp environment.

Experimental cases: To determine the impact of varied proportion of biogenic sediments on the change in carbonate systems geometries, we carried out 50 sensitivity experiments focused on the gradual introduction of Photozoan sediments in Reference A, where we defined Photozoan sediments as low-diffusion sediments

Table 4.2: Modelling parameters for the seagrass-influenced model

Model	Initial Bathymetry	Duration	Subsidence Rate (m/My)	Carbonate Production Rates (m/My)					Diffusion coefficient (km²/kyr)				
				Euphotic (seagrass environment)	Carbonate grains	Heterozoan 1	Heterozoan 2 (Rhodolith)	Carbonate Muds	Euphotic	Carbonate grains	Heterozoan 1	Heterozoan 2 (Rhodolith)	Lime Muds / Pelagics
Reference B	Figure 4.3b	4 My	20	15	10	15	12	7	0.001	0.01	0.001	0.0001	0.1
Model F	Figure 4.3b	4 My	20	30	20	15	12	7	0.001	0.01	0.001	0.0001	0.1
Model G	Figure 4.3b	4 My	20	45	30	15	12	7	0.001	0.01	0.001	0.0001	0.1
Model H	Figure 4.3b	4 My	20	60	40	7	6	3.5	0.001	0.01	0.001	0.0001	0.1
Model I	Figure 4.3b	4 My	20	60	40	3	3	1.25	0.001	0.01	0.001	0.0001	0.1

produced in the upper 40 m of the model. Photozoan proportion values were varied in the 50 sensitivity experiments by generating near-random samples using the Latin Hypercube sampling method (Agrawal et al., 2015). This varied the values of the Photozoan proportion from 0% up to about 5% more than in Reference A. Reference A with a Photozoan proportion of 49% which reflects the geometry of a rimmed platform was set as the control for the experiments, while the proportion of Photozoan sediments in the system was varied from 0 to about 55% to observe and record the change in the geometry of the model. This change is measured as the maximum slopes in degrees, which represents the maximum gradient along the platform profile, usually occurring at the coastline for homoclinal ramps, and at the steepest margins of distally steepened ramps and flat-topped platforms.

The maximum slope (MS) was also measured for 30 simulations defined by variation in the proportion of seagrass-influenced sediment in Reference B, with variations generated using the Latin Hypercube sampling method. Sampling of the Photozoan proportion rates ranged from 0 up to twice the values used in Reference B. In this case also, seagrass-influenced sediments are simplified as low-diffusion carbonate sediments deposited from sea level down to a maximum water depth of 50 m in the model. Starting with Reference B characterised by a seagrass-influenced sediment proportion of 54% and a maximum topographic gradient of 14.6o, we observed and recorded the response of 30 simulations to changing seagrass-influenced sediment proportion, to predict the possibility of seagrass-dominated systems to evolve from ramp to steep-sloped geometries.

RESULTS

Role of Photozoan sediments in the development of steep margins

To determine the effect of variation in the proportion of Photozoan sediments in carbonate systems, 50 variations of sediment production rates for the Euphotic 1 and Euphotic 2 model sediment classes were sampled without changing the production rate of the Heterozoan class. This led to variation in the geometry of the resulting

models defined by different maximum slopes. A plot of the proportion of the Photozoan sediment versus the maximum topographic gradient for the simulations (Figure 4.4) indicates that carbonate system models with Photozoan proportion up to about 40% result in geometries with maximum topographic gradients not greater than 32o. At these values of Photozoan proportion, the simulations show no significant change in geometry as Photozoan proportion changes, although the models become steeper with increasing Photozoan proportion.
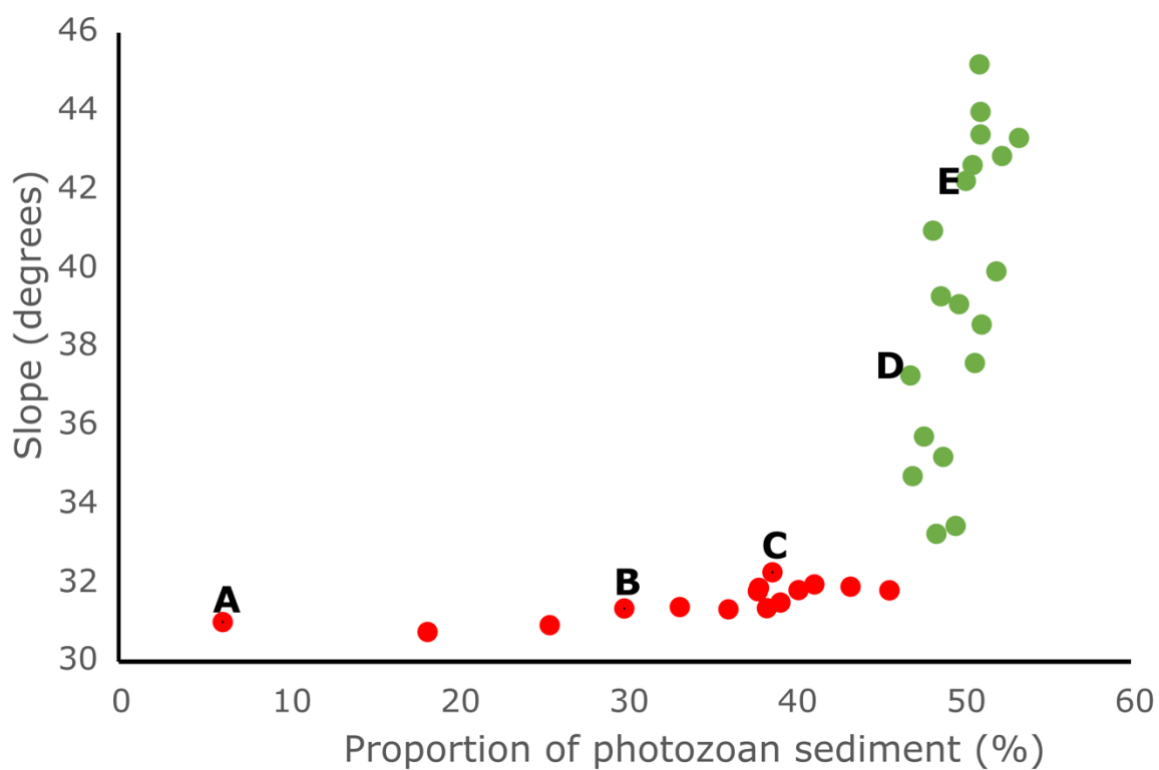
Figure 4.4: The relationship between the proportion of Photozoan sediments and the geometry of the carbonate system. Red plots represent models with Photozoan sediment proportion around the 40% mark. Green plots represent models with higher Photozoan sediment proportions. A, B, C, D and E are positions of the models in Figure 4.5.

As values of Photozoan proportion approach the 50% mark (Figures 4.4), there is an increase in the rate of change of maximum slope values as Photozoan proportion increases. At these values, slopes of the models range from above 32° to about 45°. For example, a model with Photozoan proportion of 46% shows a maximum slope of 32o, while a model with a Photozoan proportion of 48% could be characterised by a range of maximum slopes of between 33° and 40°.

To understand the implication of the maximum topographic gradient values of the models and how these are impacted by increasing or decreasing values of Photozoan proportion, five experimental models of varied Photozoan proportion and maximum slopes are presented in Figure 4.5. These models represent three simulations with Photozoan proportion values below the threshold of about 40% in Figure 4.4 (Models A, B and C) and two simulations with values above the threshold of Photozoan proportion (Models D and E). Models A, B and C are characterised by Photozoan proportions of 6%, 30% and 40 % respectively with corresponding values of slopes not exceeding 32°. Model A is characterised by a gently dipping profile that could be described as a low-angle ramp. Model B, in contrast, shows the development of some steepness along the platform margins, with more lateral extent of the model. Model C, on the hand, is characterised by a more conspicuous slope, further corroborating that the slope tends to increase as the Photozoan sediment proportion increases. As Photozoan proportion increases in Model D to 46% there is a corresponding increase in the margin steepness, with the maximum slope reaching 37o, while Model E with a Photozoan proportion of 50% is defined by a maximum slope of 42°. While the profiles of Models A, B and C could be better described as distally steepened ramps, Model E is clearly a flat-topped platform with steep margins. This indicates that the threshold of about 40% of Photozoan proportion is a cut-off below which steep margin development is not probable.

Seagrass-influenced sediments and steep margin development

Numerical experiments were also done to investigate how seagrass-dominated ramp systems in the absence of frame-building corals transition into flat-topped platforms. The assumption in this set of experiments is that seagrass causes sediment trapping up to a depth of about 50 m (Morsilli et al., 2012), thereby inhibiting the basinward transport of sediments produced in the euphotic zone of a carbonate ramp. Heterozoan sediments are produced beyond seagrass influence and are prone to redistribution by sediment transport. The production rates of these Heterozoan classes are kept constant throughout the experiments, while the seagrass-influenced sediments are varied.
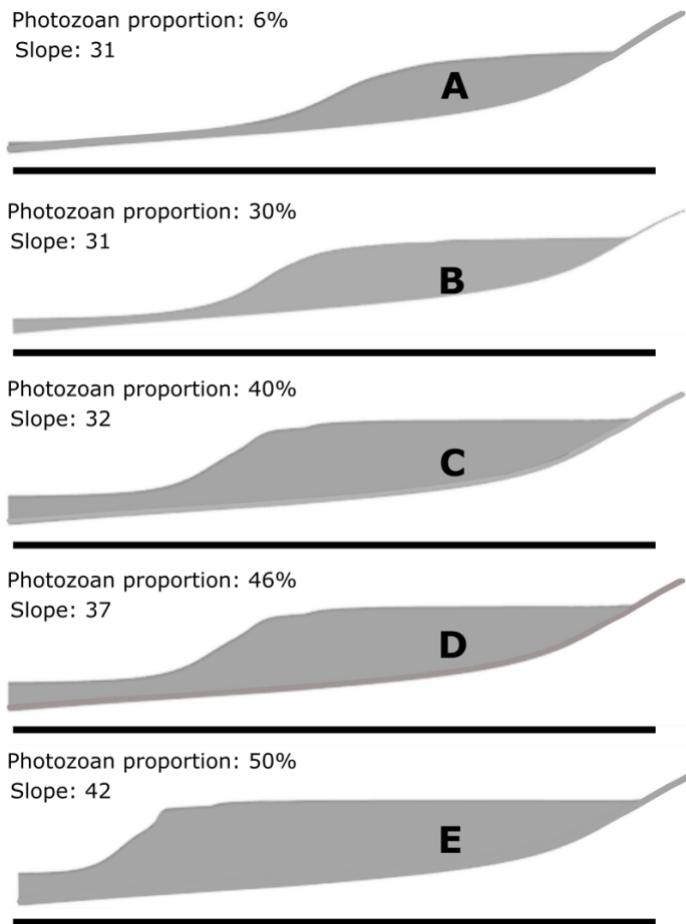
Figure 4.5: Depositional profiles of simulations with different proportion of Photozoan sediments

Figure 4.6 shows the result obtained by gradually increasing the proportion of seagrass-influenced sedimentation relative to deeper Heterozoan production. The relationship between the proportion of seagrass-influenced sediments and the maximum slope is reasonably predictable given the curve of the data spread. The curve (Figure 4.6) shows that the rate of change of geometry of the model is low for values of seagrass-influenced sediment proportion from 0 up to 62%, beyond which change in geometry becomes more significant for every change in the proportion of seagrass-influenced sediments. Models with seagrass-influenced sediment proportion values up to about 55% are characterised by maximum slope up to about 15°, while

models with seagrass-influenced sediment proportion values higher than 55% are characterised by maximum topographic gradients that can exceed 40º.
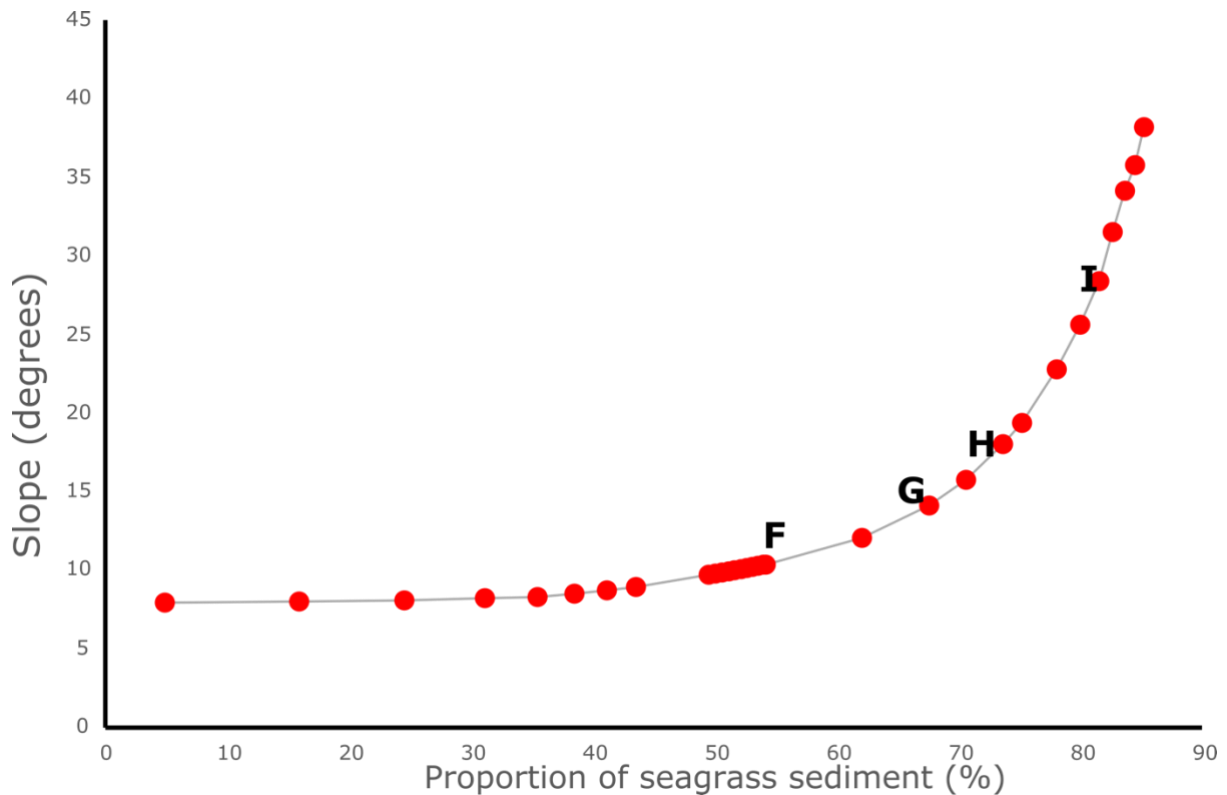
Figure 4.6: The relationship between proportion of seagrass-influenced sediments and the geometry of carbonate system. F, G, H, I are positions of models in Figure 4.7

Figure 4.7 shows the geometric implication of variation in the values of seagrass-influenced sediment proportion on the maximum topographic gradient. Model F represents a distally steepened ramp with a seagrass-influenced sediment proportion of 54% and a maximum slope of 10º. Models G, H and I, which are defined by successively increasing seagrass-influenced sediment proportions, show some responses in their geometries, as also observed in their maximum topographic

gradients. However, none of these models shows a distinct transition into a flat-topped platform.

Seagrass sediment proportion: 54%
Slope: 10º

F

Seagrass sediment proportion: 67%
Slope: 14º

G

Seagrass sediment proportion: 73%
Slope: 17º

H

Seagrass sediment proportion: 81%
Slope: 28º

I
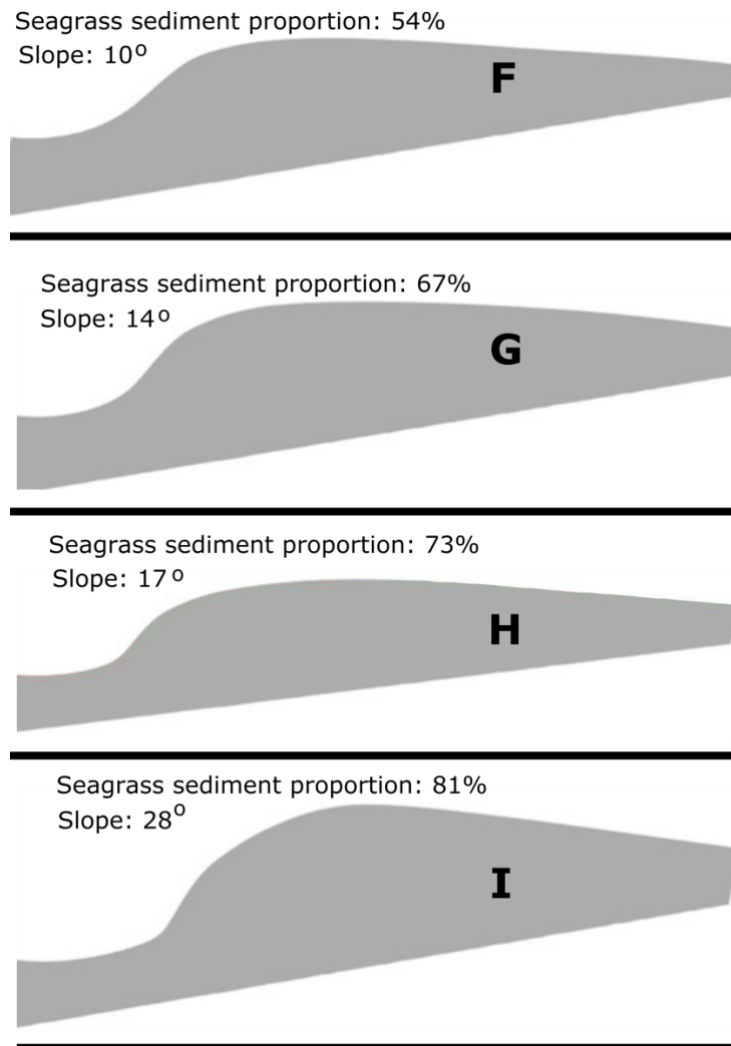
Figure 4.7: Depositional profiles of simulations with different proportions of seagrass-influenced sediments

Temporal evolution of model geometries

The evolution of platform geometries through time under conditions of high and low Photozoan proportion, as well as seagrass-influenced conditions, were simulated as shown in Figure 4.8. The Photozoan-rich system presented in Figure 4.8 is a set of time-lapse sections of Reference A (Figure 4.2d) defined by a Photozoan proportion of 50%. The Photozoan-poor system presented is defined by a Photozoan proportion

of 5%. The seagrass-influenced system in Figure 4.8 is Reference B defined by a seagrass-influenced sediment proportion of 50% (Figure 4.7).
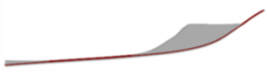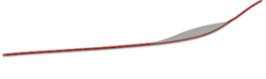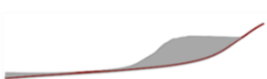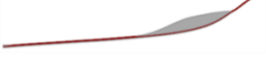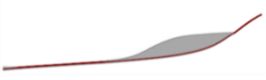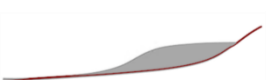
Elapsed Modelling Time (My)	Photozoan-rich system	Photozoan-poor system	Elapsed Modelling Time (My)	Seagrass-influenced system
0.1 My	Maximum slope: 23.6 degrees	Maximum slope: 10.6 degrees	0.5 My	Maximum slope: 4.4 degrees
0.42 My	Maximum slope: 26.8 degrees	Maximum slope: 11.1 degrees	1.0 My	Maximum slope: 8.9 degrees
0.68 My	Maximum slope: 25.7 degrees	Maximum slope: 12.2 degrees	1.5 My	Maximum slope: 12.2 degrees
1.18 My	Maximum slope: 32.2 degrees	Maximum slope: 14 degrees	2.0 My	Maximum slope: 16.2 degrees
1.86 My	Maximum slope: 29.8 degrees	Maximum slope: 15.2 degrees	2.5 My	Maximum slope: 20.3 degrees

Figure 4.8: Temporal evolution of carbonate geometries in different biotic settings

The Photozoan-rich system shows early indication of steep margin development, with as much as 23o of maximum slope after just 0.1 My of simulation time. While it is observed that the slope margin steepens with simulation time, there seems to be some inclination reversals at simulation time 0.68 My and 1.86 My. This may be attributed to erosion or slope margin failures under changing hydrodynamics and slope stability conditions, or due to sea level changes. It is however significant to note that the model reached a maximum topographic gradient of 30o within 1.2 My of simulation time, at an average increment of 27.3 degrees/My.

In contrast, the rate of slope margin development in the Photozoan-poor and the seagrass-influenced settings is not as intense as in the Photozoan-rich system (Figure 4.8). In the Photozoan-poor system, the maximum topographic gradient reached about 15o after 1.86 My of simulation time. with an average slope increment of 8 degrees/My,

while the seagrass-influenced setting reached a slope margin inclination of 20.3o after 2.5 My of simulation time. The seagrass-influenced setting shows homoclinal ramp development in the first 500 Ky of the simulation, after which a gradual but less noticeable slope development was initiated at 1.0 My simulation time. From 1.5 My of the simulation, the slope margin inclination becomes increasingly significant, and at 2.0 My of the simulation, a distinct distally steepened ramp geometry developed.

DISCUSSION

Establishing a link between the dominant carbonate-producing biotas and the profile of carbonate systems has been the subject of many research efforts. Pomar (2001), Schlager (2005) and many others (e.g., James and Bone, 1991; James, 1997; Light and Wilson, 1998; Moore and Wade, 2013) sought to establish the connection between carbonate geometries and their main biotic types. Such studies have led to the concept of matching Photozoan biotas with flat-topped platforms, and Heterozoan biotas typically with ramp geometries (Burchette and Wright, 1992; James, 1997; Williams et al., 2011; Michel et al., 2019). The models presented in this study essentially support Photozoan biotas as necessary requirements in the development of flat-topped platforms. Our results, however, also postulate numerically that there exists a minimum threshold of Photozoan sediment required in a system for significantly steep margins such as in flat-topped platforms to develop. This is particularly relevant in transitional systems (e.g., Brachert et al., 1996; Betzler et al., 1997) in which changing biotic composition is a main causal factor for geometric turnover from a ramp to a flat-topped platform (Bosellini, 2006; Benisek et al., 2012).

In Photozoan systems under the modelling conditions presented herein, a minimum Photozoan sediment proportion of about 40% is required for significant margin slopes to develop. This value represents a threshold of Photozoan carbonate sediments below which no significant slopes develop in the models. While there are no concrete quantitative studies comparing the relative proportions of Photozoan versus Heterozoan sediments in ancient and modern carbonate systems, the above proposition seems to have been observed in the geologic record. For example, the Miocene carbonates of Sardinia which are defined by their transition from a Heterozoan ramp to a steep-margined platform (Sowerbutts, 2000), lacked sufficient shallow water corals to develop significant slope angles (Benisek et al., 2012). In the

Holocene, the inhibition of prolific coral growth in an environment that was rather favourable for Heterozoan proliferation in the windward margins of Houtman Abrolhos reefs resulted in restricted development of steep margins (Collins et al., 1993). In the Carnarvon Ramp sector of the southwestern Australian shelf, the occurrence of Zooxanthellate corals, large foraminifera and calcareous green alga (James et al., 1999; Cathro and Austin, 2001) is also an example in which Photozoan biotas not sufficient for the development of steep platform margins.

The presence of frame-building corals or other Photozoans in a carbonate system will not necessarily translate into a flat-topped steep margin profile. The models with Photozoan proportion less than the threshold value of about 40% all have some incremental change in slope margin steepness as the Photozoan proportion increases (Figure 4.4). However, none of these 'subthreshold' models showed significant slope margins although there is some predictability between the change in Photozoan proportion and the change in geometry (Figure 4.4). These results suggest that there is a tendency for carbonate ramp development in an environment that favours Photozoan growth, provided that a critical threshold of Photozoan sediment is not exceeded. This threshold must, however, be determined through field study. An example of this scenario is the Lower Tortonian Ragusa ramp in which the presence of coral-bearing mudstones and wackestones in the inner ramp did not preclude the development of the ramp (Grasso and Lentini, 1982; Ruchonnet and Kindler, 2012). In an effective transport environment, subthreshold Photozoan production can lead to platform drowning as is the case in the Saya de Malha Bank, where a distally steepened ramp eventually drowned under extreme conditions including sediment shaving by internal waves coupled with a rapid rate of accommodation rise (Purdy and Bertram, 1993; Betzler et al., 2022). The response could have been different in a setting with high Photozoan sediment component, which often tend to keep up with accommodation creation.

The models in which seagrass influence was tested (Figures 4.6 and 4.7) indicate that with increasing sediment production and trapping efficiency by seagrass, there is a corresponding increase in the slope margin steepness. However, this raises the question of slope stability in a seagrass-dominated Heterozoan environment. The role of seagrass trapping in the modification of sedimentary environments has been

observed in modern settings (Gambi et al., 1990; Bos et al., 2007; Potouroglou et al., 2017). Although seagrass environments tend to build significant slopes by providing hydrodynamic stability (Bos et al., 2007; Hendriks et al., 2010), the steepness of the slope is additionally enhanced by the sediment fabric (Kenter, 1990; Adams et al., 2002; Schlager and Reijmer, 2009). Depending on the amount of mud proportion in the seagrass environment, the margin slope angle could range from single digits such as the 4o slopes in the Northern flank of Little Bahama bank (Austin et al., 1986) to as high as 20o such as in the Menorca ramp (Pomar et al., 2002), both of which represent high and low mud content ramps respectively.

Another factor that can aid seagrass trapping in the development of steep margins in a low-photozoan environment is early slope stabilization through microbial binding (Camoin et al., 1999; Reolid et al., 2017; Torres and Grammer, 2019). Microbial binding could present a case in principle in which unusually steeper slopes characterise the margins of a carbonate system. In such a scenario, the combination of sediment trapping by seagrass and early sediment cementation by microbial deposits could lead to steep slopes in Heterozoan settings such as presented in the experimental cases (Figures 4.6 and 4.7).

An important characteristic of Photozoan-rich carbonate systems is their high production rates compared to Heterozoan-rich systems (Bosence, 1980; Schlager, 2000). This consequently contributes to the development of their generally steep slopes (Adams and Schlager, 2000) as they tend to catch up and keep up with sea level rise through aggradation and progradation (Kendall and Schlager, 1981). The development of a flat-topped profile is thus possible, especially in cases with high production rates at the start-up phase. Such carbonate systems would be characterised by a high rate of increase in slope margin angles, as is illustrated by the rate of slope development in Figure 4.8, such that high slope angles are achieved in the carbonate system within a relatively short geologic time. In the absence of a high proportion of Photozoan sediments in the system, however, the rate of increase in the slope angles tends to be rather lower. This is largely due to the relatively lower carbonate production rates (Schlager, 2000) and in many cases, high sediment transport, leading to the flattening of the depositional profile through the redistribution

of sediments by waves and currents as is exemplified in the Middle Miocene Latium-Abruzzi ramp (Brandano et al., 2012).

The observations made in this study propose that in addition to existing classification schemes for carbonate systems, platforms can further be characterised by the proportion of Photozoan sediments in the system. Provided that field study corroborates the existence of a threshold of Photozoan sediments required for steep margins to form, subthreshold platforms can be easily distinguished by the low abundance of Photozoan sediments relative to Heterozoan sediments. The implication of this is improved reconstruction of multi-factory carbonate architecture in studies involving inconclusive data, as is the case in many geologic investigations.

It is also important to state that the results of the simulations on which this study is predicated are model-design-dependent. These means that they are biased by the assumptions set out in the modelling process. This is the case in many scientific efforts. However, irrespective of the model biases, these results predict that there is a minimum Photozoan sediment threshold required for the development of recognisable flat-topped platforms.

CONCLUSION

- In this study we present experimental cases, based on stratigraphic forward modelling, to determine the minimum Photozoan requirement for carbonate systems to develop significant slopes. We also investigated the possibility of a seagrass-dominated Heterozoan carbonate system evolving into steep margin platforms. This was achieved by carrying out sensitivity experiments on two forward models, in which one simulates a flat-topped platform with steep margins, and the other simulates a distally steepened ramp. The responses in the sensitivity experiments are measured by the maximum topographic gradients of each model. The key points of the study are summarised as follows:

- We showed through numerical modelling, that there exists a minimum threshold of Photozoan sediment proportion in a carbonate system required for carbonate ramps to transition into platforms with steep margins. In the experiments carried out in this study, this threshold is about 40% Photozoan proportion, in which platforms below this threshold (subthreshold systems), are incapable of producing steep margins. Above this threshold of Photozoan proportion, varying degrees of steep margin development is possible with increased Photozoan sediment proportion. This implies that the presence of Photozoans in a carbonate system will not automatically translate into the development of steep margin profiles. The value of this Photozoan proportion threshold should however be calibrated by field observation.

- A Heterozoan system dominated by high-transport sediments could develop some slope occasioned by effective seagrass sediment trapping. The margins of models developed with higher seagrass-influenced sediments proportions show steeper profiles than models with lower seagrass-influenced sediments proportions. We however point out that while seagrass trapping is a recognised mechanism of slope development, stabilization of such slopes would require the incorporation of other mechanisms such as sediment fabric or microbial binding.

- This study also presents an attempt at predicting the geometry of carbonate systems from the proportion of Photozoans and seagrass-influenced sediments. The plots of the sensitivity tests illustrate that profiles of carbonate systems are predictable from the relative proportion of seagrass-influenced sediments, as the models herein presented show that the proportion of seagrass-influenced sediments is directly proportional to the maximum

topographic gradient. The carbonate system geometry is however much less predictable from the proportion of Photozoan sediments in the carbonate system models.

- The implications arrived at by this numerical study provide an additional means of characterising carbonate systems based on their biogenic components. These propositions however require validation from field and laboratory studies.

ACKNOWLEDGEMENT

Chapter 5
SUMMARY AND FUTURE OUTLOOK

In this thesis, I leveraged the strengths of stratigraphic forward modelling to answer some critical questions regarding the geometric evolution of Miocene shallow marine carbonate systems, with a focus on the Mediterranean region. The numerical experiments presented herein were carried out to advance the current understanding of the significant roles of Heterozoan and Photozoan biogenic carbonate production, and how these different biotas define the geometries of carbonate systems as environmental conditions change through geologic time. To achieve this objective, stratigraphic forward models of a Photozoan-dominated carbonate platform (the Upper Miocene Llucmajor platform) and a Heterozoan-dominated carbonate ramp (Upper Miocene Menorca ramp) were developed, representing two endmembers of carbonate geometries. The main gaps in our current understanding of the evolution of shallow marine carbonate systems through geologic time, which this thesis addresses are as follows:

The sensitivity of carbonate system geometries to differential biogenic carbonate sediment production

In chapter 2 of this thesis, I demonstrated how differential carbonate sediment production by Photozoan and Heterozoan biotas in a dominantly Photozoan system influences the geometry of carbonate systems. This was done through the forward modelling of the Upper Tortonian to Lower Messinian Llucmajor Platform in Mallorca, Spain. The reference forward model was developed using a multi-class carbonate production approach which increases the flexibility of the model to study the impact of different carbonate-producing classes, an improvement over previous attempts at the numerical investigation of the evolution of the Llucmajor platform (Bosence et al., 1994; Hüssner et al., 2001). This was followed by two series of sensitivity tests. A multi-realisation global sensitivity analysis which utilizes the Latin Hypercube experimental design was used to define a set of simulations that efficiently combine the variable modelling inputs such as carbonate production rates and the production curves of the carbonate sediment classes, bathymetric configuration, sea level variation and wave energy propagation. A series of stepwise sensitivity tests were also

carried out to observe the changes in the carbonate geometry as individual parameters were varied while keeping other parameters at their reference values.

Some of the key thrusts of this study are as follows:

a) A multi-class carbonate production approach is more efficient than a single-class carbonate production approach (Bosence et al., 1994; Hüssner et al., 2001) in modelling the processes of carbonate systems development. The multi-class carbonate production curves used in the Llucmajor model allow for adequate simulation and observation of the behaviours of different carbonate-producing biotic associations in relation to bathymetry. Consequently, the model provided an efficient numerical method to explore the responses of carbonate systems to changes in the production rates or efficiencies of different carbonate-producing biotic classes. As the changes in the production rates of different biotic classes are occasioned by their unique responses to changing environmental conditions, prevalent environmental conditions can be inferred from the evolution of carbonate geometries.

b) Flat-topped platforms have hitherto been recognised as the result of the dominance of carbonate sediment production by Photozoan biotas. In addition to confirming the role of Photozoans in the development of flat-topped platforms and that of Heterozoans in the evolution of ramps, the Llucmajor model also reveals the importance of Heterozoan biotas in the progradation of flat-topped platforms. In a highly prograding platform such as the Llucmajor, Heterozoan biotas provide the necessary base for the progradation of the much shallower Photozoan sediments by providing the necessary bathymetric conditions for euphotic sediment production. This gives a numerical understanding of the concepts of ecological controls on the development of carbonate systems observed from field studies (Pomar and Ward, 1995; Pomar, 2001a).

The main controls on the evolution of steep margins in carbonate systems

In contrast to the low-transport Photozoan-dominated flat-topped Llucmajor platform, the Menorca ramp model in Chapter 3 represents a high-transport Heterozoan-dominated distally steepened carbonate ramp. The reference model was developed using data from field and laboratory studies on the distally steepened Upper Miocene Menorca ramp (e.g., Obrador et al., 1992; Pomar et al., 2002; Brandano et al., 2005;

Mateu-Vicens et al., 2008) in the western Mediterranean. The model also involved the use of a multi-class carbonate production approach with five sediment classes representing carbonate production in the euphotic, mesophotic and oligophotic zones (Mateu-Vicens et al., 2008), as well as rhodolith accumulation in the ramp slope, and pelagics (Pomar et al., 2002). The study focused on investigating the main controls on the stratal architecture of distally steepened ramps by presenting results of the sensitivity of the reference model to differences in eustatic changes, antecedent slopes, sediment transport processes and differential production of carbonate sediments in the oligophotic zone (Heterozoan) versus the seagrass-influenced euphotic zone (Photozoan).

The highlights of this study are presented below:

a) Several studies have shown the importance of antecedent slopes on the geometries of carbonate systems(e.g., Watts, 1987; Walkden and Williams, 1998). Numerical modelling has been also previously used to illustrate how high-transport ramps tend to reflect the geometry of the underlying topography (Williams et al., 2011). The study presented in Chapter 3 advances this understanding by showing that the tendency of carbonate ramps to reflect the geometry of the antecedent slope declines with higher slope inclination. For more inclined antecedent slopes like Models B4, B5 and B6, the geometry of the ramp is less controlled by the paleoslope, and more significantly controlled by the bathymetric and carbonate production rates of the biotic associations.

b) Sea level amplitudes and frequencies are significant determinants of the geometries of carbonate ramps. The sensitivity of the model to different sea-level change parameters shows that sea level fluctuations which are characterised by moderate amplitudes (about 30 to 40 m) and high frequency which persist over relatively long geologic intervals (such as 4 My in the Menorca model) in a Heterozoan-dominated environment tend to form distally steepened ramps compared to other configuration of sea level fluctuations.

c) The increase of Photozoan sediments over Heterozoan sediments resulted in a corresponding increase in the steepness of the slope. This suggests the pathway through which geometric turnovers may occur in carbonate systems as biological evolution through geologic time leads to the introduction of

Photozoans in a Heterozoan-dominated environment such as the Sedini Limestone (Benisek et al., 2012).

Minimum Photozoan sediment requirement for the development of steep margins in carbonate systems.

The results in Chapter 3, which show the impact of an increase in Photozoan sediments on the steepening of carbonate slopes in a Heterozoan-dominated system, motivated our attempt to investigate, in Chapter 4, the minimum Photozoan requirement for carbonate systems to develop steep margins. This aim was achieved by conducting sensitivity experiments on the Llucmajor and Menorca models which represent a low-transport flat-topped platform and a high-transport distally steepened ramp respectively. The results of these experiments demonstrate that not all carbonate systems with Photozoan sediments will develop steep margins. In the models presented in Chapter 4, the minimum proportion of Photozoan sediments required for steep margins to develop is 43.4%. The implication of this threshold is that a carbonate system may have significant Photozoan sediment proportion but might still not be capable of forming steep slopes. The chapter cites examples of carbonates in the geologic history that are characterised by some proportion of Photozoan sediments without the steep profiles that characterise flat-topped platforms. An example of such sub-threshold carbonate systems is the Burdigalian to Langhian Sedini Limestone (Benisek et al., 2012) which is characterised by a homoclinal ramp which transitions through time into a platform with margins that are not as strongly inclined as generally observed in flat-topped platforms. This transition is occasioned by the introduction of Photozoans into the carbonate system in the Langhian (Benisek et al., 2012). Carbonate system models with Photozoan proportion below this threshold of 43.4% show a very low correlation between the proportion of Photozoan sediment and the carbonate geometry. This relationship however improves for models with Photozoan proportions above this threshold, carbonate systems tend to develop profiles characterised by steep margins.

FUTURE RESEARCH PERSPECTIVES

The results presented in this thesis have demonstrated the impact of changing environmental conditions on biogenic carbonate production, and consequently on the geometry of carbonate systems. The flexibility and robustness of stratigraphic forward modelling as presented herein is a powerful tool for understanding carbonate systems throughout geologic history. Testing the concepts espoused through this study on a field scale is however necessary to further deepen current knowledge of the response of Heterozoan and Photozoan biotas to environmental changes. This includes investigating the relative proportion of Heterozoan versus Photozoan sediments in different geometric forms of carbonate systems in the stratigraphic record, to validate our hypothesis on the existence of a minimum Photozoan sediment requirement for steep margin development. We, therefore, recommend studying carbonates from the outcrop scale to thin sections and integrating these with stratigraphic forward models to understand the role of biologic evolution through time on carbonate geometry evolution.

Furthermore, we acknowledge that many carbonate systems develop in environments with siliciclastic inputs that may be coeval with carbonate sediment accretion. We, therefore, suggest that carbonate systems should be numerically investigated for their responses to siliciclastic sediment input, which has not hitherto been done.

REFERENCES:

Abreu, V.S., and Haddad, G.A., 1998, Glacioeustatic Fluctuations: the Mechanism Linking Stable Isotope Events and Sequence Stratigraphy From the Early Oligocene To Middle Miocene: Mesozoic and Cenozoic Sequence Stratigraphy of European Basins, p. 245–259, doi:10.2110/pec.98.02.0245.

Adams, E.W., Morsilli, M., Schlager, W., Keim, L., and van Hoek, T., 2002, Quantifying the geometry and sediment fabric of linear slopes: examples from the Tertiary of Italy (Southern Alps and Gargano Promontory): Sedimentary Geology, v. 154, p. 11–30, doi:10.1016/S0037-0738(02)00125-2.

Adams, E.W., and Schlager, W., 2000, Basic types of submarine slope curvature: Journal of Sedimentary Research, v. 70, p. 814–828, doi:10.1306/2DC4093A-0E47-11D7-8643000102C1865D.

Adey, W.H., and Vassar, J.M., 1975, Colonization, succession and growth rates of tropical crustose coralline algae (Rhodophyta, Cryptonemiales): Phycologia, v. 14, p. 55–69, doi:10.2216/i0031-8884-14-2-55.1.

Agrawal, D., Dwivedi, S., Barrois, A., Koeck, C.H., El-Wazir, Z., Al-Madani, N., and Aillud, G., 2015, Impact of environmental parameters on forward stratigraphic modelling from uncertainty analysis; Lower cretaceous, Abu Dhabi: Society of Petroleum Engineers - SPE Reservoir Characterisation and Simulation Conference and Exhibition, RCSC 2015, p. 532–543, doi:10.2118/175683-ms.

Ahr, W.M., 1973, Carbonate Ramp--Alternative to Shelf Model: ABSTRACT: AAPG Bulletin, v. 57, doi:10.1306/83D910BF-16C7-11D7-8645000102C1865D.

Al-Salmi, M., John, C.M., and Hawie, N., 2019, Quantitative controls on the regional geometries and heterogeneities of the Rayda to Shu'aiba formations (Northern Oman) using forward stratigraphic modelling: Marine and Petroleum Geology, v. 99, p. 45–60, doi:10.1016/j.marpetgeo.2018.09.030.

Asprion, U., Westphal, H., Nieman, M., and Pomar, L., 2009, Extrapolation of depositional geometries of the Menorcan Miocene carbonate ramp with ground-penetrating radar: Facies, v. 55, p. 37–46, doi:10.1007/s10347-008-0160-6.

Aurell, M., Bádenas, B., Bosence, D.W.J., and Waltham, D.A., 1998, Carbonate production and offshore transport on a Late Jurassic carbonate ramp (Kimmeridgian, Iberian basin, NE Spain): Evidence from outcrops and computer modelling: Geological Society Special Publication, v. 149, p. 137–161, doi:10.1144/GSL.SP.1999.149.01.08.

Austin, J.A., Schlager, W., Palmer, A.A., and Al, Et., 1986, Sites 629 and 630: Little Bahama Bank, *in* Proceedings of the Ocean Drilling Program, 101 Initial Reports, Ocean Drilling Program, doi:10.2973/odp.proc.ir.101.108.1986.

Benisek, M.-F., Betzler, C., Marcano, G., and Mutti, M., 2009, Coralline-algal assemblages of a Burdigalian platform slope: Implications for carbonate platform reconstruction (northern Sardinia, western Mediterranean Sea): Facies, v. 55, p. 375–386, doi:10.1007/s10347-009-0183-7.

Benisek, M.-F., Marcano, G., Betzler, C., and Mutti, M., 2012, Facies and Stratigraphic Architecture of a Miocene Warm-Temperate to Tropical Fault-Block Carbonate Platform, Sardinia (Central Mediterranean Sea), *in* Mutti, M., Piller, W., and Betzler, C. eds., Carbonate Systems during the Oligocene–Miocene Climatic Transition, Oxford, UK, Wiley, p. 129–148, doi:10.1002/9781118398364.ch8.

Berra, F., and Carminati, E., 2012, Differential compaction and early rock fracturing in high-relief carbonate platforms: Numerical modelling of a Triassic case study (Esino Limestone, Central Southern Alps, Italy): Basin Research, v. 24, p. 598–614, doi:10.1111/j.1365-2117.2012.00542.x.

Berra, F., Lanfranchi, A., Smart, P.L., Whitaker, F.F., and Ronchi, P., 2016, Forward modelling of carbonate platforms: Sedimentological and diagenetic constraints from an application to a flat-

topped greenhouse platform (Triassic, Southern Alps, Italy): Marine and Petroleum Geology, v. 78, p. 636–655, doi:10.1016/j.marpetgeo.2016.10.011.

Betzler, C. et al., 2018, Refinement of Miocene sea level and monsoon events from the sedimentary archive of the Maldives (Indian Ocean): Progress in Earth and Planetary Science, v. 5, doi:10.1186/s40645-018-0165-x.

Betzler, C., Brachert, T.C., and Nebelsick, J., 1997, The warm temperate carbonate province a review of the facies, zonations, and delimitations: CFS Courier Forschungsinstitut Senckenberg, p. 83–99.

Betzler, C., Fürstenau, J., Lüdmann, T., Hübscher, C., Lindhorst, S., Paul, A., Reijmer, J.J.G., and Droxler, A.W., 2013, Sea-level and ocean-current control on carbonate-platform growth, Maldives, Indian Ocean: Basin Research, v. 25, p. 172–196, doi:10.1111/j.1365-2117.2012.00554.x.

Betzler, C., Lindhorst, S., Lüdmann, T., Bialik, O.M., Braga, J.C., Reijmer, J., Reolid, J., Geßssner, A.-L., and Hainbucher, D., 2022, Carbonate platform drowning caught in the act: the sedimentology of Saya de Malha Bank (Indian Ocean): Sedimentology, doi:10.1111/sed.13032.

Bice, D., 1988, Synthetic stratigraphy of carbonate platform and basin systems: Geology, v. 16, p. 703–706, doi:10.1130/0091-7613(1988)016<0703:SSOCPA>2.3.CO;2.

Biddle, K.T., Schlager, W., Rudolph, K.W., and Bush, T.L., 1992, Seismic model of a progradational carbonate platform, Picco di Vallandro, the Dolomites, Northern Italy: American Association of Petroleum Geologists Bulletin, v. 76, p. 14–30, doi:10.1306/bdff8754-1718-11d7-8645000102c1865d.

Borgomano, J., Lanteaume, C., Ridet, O., Rousseau, M., and Vilasi, N., 2014, 3D Stratigraphic Forward Modelling for the Prediction of Carbonate Platform Architectures: Evaluation of Stratigraphic Trap Potential in Middle East Mesozoic Carbonate Sequences, *in* GEO-2014, 11th Middle East Geosciences Conference and Exhibition, 10-12 March 2014, v. 41328.

Bos, A.R., Bouma, T.J., de Kort, G.L.J., and van Katwijk, M.M., 2007, Ecosystem engineering by annual intertidal seagrass beds: Sediment accretion and modification: Estuarine, Coastal and Shelf Science, v. 74, p. 344–348, doi:10.1016/j.ecss.2007.04.006.

Bosellini, F.R., 2006, Biotic changes and their control on Oligocene-Miocene reefs: A case study from the Apulia Platform margin (southern Italy): Palaeogeography, Palaeoclimatology, Palaeoecology, v. 241, p. 393–409, doi:10.1016/j.palaeo.2006.04.001.

Bosellini, A., and Ginsburg, R.N., 1971, Form and Internal Structure of Recent Algal Nodules (Rhodolites) from Bermuda: The Journal of Geology, v. 79, doi:https://doi.org/10.1086/627697.

Bosence, D., 2005, A genetic classification of carbonate platforms based on their basinal and tectonic settings in the Cenozoic: Sedimentary Geology, v. 175, p. 49–72, doi:10.1016/j.sedgeo.2004.12.030.

Bosence, D.W.J., 1980, Sedimentary facies, production rates and facies models for recent coralline algal gravels, Co. Galway, Ireland: Geological Journal, v. 15, p. 91–111, doi:10.1002/gj.3350150203.

Bosence, D.W.J., 1983, The Occurrence and Ecology of Recent Rhodoliths — A Review, *in* Coated Grains, Berlin, Heidelberg, Springer Berlin Heidelberg, p. 225–242, doi:10.1007/978-3-642-68869-0_20.

Bosence, D., Pomar, L., Waltham, D.A., and Lankester, T.H.G., 1994, Computer modeling a Miocene carbonate platform, Mallorca, Spain: American Association of Petroleum Geologists Bulletin, v. 78, p. 247–266, doi:10.1306/bdff9078-1718-11d7-8645000102c1865d.

Bosence, D., and Waltham, D., 1990, Computer modeling the internal architecture of carbonate platforms: Geology, v. 18, p. 26–30, doi:10.1130/0091-7613(1990)018<0026:CMTIAO>2.3.CO;2.

Bosence, D., and Wilson, J., 2003, Maerl growth, carbonate production rates and accumulation rates in the northeast Atlantic: Aquatic Conservation: Marine and Freshwater Ecosystems, v. 13, doi:10.1002/aqc.565.

Bosscher, H., and Schlager, W., 1993, Accumulation Rates of Carbonate Platforms: The Journal of Geology, v. 101, p. 345–355, doi:10.1086/648228.

Bosscher, H., and Schlager, W., 1992, Computer simulation of reef growth: Sedimentology, v. 39, p. 503–512, doi:10.1111/j.1365-3091.1992.tb02130.x.

Bosworth, W., Crevello, P., Winn, R.D., and Steinmetz, J., 1998, Structure, sedimentation, and basin dynamics during rifting of the Gulf of Suez and north-western Red Sea: Sedimentation and Tectonics in Rift Basins Red Sea:- Gulf of Aden, p. 77–96, doi:10.1007/978-94-011-4930-3_6.

Bourrouilh-Le Jan, F.G., and Hottinger, L.C., 1988, Occurrence of rhodolites in the tropical Pacific - a consequence of Mid-Miocene paleo-oceanographic change: Sedimentary Geology, v. 60, doi:10.1016/0037-0738(88)90130-3.

Boylan, A.L., Waltham, D.A., Bosence, D.W.J., Badenas, B., and Aurell, M., 2002, Digital rocks: Linking forward modelling to carbonate facies: Basin Research, v. 14, p. 401–415, doi:10.1046/j.1365-2117.2002.00180.x.

Brachert, T.C., Betzler, C., Braga, J.C., and Martin, J.M., 1996, Record of climatic change in neritic carbonates: Turnover in biogenic associations and depositional modes (Late Miocene, southern Spain): International Journal of Earth Sciences, v. 85, p. 327–337, doi:10.1007/s005310050078.

Braga, J.C., Martín, J.M., Betzler, C., and Aguirre, J., 2006, Models of temperate carbonate deposition in Neogene basins in SE Spain: a synthesis: Geological Society, London, Special Publications, v. 255, p. 121–135, doi:10.1144/GSL.SP.2006.255.01.09.

Brandano, M., 2003, Tropical/subtropical inner ramp facies in lower Miocene Calcari a Briozoi e Litotamni of the Monte Lungo area (Cassino Plain, Central Apennines, Italy): Bollettino Della Societa Geologica Italiana, v. 122, p. 85–98.

Brandano, M., Corda, L., and Castorina, F., 2012, Facies and Sequence Architecture of a Tropical Foramol-Rhodalgal Carbonate Ramp: Miocene of the Central Apennines (Italy): Carbonate Systems during the Oligocene-Miocene Climatic Transition, p. 107–127, doi:10.1002/9781118398364.ch7.

Brandano, M., Tomassetti, L., Mateu-Vicens, G., and Gaglianone, G., 2019, The seagrass skeletal assemblage from modern to fossil and from tropical to temperate: Insight from Maldivian and Mediterranean examples: Sedimentology, v. 66, p. 2268–2296, doi:10.1111/sed.12589.

Brandano, M., Vannucci, G., Pomar, L., and Obrador, A., 2005, Rhodolith assemblages from the lower Tortonian carbonate ramp of Menorca (Spain): Environmental and paleoclimatic implications: Palaeogeography, Palaeoclimatology, Palaeoecology, v. 226, p. 307–323, doi:10.1016/j.palaeo.2005.04.034.

Brown, K.M., 2005, Calcareous Epiphytes on Modern Seagrasses as Carbonate Sediment Producers in Shallow Cool-Water Marine Environments, South Australia: University of Adelaide.

Burchette, T.P., 1988, Tectonic control on carbonate platform facies distribution and sequence development: Miocene, Gulf of Suez: Sedimentary Geology, v. 59, p. 179–204, doi:10.1016/0037-0738(88)90076-0.

Burchette, T.P., and Wright, V.P., 1992, Carbonate ramp depositional systems: Sedimentary Geology, v. 79, p. 3–57, doi:10.1016/0037-0738(92)90003-A.

Burgess, P.M., 2012, A brief review of developments in stratigraphic forward modelling, 2000-2009, in Regional Geology and Tectonics, Elsevier, p. 378–404, doi:10.1016/B978-0-444-53042-4.00014-5.

Burgess, P.M., Lammers, H., van Oosterhout, C., and Granjeon, D., 2006, Multivariate sequence stratigraphy: Tackling complexity and uncertainty with stratigraphic forward modeling, multiple scenarios, and conditional frequency maps: AAPG Bulletin, v. 90, p. 1883–1901, doi:10.1306/06260605081.

Burgess, P.M., and Prince, G.D., 2015, Non-unique stratal geometries: Implications for sequence stratigraphic interpretations: Basin Research, v. 27, p. 351–365, doi:10.1111/bre.12082.

Burgess, P.M., Winefield, P., Minzoni, M., and Elders, C., 2013, Methods for identification of isolated carbonate buildups from seismic reflection data: AAPG Bulletin, v. 97, p. 1071–1098, doi:10.1306/12051212011.

Busson, J., Joseph, P., Mulder, T., Teles, V., Borgomano, J., Granjeon, D., Betzler, C., Poli, E., and Wunsch, M., 2019, High-resolution stratigraphic forward modeling of a Quaternary carbonate margin: Controls and dynamic of the progradation: Sedimentary Geology, v. 379, p. 77–96, doi:10.1016/j.sedgeo.2018.11.004.

Cabioch, G., Montaggioni, L.F., Faure, G., and Ribaud-Lamenti, A., 1999, Reef coralgal assemblages as recorders of paleobathymetry and sea level changes in the Indo-Pacific province: v. 18, p. 1681–1695, doi:1016/S0277-3791(99)00014-1.

Calvo, J.P. et al., 1993, Up-to-date Spanish continental Neogene synthesis and paleoclimatic interpretation: Revista de la Sociedad Geológica de España, v. 6, http://oa.upm.es/3670/.

Camoin, G.F., Gautret, P., Montaggioni, L.F., and Cabioch, G., 1999, Nature and environmental significance of microbialites in Quaternary reefs: The Tahiti paradox: Sedimentary Geology, v. 126, p. 271–304, doi:10.1016/S0037-0738(99)00045-7.

Canals, M., and Ballesteros, E., 1997, Production of carbonate particles by phytobenthic communities on the Mallorca-Menorca shelf, northwestern Mediterranean Sea: Deep-Sea Research Part II: Topical Studies in Oceanography, v. 44, p. 611–629, doi:10.1016/S0967-0645(96)00095-1.

Capó, A., and Garcia, C., 2019, Basin filling evolution of the central basins of Mallorca since the Pliocene: Basin Research, v. 31, p. 948–966, doi:10.1111/bre.12352.

Carannante, G., Esteban, M., Milliman, J.D., and Simone, L., 1988, Carbonate lithofacies as paleolatitude indicators: problems and limitations: Sedimentary Geology, v. 60, p. 333–346, doi:10.1016/0037-0738(88)90128-5.

Cathro, D.L., and Austin, J.A., 2001, An early mid-Miocene, strike-parallel shelfal trough and possible karstification in the Northern Carnarvon Basin, northwest Australia: Marine Geology, v. 178, p. 157–169, doi:10.1016/S0025-3227(01)00177-3.

Cathro, D.L., Austin James A., J.A., and Moss, G.D., 2003, Progradation along a deeply submerged Oligocene-Miocene heterozoan carbonate shelf: How sensitive are clinoforms to sea level variations? American Association of Petroleum Geologists Bulletin, v. 87, p. 1547–1574, doi:10.1306/05210300177.

Chave, K.E., 1967, Recent Carbonate Sediments–An Unconventional View: Journal of Geological Education, v. 15, p. 200–204, doi:10.5408/0022-1368-xv.5.200.

Choi, Y.S., and Simo, J.A., 1998, Ramp facies and sequence stratigraphic models in an epeiric sea: The Upper Ordovician mixed carbonate-siliciclastic Glenwood and Platteville Formations, Wisconsin, USA: Geological Society Special Publication, v. 149, p. 437–456, doi:10.1144/GSL.SP.1999.149.01.20.

Cita, M.B., Bryan, W.B.F., and Kidd, R.B., 1978, Sedimentation Rates in Neogene Deep-Sea Sediments from the Mediterranean and Geodynamic Implications of Their Changes, *in* Initial Reports of the Deep Sea Drilling Project, 42 Pt. 1, U.S. Government Printing Office, doi:10.2973/dsdp.proc.42-1.152.1978.

Coe, A.L., Bosence, D.W.J., Church, K.D., Flint, S.S., Howell, J.A., Wilson, R., and Chris, L., 2003, The sedimentary record of Sea-level change: v. 8, 113–114 p., doi:10.2277/0521831113.

Collins, L.B., Zhu, Z.R., Wyrwoll, K.H., Hatcher, B.G., Playford, P.E., Eisenhauer, A., Chen, J.H., Wasserburg, G.J., and Bonani, G., 1993, Holocene growth history of a reef complex on a cool-water carbonate margin: Easter Group of the Houtman Abrolhos, Eastern Indian Ocean: Marine Geology, v. 115, p. 29–46, doi:10.1016/0025-3227(93)90073-5.

Cornacchia, I., Brandano, M., and Agostini, S., 2021, Miocene paleoceanographic evolution of the Mediterranean area and carbonate production changes: A review: Earth-Science Reviews, v. 221, p. 103785, doi:10.1016/j.earscirev.2021.103785.

Davies, P.J., and Hopley, D., 1983, Growth fabrics and growth rates of Holocene reefs in the Great Barrier Reef (Australia).: BMR Journal of Australian Geology & Geophysics, v. 8, p. 237–251.

Doglioni, C., Gueguen, E., Sàbat, F., and Fernandez, M., 1997, The Western Mediterranean extensional basins and the Alpine orogen: Terra Nova, v. 9, p. 109–112, doi:10.1046/j.1365-3121.1997.d01-18.x.

Doligez, B., Granjeon, D., Joseph, P., Eschard, R., and Beucher, H., 1999, How Can Stratigraphic Modeling Help Constrain Geostatistical Reservoir Simulations?, *in* Numerical Experiments in Stratigraphy<subtitle>Recent Advances in Stratigraphic and Sedimentologic Computer Simulations</subtitle>, SEPM Society for Sedimentary Geology, doi:10.2110/pec.99.62.0239.

Droxler, A.W., and Schlager, W., 1985, Glacial versus interglacial sedimentation rates and turbidite frequency in the Bahamas.: Geology, v. 13, p. 799–802, doi:10.1130/0091-7613(1985)13<799:GVISRA>2.0.CO;2.

Eberli, G.P., and Ginsburg, R.N., 1989, Cenozoic progradation of northwestern Great Bahama Bank, a record of lateral platform growth and sea-level fluctuations: Controls on carbonate platform and basin development, p. 339–351, doi:10.2110/pec.89.44.0339.

Edinger, E.N., and Risk, M.J., 1995, Preferential survivorship of brooding corals in a regional extinction: Paleobiology, v. 21, p. 200–219, doi:10.1017/S0094837300013208.

Elrick, M., and Read, J.F., 1991, Cyclic ramp-to-basin carbonate deposits, Lower Mississippian, Wyoming and Montana: a combined field and computer modeling study: Journal of Sedimentary Petrology, v. 61, p. 1194–1224, doi:10.1306/D4267866-2B26-11D7-8648000102C1865D.

Elvebakk, G., Hunt, D.W., and Stemmerik, L., 2002, From isolated buildups to buildup mosaics: 3D seismic sheds new light on upper Carboniferous-Permian fault controlled carbonate buildups, Norwegian Barents Sea: Sedimentary Geology, v. 152, p. 7–17, doi:10.1016/S0037-0738(02)00232-4.

Esteban, M., 1979, Significance of the upper miocene coral reefs of the Western Mediterranean: Palaeogeography, Palaeoclimatology, Palaeoecology, v. 29, p. 169–188, doi:10.1016/0031-0182(79)90080-4.

Franseen, E.K., and Esteban, M., 1996, Models for carbonate stratigraphy from Miocene reef complexes of Mediterranean regions:, doi:10.2110/csp.96.05.

Franseen, E.K., Goldstein, R.H., and Farr, M.R., 1997, Substrate-slope and temperature controls on carbonate ramps: revelation from Upper Miocene outcrops, SE Spain., *in* Cool-Water Carbonates, SEPM (Society for Sedimentary Geology), p. 271–290, doi:10.2110/pec.97.56.0271.

Frost, E.L., and Kerans, C., 2010, Controls on syndepositional fracture patterns, Devonian reef complexes, Canning Basin, Western Australia: Journal of Structural Geology, v. 32, p. 1231–1249, doi:10.1016/j.jsg.2009.04.019.

Frost, E.L., and Kerans, C., 2009, Platform-Margin Trajectory as a Control on Syndepositional Fracture Patterns, Canning Basin, Western Australia: Journal of Sedimentary Research, v. 79, p. 44–55, doi:10.2110/jsr.2009.014.

Gambi, M., Nowell, A., and Jumars, P., 1990, Flume observations on flow dynamics in Zostera marina (eelgrass) beds: Marine Ecology Progress Series, v. 61, p. 159–169, doi:10.3354/meps061159.

Gervais, V., Ducros, M., and Granjeon, D., 2018, Probability maps of reservoir presence and sensitivity analysis in stratigraphic forward modeling: AAPG Bulletin, v. 102, p. 545–547, doi:10.1306/0913171611517242.

Gervais, V., Ducros, M., and Granjeon, D., 2016, Uncertainty quantification for stratigraphic modeling Uncertainty quantification for stratigraphic modeling:, doi:10.13140/RG.2.1.4375.8488.

Ginés, A., Ginés, J., Gómez-Pujol, L., Onac, B.P., and Fornós, J.J., 2012, Mallorca : a Mediterranean Benchmark for Quaternary Studies: v. 18.

Ginsburg, R.N., and James, N.P., 1974, Holocene Carbonate Sediments of Continental Shelves: The Geology of Continental Margins, p. 137–155, doi:10.1007/978-3-662-01141-6_11.

Gómez-Pérez, I., Fernández-Mendiola, P.A., and García-Mondéjar, J., 1999, Depositional architecture of a rimmed carbonate platform (Albian, Gorbea, western Pyrenees): Sedimentology, v. 46, p. 337–356, doi:10.1046/j.1365-3091.1999.00217.x.

Goodwin, P.W., and Anderson, E.J., 1985, Punctuated aggradational cycles: a general hypothesis of episodic stratigraphic accumulation.: Journal of Geology, v. 93, p. 515–533.

Granjeon, D., 2014, 3D forward modelling of the impact of sediment transport and base level cycles on continental margins and incised valleys, *in* From Depositional Systems to Sedimentary

Successions on the Norwegian Continental Margin, Chichester, UK, John Wiley & Sons, Ltd, v. 9781118920, p. 453–472, doi:10.1002/9781118920435.ch16.

Granjeon, D., 1996, Modélisation stratigraphique déterministe : conception et applications d'un modèle diffusif 3d multilithologique: Université de Rennes 1., https://www.worldcat.org/title/modelisation-stratigraphique-deterministe-conception-et-applications-dun-modele-diffusif-3d-multilithologique/oclc/490267137.

Granjeon, D., and Joseph, P., 1999, Concepts and Applications of A 3-D Multiple Lithology, Diffusive Model in Stratigraphic Modeling, *in* Harbaugh, J.W., Watney, W.L., Rankey, E.C., Slingerland, R., Goldstein, R.H., and Franseen, E.K. eds., Numerical Experiments in Stratigraphy<subtitle>Recent Advances in Stratigraphic and Sedimentologic Computer Simulations</subtitle>, SEPM Society for Sedimentary Geology, doi:10.2110/pec.99.62.0197.

Grant, G.R., Naish, T.R., Dunbar, G.B., Stocchi, P., Kominz, M.A., Kamp, P.J.J., Tapia, C.A., McKay, R.M., Levy, R.H., and Patterson, M.O., 2019, The amplitude and origin of sea-level variability during the Pliocene epoch: Nature, v. 574, p. 237–241, doi:10.1038/s41586-019-1619-z.

Grasso, M., and Lentini, F., 1982, Sedimentary and tectonic evolution of the eastern Hyblean Plateau (southeastern Sicily) during late Cretaceous to Quaternary time: Palaeogeography, Palaeoclimatology, Palaeoecology, v. 39, p. 261–280, doi:10.1016/0031-0182(82)90025-6.

Halfar, J., Godinez-Orta, L., Goodfriend, G.A., Mucciarone, D.A., Ingle, J.C., and Holden, P., 2001, Holocene-late Pleistocene non-tropical carbonate sediments and tectonic history of the western rift basin margin of the southern Gulf of California: Sedimentary Geology, v. 144, p. 149–157, doi:10.1016/S0037-0738(01)00139-7.

Halfar, J., Godinez-Orta, L., Mutti, M., Valdez-Holguín, J.E., and Borges, J.M., 2004, Nutrient and temperature controls on modern carbonate production: An example from the Gulf of California, Mexico: Geology, v. 32, p. 213–216, doi:10.1130/G20298.1.

Hallock, P., 1988, The role of nutrient availability in bioerosion: Consequences to carbonate buildups: Palaeogeography, Palaeoclimatology, Palaeoecology, v. 63, p. 275–291, doi:10.1016/0031-0182(88)90100-9.

Hallock, P., and Glenn, E.C., 1986, Larger foraminifera: a tool for paleoenvironmental analysis of Cenozoic carbonate depositional facies.: Palaios, v. 1, p. 55–64, doi:10.2307/3514459.

Handford, C.R., and Loucks, R.G., 1993, Carbonate Depositional Sequences and Systems Tracts—Responses of Carbonate Platforms to Relative Sea-Level Changes, *in* Carbonate Sequence Stratigraphy, American Association of Petroleum Geologists, p. 3–41, doi:10.1306/M57579C1.

Haq, B.U., 2014, Cretaceous eustasy revisited: Global and Planetary Change, v. 113, p. 44–58, doi:10.1016/j.gloplacha.2013.12.007.

Haq, B.U., Hardenbol, J., and Vail, P.R., 1988, Mesozoic and Cenozoic Chronostratigraphy and Cycles of Sea-Level Change, *in* Sea-Level Changes, SEPM (Society for Sedimentary Geology), p. 71–108, doi:10.2110/pec.88.01.0071.

Hawie, N., Barrois, A., Marfisi, E., Murat, B., Hall, J., El-Wazir, Z., Al-Madani, N., and Aillud, G., 2015, Forward stratigraphic modelling, deterministic approach to improve carbonate heterogeneity prediction; Lower cretaceous, Abu Dhabi: Society of Petroleum Engineers - Abu Dhabi International Petroleum Exhibition and Conference, ADIPEC 2015, doi:10.2118/177519-ms.

Hawie, N., Callies, M., and Marfisi, E., 2017, Integrated multi-disciplinary forward stratigraphic modelling workflow in petroleum systems assessment: SPE Middle East Oil and Gas Show and Conference, MEOS, Proceedings, v. 2017-March, p. 1405–1412, doi:10.2118/183835-ms.

Hawie, N., Marfisi, E., Saint-Ange, F., and MacDonald, A.W.A., 2019, Statistical analysis of forward stratigraphic models in complex salt provinces: The central Scotian Basin case study: AAPG Bulletin, v. 103, p. 433–467, doi:10.1306/07031817054.

Hendriks, I.E., Bouma, T.J., Morris, E.P., and Duarte, C.M., 2010, Effects of seagrasses and algae of the Caulerpa family on hydrodynamics and particle-trapping rates: Marine Biology, v. 157, p. 473–481, doi:10.1007/s00227-009-1333-8.

Henrich, R., Freiwald, A., Betzler, C., Bader, B., Schäfer, P., Samtleben, C., Brachert, T.C., Wehrmann, A., Zankl, H., and Kühlmann, D.H.H., 1995, Controls on modern carbonate sedimentation on warm-temperate to arctic coasts, shelves and seamounts in the Northern Hemisphere: Implications for fossil counterparts: Facies, v. 32, p. 71–108, doi:10.1007/BF02536865.

Hongo, C., and Kayanne, H., 2011, Key species of hermatypic coral for reef formation in the northwest Pacific during Holocene sea-level change: Marine Geology, v. 279, p. 162–177, doi:10.1016/j.margeo.2010.10.023.

Huang, X., Griffiths, C.M., and Liu, J., 2015, Recent development in stratigraphic forward modelling and its application in petroleum exploration: Australian Journal of Earth Sciences, v. 62, p. 903–919, doi:10.1080/08120099.2015.1125389.

Hüssner, H., Roessler, J., Betzler, C., Petschick, R., and Peinl, M., 2001, Testing 3D computer simulation of carbonate platform growth with REPRO: The Miocene Llucmajor carbonate platform (Mallorca): Palaeogeography, Palaeoclimatology, Palaeoecology, v. 175, p. 239–247, doi:10.1016/S0031-0182(01)00374-1.

James, N.P., 1997, The Cool-Water Carbonate Depositional Realm, *in* James, N.P. and Clarke, J.A.D. eds., Cool-Water Carbonates, SEPM (Society for Sedimentary Geology), p. 1–20, doi:10.2110/pec.97.56.0001.

James, N.P., and Bone, Y., 1991, Origin of a cool-water, Oligo-Miocene deep shelf limestone, Eucla Platform, southern Australia: Sedimentology, v. 38, p. 323–341, doi:10.1111/j.1365-3091.1991.tb01263.x.

James, N.P., Bone, Y., Brown, K.M., and Cheshire, A., 2009, Calcareous Epiphyte Production in Cool-Water Carbonate Seagrass Depositional Environments — Southern Australia, *in* Perspectives in Carbonate Geology, v. 41, p. 123–148, doi:10.1002/9781444312065.ch9.

James, N.P., Collins, L.B., Bone, Y., and Hallock, P., 1999, Subtropical carbonates in a temperate realm: Modern sediments on the southwest australian shelf: Journal of Sedimentary Research, v. 69, p. 1297–1321, doi:10.2110/jsr.69.1297.

James, N.P., and Mountjoy, E., 1983, Shelf-Slope Break in Fossil Carbonate Platforms: An Overview, *in* The Shelfbreak, SEPM (Society for Sedimentary Geology), p. 189–206, doi:10.2110/pec.83.06.0189.

Janson, X., van Buchem, F.S.P., Dromart, G., Eichenseer, H.T., Dellamonica, X., Boichard, R., Bonnaffe, F., and Eberli, G., 2010, Architecture and facies differentiation within a Middle Miocene carbonate platform, Ermenek, Mut Basin, southern Turkey: Geological Society Special Publication, v. 329, p. 265–290, doi:10.1144/SP329.11.

John, C.M., and Mutti, M., 2005, Relative control of paleoceanography, climate, and eustasy over heterozoan carbonates: A perspective from slope sediments of the Marion Plateau (ODP LEG 194): Journal of Sedimentary Research, v. 75, p. 216–230, doi:10.2110/jsr.2005.017.

Jones, B., and Desrochers, A., 1992, Shallow carbonate platforms, *in* Walker, R.G. and James, N.P. eds., Facies Models – Response to Sea Level Change, Geological Association, Canada, p. 277– 301.

Kendall, C.G.St.C., and Schlager, W., 1981, Carbonates and relative changes in sea level: Marine Geology, v. 44, p. 181–212, doi:10.1016/0025-3227(81)90118-3.

Kenter, J.A.M., 1990, Carbonate platform flanks: slope angle and sediment fabric: Sedimentology, v. 37, p. 777–794, doi:10.1111/j.1365-3091.1990.tb01825.x.

Kenter, J.A.M., Harris, P.M., and della Porta, G., 2005, Steep microbial boundstone-dominated platform margins - Examples and implications: Sedimentary Geology, v. 178, p. 5–30, doi:10.1016/j.sedgeo.2004.12.033.

Kershaw, S., and Guo, L., 2006, Pleistocene calcified cyanobacterial mounds, Perachora Peninsula, central Greece: a controversy of growth and history: Geological Society, London, Special Publications, v. 255, p. 53–69, doi:10.1144/GSL.SP.2006.255.01.05.

Kim, W., Fouke, B.W., Petter, A.L., Quinn, T.M., Kerans, C., and Taylor, F., 2012, Sea-level rise, depth-dependent carbonate sedimentation and the paradox of drowned platforms: Sedimentology, v. 59, p. 1677–1694, doi:10.1111/j.1365-3091.2012.01321.x.

Kindler, P., and Wilson, M.E.J., 2012, Carbonate Grain Associations: their Use and Environmental Significance, a Brief Review, *in* Carbonate Systems during the Oligocene–Miocene Climatic Transition, p. 35–47, doi:10.1002/9781118398364.ch3.

King, T.K., Pierson, B.J., Al-Jaaidi, O., and Hague, P., 2012, Effects of syn-depositional tectonics on platform geometry and reservoir characters in miocene carbonate platforms of Central Luconia, Sarawak: Society of Petroleum Engineers - International Petroleum Technology Conference 2012, IPTC 2012, v. 1, p. 245–261, doi:10.2523/iptc-14247-ms.

Kinsey, D.W., 1978, Productivity and calcification estimates using slack-water periods and field enclosures, *in* Stoddart, D.R. and Johannes, R.E. eds., Coral reefs: research methods, UNESCO, https://unesdoc.unesco.org/search/N-EXPLORE-33fac11c-2c87-426e-ba2c-93fececdd821.

Knoerich, A.C., and Mutti, M., 2003, Controls of facies and sediment composition on the diagenetic pathway of hallow-water Heterozoan carbonates: The Oligocene of the Maltese Islands: International Journal of Earth Sciences, v. 92, p. 494–510, doi:10.1007/s00531-003-0329-8.

Kolodka, C., Vennin, E., Bourillot, R., Granjeon, D., and Desaubliaux, G., 2016, Stratigraphic modelling of platform architecture and carbonate production: a Messinian case study (Sorbas Basin, SE Spain): Basin Research, v. 28, p. 658–684, doi:10.1111/bre.12125.

Lanteaume, C., Fournier, F., Pellerin, M., and Borgomano, J., 2018, Testing geologic assumptions and scenarios in carbonate exploration: Insights from integrated stratigraphic, diagenetic, and seismic forward modeling: Leading Edge, v. 37, p. 672–680, doi:10.1190/tle37090672.1.

Lees, A., 1975, Possible influence of salinity and temperature on modern shelf carbonate sedimentation: Marine Geology, v. 19, p. 159–198, doi:10.1016/0025-3227(75)90067-5.

Lees, A., and Buller, A.T., 1972, Modern temperate-water and warm-water shelf carbonate sediments contrasted: Marine Geology, v. 13, doi:10.1016/0025-3227(72)90011-4.

Li, X., Falivene, O., Minzoni, M., Lehrmann, D.J., Reijmer, J.J.G., Morsilli, M., Al-Ramadan, K.A.H., Yu, M., and Payne, J.L., 2020, Interactions between sediment production and transport in the geometry of carbonate platforms: Insights from forward modeling of the Great Bank of Guizhou (Early to Middle Triassic), south China: Marine and Petroleum Geology, v. 118, p. 104416, doi:10.1016/j.marpetgeo.2020.104416.

Light, J.M., and Wilson, J.B., 1998, Cool-water carbonate deposition on the West Shetland Shelf: A modern distally steepened ramp: Geological Society Special Publication, v. 149, p. 73–105, doi:10.1144/GSL.SP.1999.149.01.06.

Lüdmann, T., Wiggershaus, S., Betzler, C., and Hübscher, C., 2012, Southwest Mallorca Island: A cool-water carbonate margin dominated by drift deposition associated with giant mass wasting: Marine Geology, v. 307–310, p. 73–87, doi:10.1016/j.margeo.2011.09.008.

Mateu-Vicens, G., Hallock, P., and Brandano, M., 2008, A depositional model and paleoecological reconstruction of the lower Tortonian distally steepened ramp of Menorca (Balearic Islands, Spain): Palaios, v. 23, p. 465–481, doi:10.2110/palo.2007.p07-061r.

Matsuda, S., 1989, Succession and growth rates of encrusting crustose coralline algae (Rhodophyta, Cryptonemiales) in the upper fore-reef environment off Ishigaki Island, Ryukyu Islands: Coral Reefs, v. 7, p. 185–195, doi:10.1007/BF00301597.

Miall, A.D., 1992, Exxon global cycle chart: an event for every occasion? Geology, v. 20, p. 787–790, doi:10.1130/0091-7613(1992)020<0787:EGCCAE>2.3.CO;2.

Michel, J., Borgomano, J., and Reijmer, J.J.G., 2018, Heterozoan carbonates: When, where and why? A synthesis on parameters controlling carbonate production and occurrences: Earth-Science Reviews, v. 182, p. 50–67, doi:10.1016/j.earscirev.2018.05.003.

Michel, J., Laugié, M., Pohl, A., Lanteaume, C., Masse, J.P., Donnadieu, Y., and Borgomano, J., 2019, Marine carbonate factories: a global model of carbonate platform distribution: International Journal of Earth Sciences, v. 108, p. 1773–1792, doi:10.1007/s00531-019-01742-6.

Miller, K.G., Browning, J. v, Schmelz, W.J., Kopp, R.E., Mountain, G.S., and Wright, J.D., 2020, Cenozoic sea-level and cryospheric evolution from deep-sea geochemical and continental margin records: Science Advances, v. 6, p. eaaz1346, doi:10.1126/sciadv.aaz1346.

Miller, K.G., Kominz, M.A., Browning, J. v., Wright, J.D., Mountain, G.S., Katz, M.E., Sugarman, P.J., Cramer, B.S., Christie-Blick, N., and Pekar, S.F., 2005a, The phanerozoic record of global sea-level change: Science, v. 310, p. 1293–1298, doi:10.1126/science.1116412.

Miller, K.G., Kominz, M.A., Browning, J. v., Wright, J.D., Mountain, G.S., Katz, M.E., Sugarman, P.J., Cramer, B.S., Christie-Blick, N., and Pekar, S.F., 2005b, The phanerozoic record of global sea-level change: Science, v. 310, p. 1293–1298, doi:10.1126/science.1116412.

Milliman, J.D., Müller, G., and Förstner, U., 1974, Recent Sedimentary Carbonates: Berlin, Heidelberg, Springer Berlin Heidelberg, doi:10.1007/978-3-642-65528-9.

Montaggioni, L.F., 2005, History of Indo-Pacific coral reef systems since the last glaciation: Development patterns and controlling factors: Earth-Science Reviews, v. 71, p. 1–75, doi:10.1016/j.earscirev.2005.01.002.

Moore, C.H., and Wade, W.J., 2013a, Natural Fracturing in Carbonate Reservoirs, *in* Developments in Sedimentology, v. 67, p. 285–300, doi:10.1016/B978-0-444-53831-4.00011-2.

Moore, C.H., and Wade, W.J., 2013b, The basic nature of carbonate sediments and sedimentation: Developments in Sedimentology, v. 67, p. 3–21, doi:10.1016/B978-0-444-53831-4.00001-X.

Morsilli, M., Bosellini, F.R., Pomar, L., Hallock, P., Aurell, M., and Papazzoni, C.A., 2012, Mesophotic coral buildups in a prodelta setting (Late Eocene, southern Pyrenees, Spain): A mixed carbonate-siliciclastic system: Sedimentology, v. 59, p. 766–794, doi:10.1111/j.1365-3091.2011.01275.x.

Morsilli, M., and Pomar, L., 2012, Internal waves vs. surface storm waves: A review on the origin of hummocky cross-stratification: Terra Nova, v. 24, p. 273–282, doi:10.1111/j.1365-3121.2012.01070.x.

Mutti, M., 2019, Latitudinal Variability of Carbonate Systems Today and During Icehouse and Greenhouse Worlds, *in* Latitudinal Controls on Stratigraphic Models and Sedimentary Concepts, SEPM (Society for Sedimentary Geology), p. 46–58, doi:10.2110/sepmsp.108.11.

Mutti, M., Bernoulli, D., and Stille, P., 1997, Temperate carbonate platform drowning linked to Miocene oceanographic events: Maiella platform margin, Italy: Terra Nova, v. 9, p. 122–125, doi:10.1046/j.1365-3121.1997.d01-19.x.

Mutti, M., and Hallock, P., 2003a, Carbonate systems along nutrient and temperature gradients: Some sedimentological and geochemical constraints: International Journal of Earth Sciences, v. 92, p. 465–475, doi:10.1007/s00531-003-0350-y.

Mutti, M., and Hallock, P., 2003b, Carbonate systems along nutrient and temperature gradients: Some sedimentological and geochemical constraints: International Journal of Earth Sciences, v. 92, p. 465–475, doi:10.1007/s00531-003-0350-y.

Nader, F.H., Souque, C., Lecomte, J., Deschamps, R., Chauveau, B., Granjeon, D., Staples, R., Woon, E., Tricker, P., and Frascati, A., 2018, Advanced 3-D Forward Stratigraphic Modeling of the East-Mediterranean Frontier Deepwater Basins : An Approach for Enhancing Reservoir Fairways Predictions *: v. 11133, doi:10.1306/11133Nader2018.

Nelson, C.S., 1988, An introductory perspective on non-tropical shelf carbonates: Sedimentary Geology, v. 60, p. 3–12, doi:10.1016/0037-0738(88)90108-X.

Nolting, A., Zahm, C.K., Kerans, C., and Nikolinakou, M.A., 2018, Effect of carbonate platform morphology on syndepositional deformation: Insights from numerical modeling: Journal of Structural Geology, v. 115, p. 91–102, doi:10.1016/j.jsg.2018.07.003.

Obrador, A., 1970, Estudio estratigráfico y sedimentológico de los materiales miocénicos de la isla de Menorca: Acta geológica hispánica, v. 5, https://raco.cat/index.php/ActaGeologica/article/view/74641.

Obrador, A., Pomar, L., and Taberner, C., 1992, Late Miocene breccia of Menorca (Balearic Islands) a basis for the interpretation of a Neogene ramp deposit: Sedimentary Geology, v. 79, p. 203–223, doi:10.1016/0037-0738(92)90012-G.

Olsson, R.K., 1988, Foraminiferal Modeling of Sea-Level Change in the Late Cretaceous of New Jersey, *in* Sea-Level Changes, SEPM (Society for Sedimentary Geology), p. 289–297, doi:10.2110/pec.88.01.0289.

Otoo, D., and Hodgetts, D., 2021, Porosity and permeability prediction through forward stratigraphic simulations using GPM^TM and Petrel^TM: Application in shallow marine depositional settings: Geoscientific Model Development, v. 14, p. 2075–2095, doi:10.5194/gmd-14-2075-2021.

Pall, J., Chandra, R., Azam, D., Salles, T., Webster, J.M., Scalzo, R., and Cripps, S., 2020, Bayesreef: A Bayesian inference framework for modelling reef growth in response to environmental change and biological dynamics: Environmental Modelling and Software, v. 125, doi:10.1016/j.envsoft.2019.104610.

Pedley, H.M., and Carannante, G., 2006, Cool-Water Carbonates: Depositional Systems and Palaeoenvironmental Controls: Geological Society of London, doi:https://doi.org/10.1144/GSL.SP.2006.255.

Pedley, M., and Grasso, M., 2006, The response of cool-water carbonates to eustatic change in microtidal, Mediterranean Quaternary settings of Sicily: Geological Society Special Publication, v. 255, p. 137–156, doi:10.1144/GSL.SP.2006.255.01.10.

Pomar, L., 2020, Carbonate systems, *in* Regional Geology and Tectonics: Principles of Geologic Analysis, Elsevier, p. 235–311, doi:10.1016/B978-0-444-64134-2.00013-4.

Pomar, L., 2001a, Ecological control of sedimentary accommodation: evolution from a carbonate ramp to rimmed shelf, Upper Miocene, Balearic Islands: Palaeogeography, Palaeoclimatology, Palaeoecology, v. 175, p. 249–272, doi:10.1016/S0031-0182(01)00375-3.

Pomar, L., 1993, High-resolution sequence stratigraphy in prograding Miocene carbonates: application to seismic interpretation: Carbonate sequence stratigraphy: recent developments and applications, p. 389–407.

Pomar, L., 1991, Reef geometries, erosion surfaces and high-frequency sea-level changes, upper Miocene Reef Complex, Mallorca, Spain: Sedimentology, v. 38, p. 243–269, doi:10.1111/j.1365-3091.1991.tb01259.x.

Pomar, L., 2001b, Types of carbonate platforms: a genetic approach: Basin Research, v. 13, p. 313–334, doi:10.1046/j.0950-091x.2001.00152.x.

Pomar, L., Baceta, J.I., Hallock, P., Mateu-Vicens, G., and Basso, D., 2017, Reef building and carbonate production modes in the west-central Tethys during the Cenozoic: Marine and Petroleum Geology, v. 83, p. 261–304, doi:10.1016/j.marpetgeo.2017.03.015.

Pomar, L., Bassant, P., Brandano, M., Ruchonnet, C., and Janson, X., 2012a, Impact of carbonate producing biota on platform architecture: Insights from Miocene examples of the Mediterranean region: Earth-Science Reviews, v. 113, p. 186–211, doi:10.1016/j.earscirev.2012.03.007.

Pomar, L., Esteban, M., Calvet, F., and Baron, A., 1983, La unidad arrecifal del Mioceno superior de Mallorca (L. Pomar, A. Obrador, J. Fornos, & A. Rodriguez-Perea, Eds.): Inst. Est. Balearics and Universidad de Palma de Mallorca, 139–175 p.

Pomar, L., and Hallock, P., 2008, Carbonate factories: A conundrum in sedimentary geology: Earth-Science Reviews, v. 87, p. 134–169, doi:10.1016/j.earscirev.2007.12.002.

Pomar, L., and Hallock, P., 2007, Changes in coral-reef structure through the Miocene in the Mediterranean province: Adaptive versus environmental influence: Geology, v. 35, p. 899–902, doi:10.1130/G24034A.1.

Pomar, L., and Haq, B.U., 2016, Decoding depositional sequences in carbonate systems: Concepts vs experience: Global and Planetary Change, v. 146, p. 190–225, doi:10.1016/j.gloplacha.2016.10.001.

Pomar, L., and Kendall, C.G.St.C., 2008a, Architecture of Carbonate Platforms: A Response to Hydrodynamics and Evolving Ecology, *in* Controls on Carbonate Platform and Reef Development, p. 187–216, doi:10.2110/pec.08.89.0187.

Pomar, L., and Kendall, C.G.St.C., 2008b, Ecological Accommodation: A Key to the Interpretation of Carbonate Platform Architecture Variability: Search and Discovery Article #50150 (2008)., v. 50150.

Pomar, L., Mateu-Vicens, G., Morsilli, M., and Brandano, M., 2014, Carbonate ramp evolution during the Late Oligocene (Chattian), Salento Peninsula, southern Italy: Palaeogeography, Palaeoclimatology, Palaeoecology, v. 404, p. 109–132, doi:10.1016/j.palaeo.2014.03.023.

Pomar, L., Morsilli, M., Hallock, P., and Bádenas, B., 2012b, Internal waves, an under-explored source of turbulence events in the sedimentary record: Earth-Science Reviews, v. 111, p. 56–81, doi:10.1016/j.earscirev.2011.12.005.

Pomar, L., Obrador, A., and Westphal, H., 2002, Sub-wavebase cross-bedded grainstones on a distally steepened carbonate ramp, Upper Miocene, Menorca, Spain: Sedimentology, v. 49, p. 139–169, doi:10.1046/j.1365-3091.2002.00436.x.

Pomar, L., and Ward, W.C., 1999, Reservoir-scale heterogeneity in depositional packages and diagenetic patterns on a reef-rimmed platform, upper Miocene, Mallorca, Spain: AAPG Bulletin, v. 83, p. 1759–1773, doi:10.1306/e4fd425b-1732-11d7-8645000102c1865d.

Pomar, L., and Ward, W.C., 1994, Response of a late Miocene Mediterranean reef platform to high-frequency eustasy: Geology, v. 22, p. 131, doi:10.1130/0091-7613(1994)022<0131:ROALMM>2.3.CO;2.

Pomar, L., and Ward, W.C., 1995, Sea-Level Changes, Carbonate Production and Platform Architecture: The Llucmajor Platform, Mallorca, Spain, in Haq, B.U. ed., Sequence Stratigraphy and Depositional Response to Eustatic, Tectonic and Climate Forcing, p. 87–112, doi:10.1007/978-94-015-8583-5_4.

Pomar, L., Ward, W.C., and Green, D.G., 1996, Upper Miocene reef complex of the Llucmajor area, Mallorca, Spain: 191–225 p., doi:10.2110/csp.96.01.0191.

Potouroglou, M., Bull, J.C., Krauss, K.W., Kennedy, H.A., Fusi, M., Daffonchio, D., Mangora, M.M., Githaiga, M.N., Diele, K., and Huxham, M., 2017, Measuring the role of seagrasses in regulating sediment surface elevation: Scientific Reports, v. 7, p. 11917, doi:10.1038/s41598-017-12354-y.

Purdy, E.G., 1963, Recent Calcium Carbonate Facies of the Great Bahama Bank. 2. Sedimentary Facies: The Journal of Geology, v. 71, p. 472–497, doi:10.1086/626920.

Purdy, E.G., and Bertram, G.T., 1993, Carbonate Concepts from the Maldives, Indian Ocean: American Association of Petroleum Geologists, doi:10.1306/St34568.

Qing Sun, S., and Esteban, M., 1994, Paleoclimatic controls on sedimentation, diagenesis, and reservoir quality: lessons from Miocene carbonates: American Association of Petroleum Geologists Bulletin, v. 78, p. 519–543, doi:10.1306/bdff924e-1718-11d7-8645000102c1865d.

Read, J.F., 1985, Carbonate Platform Facies Models.: American Association of Petroleum Geologists Bulletin, v. 69, p. 1–21, doi:10.1306/ad461b79-16f7-11d7-8645000102c1865d.

Read, J.F., 1982, Carbonate platforms of passive (extensional) continental margins: Types, characteristics and evolution: Tectonophysics, v. 81, p. 195–212, doi:10.1016/0040-1951(82)90129-9.

Read, J.F., 1998, Phanerozoic carbonate ramps from greenhouse, transitional and ice-house worlds: Clues from field and modelling studies: Geological Society Special Publication, v. 149, p. 107–135, doi:10.1144/GSL.SP.1999.149.01.07.

Read, J.F., and Horbury, A.D., 1993, Eustatic and Tectonic Controls on Porosity Evolution Beneath Sequence-Bounding Unconformities and Parasequence Disconformities on Carbonate Platforms (A. D. Horbury & A. G. Robinson, Eds.): Diagenesis and Basin Development, v. 36, p. 0, doi:10.1306/St36574C11.

Reijmer, J.J.G., 2021, Marine carbonate factories: Review and update: Sedimentology, doi:10.1111/sed.12878.

Reolid, J., Betzler, C., Eberli, G.P., and Grammer, G.M., 2017, The Importance of Microbial Binding In Neogene–Quaternary Steep Slopes: Journal of Sedimentary Research, v. 87, p. 567–577, doi:10.2110/jsr.2017.28.

Resor, P.G., and Flodin, E.A., 2010, Forward modeling synsedimentary deformation associated with a prograding steep-sloped carbonate margin: Journal of Structural Geology, v. 32, p. 1187–1200, doi:10.1016/j.jsg.2009.04.015.

Rinke-Hardekopf, L., Reuning, L., Bourget, J., and Back, S., 2018, Syn-sedimentary deformation as a mechanism for the initiation of submarine gullies on a carbonate platform to slope transition, Browse Basin, Australian North West Shelf: Marine and Petroleum Geology, v. 91, p. 622–630, doi:10.1016/j.marpetgeo.2017.12.034.

Roberts, D.G., and Bally, A.W., 2012, Regional Geology And Tectonics: Elsevier, v. 110, 1689–1699 p., doi:10.1016/C2009-0-17259-8.

Ros, J.D., Romero, J., Enric, B., and Gili, J.M., 1985, Diving in blue water . The benthos, *in* Margalef, R. ed., The Western Mediterranean, Oxford, Pergamon Press, p. 233–295.

Ruchonnet, C., and Kindler, P., 2012a, Facies Models and Geometries of the Ragusa Platform (SE Sicily, Italy) Near the Serravallian-Tortonian Boundary, *in* Carbonate Systems during the Oligocene-Miocene Climatic Transition, Oxford, UK, Wiley-Blackwell, p. 71–88, doi:10.1002/9781118398364.ch5.

Ruchonnet, C., and Kindler, P., 2012b, Facies Models and Geometries of the Ragusa Platform (SE Sicily, Italy) Near the Serravallian–Tortonian Boundary, *in* Carbonate Systems during the Oligocene–Miocene Climatic Transition, p. 71–88, doi:10.1002/9781118398364.ch5.

Sàbat, F., Gelabert, B., and Rodriguez-Perea, A., 2018, Minorca, an exotic Balearic island (western Mediterranean): Geologica Acta, v. 16, p. 411–426, doi:10.1344/GeologicaActa2018.16.4.5.

Sàbat, F., Gelabert, B., Rodríguez-Perea, A., and Giménez, J., 2011a, Geological structure and evolution of Majorca: Implications for the origin of the Western Mediterranean: Tectonophysics, v. 510, p. 217–238, doi:10.1016/j.tecto.2011.07.005.

Sàbat, F., Gelabert, B., Rodríguez-Perea, A., and Giménez, J., 2011b, Geological structure and evolution of Majorca: Implications for the origin of the Western Mediterranean: Tectonophysics, v. 510, p. 217–238, doi:10.1016/j.tecto.2011.07.005.

Sàbat, F., Roca, E., Muñoz, J.A., Vergés, J., Santanach, P., Sans, M., Masana, E., Estévez, A., and Santisteban, C. de, 1994, Role of extension and compression in the evolution of the eastem margin of Iberia: the ESCI- València Trough seismic profile: Revista de la Sociedad Geológica de España, v. 8.

Salles, T., Ding, X., and Brocard, G., 2018a, pyBadlands: A framework to simulate sediment transport, landscape dynamics and basin stratigraphic evolution through space and time: PLoS ONE, v. 13, p. 1–24, doi:10.1371/journal.pone.0195557.

Salles, T., Pall, J., Webster, J.M., and Dechnik, B., 2018b, Exploring coral reef responses to millennial-scale climatic forcings: Insights from the 1-D numerical tool pyReef-Core v1.0: Geoscientific Model Development, v. 11, p. 2093–2110, doi:10.5194/gmd-11-2093-2018.

Sarkar, S., 2017, Ecology of coralline red algae and their fossil evidences from India: Thalassas, v. 33, p. 15–28, doi:10.1007/s41208-016-0017-7.

Schäfer, P., Fortunato, H., Bader, B., Liebetrau, V., Bauch, T., and Reijmer, J.J.G., 2011, Growth rates and carbonate production by coralline red algae in upwelling and non-upwelling settings along the pacific coast of panama: Palaios, v. 26, p. 420–432, doi:10.2110/palo.2010.p10-138r.

Scheibner, C., Rasser, M.W., and Mutti, M., 2007, The Campo section (Pyrenees, Spain) revisited: Implications for changing benthic carbonate assemblages across the Paleocene-Eocene boundary: Palaeogeography, Palaeoclimatology, Palaeoecology, v. 248, p. 145–168, doi:10.1016/j.palaeo.2006.12.007.

Schlager, W., 1993, Accommodation and supply-a dual control on stratigraphic sequences: Sedimentary Geology, v. 86, p. 111–136, doi:10.1016/0037-0738(93)90136-S.

Schlager, W., 2003, Benthic carbonate factories of the Phanerozoic: International Journal of Earth Sciences, v. 92, p. 445–464, doi:10.1007/s00531-003-0327-x.

Schlager, W., 2005, Carbonate Sedimentology and Sequence Stratigraphy:, doi:10.2110/csp.05.08.

Schlager, W., 2000, Sedimentation rates and growth potential of tropical, cool water and mud-mound carbonate systems: Geological Society Special Publication, v. 178, p. 217–227, doi:10.1144/GSL.SP.2000.178.01.14.

Schlager, W., 1992, Sedimentology and sequence stratigraphy of reefs and carbonate platforms:, doi:10.1016/0264-8172(94)90087-6.

Schlager, W., and Camber, O., 1986, Submarine slope angles, drowning unconformities, and self-erosion of limestone escarpments.: Geology, v. 14, p. 762–765, doi:10.1130/0091-7613(1986)14<762:SSADUA>2.0.CO;2.

Schlager, W., and Reijmer, J.J.G., 2009, Carbonate platform slopes of the Alpine Triassic and the Neogene - A comparison: Austrian Journal of Earth Sciences, v. 102, p. 4–14.

Schlager, W., Reijmer, J.J.G., and Droxler, A., 1994, Highstand shedding of carbonate platforms: Journal of Sedimentary Research B: Stratigraphy & Global Studies, p. 270–281, doi:10.1306/d4267faa-2b26-11d7-8648000102c1865d.

Scholle, P.A., Arthur, M.A., and Ekdale, A.A., 1983, Pelagic Environment (P. A. Scholle, D. G. Bebout, & C. H. Moore, Eds.): Carbonate Depositional Environments, v. 33, p. 0, doi:10.1306/M33429C19.

Seard, C., Borgomano, J., Granjeon, D., and Camoin, G., 2013, Impact of environmental parameters on coral reef development and drowning: Forward modelling of the last deglacial reefs from Tahiti (French Polynesia; IODP Expedition #310): Sedimentology, v. 60, p. 1357–1388, doi:10.1111/sed.12030.

Smith, S. v., and Kinsey, D.W., 1976, Calcium carbonate production, coral reef growth, and sea level change: Science, v. 194, p. 937–939, doi:10.1126/science.194.4268.937.

Sowerbutts, A., 2000, Sedimentation and volcanism linked to multiphase rifting in an Oligo-Miocene intra-arc basin, Anglona, Sardinia: Geological Magazine, v. 137, p. 395–418, doi:10.1017/S0016756800004246.

Stanley, S.M., and Hardie, L.A., 1998, Secular oscillations in the carbonate mineralogy of reef-building and sediment-producing organisms driven by tectonically forced shifts in seawater chemistry: Palaeogeography, Palaeoclimatology, Palaeoecology, v. 144, p. 3–19, doi:10.1016/S0031-0182(98)00109-6.

Strasser, A., and Samankassou, E., 2003, Carbonate sedimentation rates today and in the past: Holocene of Florida Bay, Bahamas, and Bermuda vs. Upper Jurassic and lower cretaceous of the Jura mountains (Switzerland and France): Geologia Croatica, v. 56, p. 1–18, doi:10.4154/GC.2003.01.

Strobel, J., Cannon, R., Christopher, G.S., Kendall, C.S., Biswas, G., and Bezdek, J., 1989, Interactive (SEDPAK) simulation of clastic and carbonate sediments in shelf to basin settings: Computers and Geosciences, v. 15, p. 1279–1290, doi:10.1016/0098-3004(89)90092-7.

Sultana, D., Burgess, P., and Bosence, D., 2021, How do carbonate factories influence carbonate platform morphology? Exploring production–transport interactions with numerical forward modelling: Sedimentology, doi:10.1111/sed.12943.

Swift, D.J.P., and Thorne, J.A., 1991, Sedimentation on Continental Margins, I: A General Model for Shelf Sedimentation, *in* Shelf Sand and Sandstone Bodies, Oxford, UK, Blackwell Publishing Ltd., p. 1–31, doi:10.1002/9781444303933.ch1.

Tella, T.O., Winterleitner, G., Morsilli, M., and Mutti, M., 2022a, Testing sea-level and carbonate production effects on stratal architecture of a distally steepened carbonate ramp (Upper Miocene, Menorca): A 3D forward modelling approach: Sedimentary Geology, v. 441, p. 106267, doi:10.1016/j.sedgeo.2022.106267.

Tella, T.O., Winterleitner, G., and Mutti, M., 2022b, Investigating the role of differential biotic production on carbonate geometries through stratigraphic forward modelling and sensitivity analysis: the Llucmajor example: Petroleum Geoscience, v. 28, p. petgeo2021- 053, doi:10.1144/petgeo2021-053.

Tomás, S., Zitzmann, M., Homann, M., Rumpf, M., Amour, F., Benisek, M.-F., Marcano, G., Mutti, M., and Betzler, C., 2010, From ramp to platform: Building a 3D model of depositional geometries and facies architectures in transitional carbonates in the Miocene, Northern Sardinia: Facies, v. 56, p. 195–210, doi:10.1007/s10347-009-0203-7.

Torres, A.S., and Grammer, G.M., 2019, Significance of Microbial Binding in the Formation and Stabilization of Carbonate Forereef Slope Deposits: v. 51583, doi:10.1306/51583Torres2019.

Tucker, M.E., Calvet, F., and Hunt, D., 2009a, Sequence Stratigraphy of Carbonate Ramps: Systems Tracts, Models and Application to the Muschelkalk Carbonate Platforms of Eastern Spain, *in* Posamentier, H.W., Summerhayes, C.P., Haq, B.U., and Allen, G.P. eds., Sequence Stratigraphy and Facies Associations, Oxford, UK, Blackwell Publishing Ltd., p. 397–415, doi:10.1002/9781444304015.ch20.

Tucker, M.E., Wilson, J.L., Crevello, P.D., Sarg, J.F., and Read, J.F., 1990, Carbonate Platforms (M. E. Tucker, J. L. Wilson, P. D. Crevello, J. Rick Sarg, & J. F. Read, Eds.): Oxford, UK, Blackwell Publishing Ltd., v. 9, 1–328 p., doi:10.1002/9781444303834.

Tucker, M.E., Wright, V.P., and Dickson, J.A.D., 2009b, Carbonate Sedimentology: 1–482 p., doi:10.1002/9781444314175.

Walkden, G., and Williams, A., 1998, Carbonate ramps and the Pleistocene-Recent depositional systems of the Arabian Gulf: Geological Society Special Publication, v. 149, p. 43–53, doi:10.1144/GSL.SP.1999.149.01.04.

Warrlich, G., Bosence, D., Waltham, D., Wood, C., Boylan, A., and Badenas, B., 2008, 3D stratigraphic forward modelling for analysis and prediction of carbonate platform stratigraphies in exploration and production: Marine and Petroleum Geology, v. 25, p. 35–58, doi:10.1016/j.marpetgeo.2007.04.005.

Warrlich, G.M.D., Waltham, D.A., and Bosence, D., 2002, Quantifying the sequence stratigraphy and drowning mechanisms of atolls using a new 3-D forward stratigraphic modelling program (CARBONATE 3D): Basin Research, v. 14, p. 379–400, doi:10.1046/j.1365-2117.2002.00181.x.

Watts, N.R., 1987, Carbonate Sedimentology and Depositional History of the Nisku Formation (Within the Western Canadian Sedimentary Basin) in South Central Alberta, *in* 13th CSPG Core Conference and Display, p. 87–152, https://archives.datapages.com/data/cspg_sp/data/CSPG-SP-010/010001/87_cspgsp100087.htm.

Watts, A.B., and Torne, M., 1992, Subsidence history, crustal structure, and thermal evolution of the Valencia Trough: a young extensional basin in the western Mediterranean: Journal of Geophysical Research, v. 97, doi:10.1029/92jb00583.

Whitaker, F., Smart, P., Hague, Y., Waltham, D., and Bosence, D., 1997, Coupled two-dimensional diagenetic and sedimentological modeling of carbonate platform evolution: Geology, v. 25, p. 175–178, doi:10.1130/0091-7613(1997)025<0175:CTDDAS>2.3.CO;2.

Williams, H.D., Burgess, P.M., Wright, V.P., della Porta, G., and Granjeon, D., 2011, Investigating Carbonate Platform Types: Multiple Controls and a Continuum of Geometries: Journal of Sedimentary Research, v. 81, p. 18–37, doi:10.2110/jsr.2011.6.

Wilson, J.L., 1975, Carbonate Facies in Geologic History: New York, NY, Springer New York, doi:10.1007/978-1-4612-6383-8.

Wilson, M., and Vecsei, A., 2005, The apparent paradox of abundant foramol facies in low latitudes: their environmental significance and effect on platform development: Earth-Science Reviews, v. 69, p. 133–168, doi:10.1016/j.earscirev.2004.08.003.

Wright, V.P., 1986, Facies sequences on a carbonate ramp: the Carboniferous Limestone of South Wales: Sedimentology, v. 33, p. 221–241, doi:10.1111/j.1365-3091.1986.tb00533.x.

Wright, V.P., and Burgess, P.M., 2005, The carbonate factory continuum, facies mosaics and microfacies: An appraisal of some of the key concepts underpinning carbonate sedimentology: Facies, v. 51, p. 17–23, doi:10.1007/s10347-005-0049-6.

Wunsch, M., 2017, The Sedimentology and Architecture of Carbonate Platform Slopes: , p. 1–118, https://d-nb.info/1151639044/34.

Zhang, J., Burgess, P.M., Granjeon, D., and Steel, R., 2019, Can sediment supply variations create sequences? Insights from stratigraphic forward modelling: Basin Research, v. 31, p. 274–289, doi:10.1111/bre.12320.